WEAR BEHAVIOUR OF ALUMINIUM BASED METAL MATRIX COMPOSITES REINFORCED WITH RED MUD, SiC AND Al_2O_3

A Thesis Submitted in partial fulfilment of the requirement for the award of degree of

MASTER OF ENGINEERING
IN
PRODUCTION & INDUSTRIAL ENGINEERING

Submitted By
Hitesh Bansal
Roll No. 800982006

Under the Guidance of

Yogesh Kumar Singla
Lecturer,
Deptt. Of Mechanical Engg.
Thapar University, Patiala
Patiala-147004

Anil Kalra
Lecturer,
Deptt. Of Mechanical Engg.
Thapar University, Patiala
Patiala-147004

DEPARTMENT OF MECHANICAL ENGINEERING
THAPAR UNIVERSITY, PATIALA
PATIALA- 147004, INDIA

JUNE- 2011

CERTIFICATE

This is to certify that the work done in this thesis report entitled " **WEAR BEHAVIOUR OF ALUMINIUM BASED METAL MATRIX COMPOSITES REINFORCED WITH RED MUD, SILICON CARBIDE AND ALUMINIUM OXIDE** " submitted in partial fulfilment of requirement for the award of **Master of Engineering degree in Production & Industrial engineering** submitted in the mechanical engineering department of Thapar University, Patiala, is an authentic record of work carried out by me under the guidance of **Mr. Yogesh Kumar Singla, Lecturer, Mechanical Engineering Department, Thapar University, Patiala and Mr. Anil Kalra, Lecturer, Mechanical Engineering Department, Thapar University, Patiala.**

The matter embodied in this report has not been submitted in part or full to any other university or institute for the award of any degree.

Hitesh Bansal

(Hitesh Bansal)

This is to certify that above declaration made by the student concerned is correct to the best of my knowledge & belief.

Mr. Yogesh Kumar Singla
Lecturer,
Deptt. of Mechanical Engg.
Thapar University,
Patiala-147004

Anil Kalra 4/7/2011

Mr. Anil Kalra
Lecturer,
Deptt. of Mechanical Engg.
Thapar University,
Patiala-147004

Countersigned by

Dr. Ajay Batish
Professor & HOD
Deptt. of Mechanical Engg.
Thapar University,
Patiala-147004

Dr. S.K. Mohapatra
Dean of Academic Affairs
Thapar University,
Patiala-147004

ACKNOWLEDGEMENT

To achieve success in any work, guidance plays an important role. It makes us put right amount of energy in the right direction and at right time to obtain the desired result. I express my sincere gratitude to my guides, **Mr. Yogesh Kumar Singla**, Lecturer, Mechanical engineering department and **Mr. Anil Kalra**, Lecturer, Mechanical Engineering Department, Thapar University, Patiala, for giving valuable guidance during the course of this work, for their ever encouraging and timely moral support. Their enormous knowledge always helped me unconditionally to solve various problems.

I am also very thankful **Dr. Rahul Chibber**, Assistant Professor, Mechanical engineering department, Thapar University, Patiala for help me a lot during my work.

I am also greatful to my loving parents who have given me moral support at each moment during my thesis work.

I am greatly thankful to **Dr. Ajay Batish**, Professor and Head, Mechanical Engineering Department, Thapar University, Patiala and **Dr. S.K. Mohapatra** Dean of Academic Affairs, Thapar University, Patiala for his encouragement and inspiration for execution of the thesis work. I express my feelings of thanks to the entire faculty and staff, Department of Mechanical Engineering, Thapar University, Patiala for their help, inspiration and moral support, which went a long way in the successful completion of my Thesis.

Last but not least, I would like to thank God for all good deeds.

Hitesh Bansal

ABSTRACT

Metal matrix composites are used mostly in space ships, aerospace, automotive, nuclear, biotechnology, electronic and sporting goods industries, but due to their high cost, experiments are usually done to reduce the cost of the composites and inexpensive materials are utilised for metal matrix composites.

Red mud emerges as the major waste material during production of alumina from bauxite by the Bayer's process. It comprises of oxides of iron, titanium, aluminium and silica along with some other minor constituents. Based on economics as well as environmental related issues, enormous efforts have been directed worldwide towards red mud management issues i.e. of utilization, storage and disposal. Different avenues of red mud utilization are more or less known but none of them have so far proved to be economically viable or commercially feasible. It is generally agreed that micro hardness and resistance to wear of MMCs is created by reinforcement and also the wear properties are improved remarkably by introducing hard intermetallic compound into the aluminium matrix. The reinforcing materials are generally SiC, Al_2O_3, TiO_2 etc and are costly. The present research work has been undertaken with an objective to explore the use of red mud as a reinforcing material due to its easy availability and contains all these reinforcement elements.

In the present investigation a comparative study on abrasive wear behaviour of Aluminium metal matrix composite reinforced with Red Mud, SiC and Al_2O_3 (produced by the stir casting technique) has been carried out. During this investigation, Red Mud was received from CBRI, IIT Roorkee and SiC and Al_2O_3 was received from the market (local source). In this research, wear performance and microhardness studies were carried out by varying the percentage of reinforcements in the matrix. All experiments were conducted under room temperature condition. To assess the wear characteristics of the aluminium alloy 6061 with red mud, SiC and Al_2O_3 composites (in pure sliding mode) a computerized pin-on-disc machine was used.

Microhardness tester was employed to measure the value of microhardness number (VHN) of different MMCs by indenting the diamond indenter on the specimen with a constant load of 200 gram and constant dwell time of 20 seconds at 10X optical zoom.
The specimens were studied under optical microscope and SEM to get an idea about the

distribution pattern of the reinforcement in the matrix alloy and effect of these particulate reinforcements on the wear behaviour and microhardness of the composites. Dispersion of particulates in aluminium matrix improves the hardness of the matrix material and also the wear behaviour of the composite.

X-ray Diffraction (XRD) was performed to know the presence of the phases of reinforced material.

There are other fabrication techniques available where the volume fraction of reinforcements could be increased and are likely to vary the wear performances of the composite. This work can be further extended to those techniques. However these results can act as a starting point for both industrial designers and researchers to design and develop MMC components using this industrial waste.

CONTENTS

CHAPTER 2

CHAPTER 3

CHAPTER 4

CHAPTER 5

LIST OF FIGURES

LIST OF TABLES

CHAPTER 1 INTRODUCTION

Major concentration on this thesis project is to study the wear behavior and hardness of aluminium (Al) based metal matrix composites AMCs which are used in aerospace, automotive and agricultural industries etc. But for further study firstly we should know about the Metal Matrix composites.

1.1 COMPOSITE MATERIALS

A composite material is a material composed of two or more constituents. The constituents are combined at a microscopic level and are not soluble in each other. Generally, a composite material is composed of reinforcement (fibers, particles/ particulates, flakes, and/or fillers) embedded in a matrix (metals, polymers). The matrix holds the reinforcement to form the desired shape while the reinforcement improves the overall mechanical properties of the matrix. When designed properly, the new combined material exhibits better strength than would each individual material. The most primitive man-made composite materials are straw and mud combined to form bricks for building construction [1, 2].

1.2 PROPERTIES OF COMPOSITES [2]

The following are the various properties of composites:

- Composites posses excellent Strength and Stiffness
- They are very light Materials
- They possess high resistance to corrosion, chemicals and other weathering agents.
- High strength to weight ratio (low density high tensile strength)
- High creep resistance
- High tensile strength at elevated temperature
- High toughness

1.3 INTRODUCTION OF METAL MATRIX COMPOSITES

Metal matrix composites (MMCs), like all composites; consist of at least two chemically and physically distinct phases, suitably distributed to provide properties not obtainable with either of

the individual phases. Generally, there are two phases either a fibrous or particulate phase in a metallic matrix. For e.g. Al_2O_3 fiber reinforced in a copper matrix for superconducting magnets and SiC particle reinforced with in the Al matrix composites used in aero space, automotive and thermal management applications.

For many researchers the term metal matrix composites is often equated with the term light metal matrix composites (MMCs). Substantial progress in the development of light metal matrix composites has been achieved in recent decades, so that they could be introduced into the most important applications. In traffic engineering, especially in the automotive industry, MMCs have been used commercially in fiber reinforced pistons and aluminium crank cases with strengthened cylinder surfaces as well as particle strengthened brake disks. These innovative materials open up unlimited possibilities for modern material science and development; the characteristics of MMCs can be designed into the material, custom-made, dependent on the application [3].

1.4 OBJECTIVES OF METAL MATRIX COMPOSITES [3]

The objectives for metal composite materials are:

- Increase in yield strength and tensile strength at room temperature and above while maintaining the minimum ductility or rather toughness
- Increase in creep resistance at higher temperatures compared to that of conventional alloys, Increase in fatigue strength, especially at higher temperatures
- Improvement of Thermal Shock Resistance
- Improvement of Corrosion Resistance
- Increase in Young's Modulus
- Reduction of Thermal Elongation

1.5 MATRIX

The matrix is the monolithic material into which the reinforcement is embedded, and is completely continuous. This means that there is a path through the matrix to any point in the material, unlike two materials sandwiched together. In structural applications, the matrix is usually a lighter metal such as aluminium, magnesium, or titanium, and provides a compliant

support for the reinforcement. In high temperature applications, cobalt and cobalt-nickel alloy matrices are common [3].

1.6 MATRIX MATERIAL

The most common matrix materials used in composite are as follows:

- Aluminium matrix
- Copper Matrix
- Titanium Matrix

1.7 DIFFERENT METHODS USED TO MANUFACTURE PARTICULATE REINFORCED MMCs [4]

MMC manufacturing can be of two types: solid and liquid.

1.7.1 Solid-phase fabrication methods:

- Powder blending and consolidation (powder metallurgy): Powdered metal and discontinuous reinforcement are mixed and then bonded through a process of compaction, degassing, and thermo-mechanical treatment (extrusion).
- Foil diffusion bonding: Layers of metal foil are sandwiched with long fibers, and then pressed through to form a matrix.

1.7.2 Liquid-phase fabrication methods:

Liquid-phase fabrication method is more efficient than the solid-phase fabrication method because solid-phase processing requires a longer time.

- Electroplating / Electroforming: A solution containing metal ions loaded with reinforcing particles is co-deposited forming a composite material.
- Stir casting: Discontinuous reinforcement is stirred into molten metal, which is allowed to solidify.
- Squeeze casting: Molten metal is injected into a form with fibers preplaced inside it.
- Spray deposition: Molten metal is sprayed onto a continuous fiber substrate.

1.7.2.1 Stir casting

Stir casting set-up mainly consists a furnace and a stirring assembly as shown in Figure 1.1. In general, the solidification synthesis of metal matrix composites involves a melt of the selected matrix material followed by the introduction of a reinforcement material into the melt, obtaining a suitable dispersion. The next step is the solidification of the melt containing suspended dispersoids under selected conditions to obtain the desired distribution of the dispersed phase in the cast matrix. In preparing metal matrix composites by the stir casting method, there are several factors that need considerable attention, including

- The difficulty in achieving a uniform distribution of the reinforcement material.
- Wettability between the two main substances.
- Porosity in the cast metal matrix composites.
- Chemical reactions between the reinforcement material and the matrix alloy.

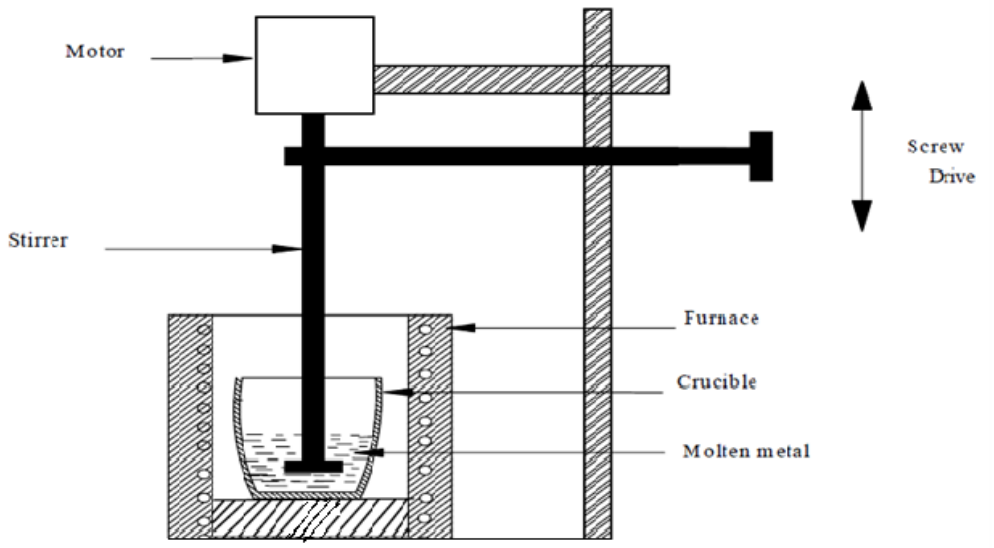

Figure 1.1- Stir Casting [1]

In order to achieve the optimum properties of the metal matrix composite, the distribution of the reinforcement material in the matrix alloy must be uniform, and the wettability or bonding between these substances should be optimized. The porosity levels need to be minimized.

1.7.2.1.1 Characterization of Stir Casting:

1. Contents of dispersed phase are limited (usually not more than 30% by volume).
2. Distribution of dispersed phase throughout the matrix is not perfectly homogeneous:
   - There are local clouds (clusters) of the dispersed particles (fibers).
   - There may be gravity segregation of the dispersed phase due to a difference in the densities of the dispersed and matrix phase.
3. The technology is relatively simple and low cost.

1.8 ADVANTAGES OF METAL MATRIX COMPOSITES [2]

The following are the various advantages of MMCs:

- Dimensional stability
- Wear and Corrosion resistance
- Reduced Weight

1.9 DISADVANTAGES OF METAL MATRIX COMPOSITES [2]

The following are the various disadvantages of MMCs:

- High production cost
- Difficult to repair
- Complex fabrication methods for fiber- reinforced systems (except for casting)

1.10 APPLICATION OF METAL MATRIX COMPOSITES

Table 1.1- Application of MMC [21]

Potential and Existing Applications / Benefits	Weight Reduction	Wear Resistance	Stiffness	Tailorable Thermal Conductivity	Increased Performance at Elevated Temperatures	Tailorable CTE	Corrosion Resistance	Resistance to Radiation	High Strength
Aircraft Skins	•				•				•
Bearings	•	•					•		•
Bicycle Frames	•		•						•
Boat Masts & Spars	•		•						•
Brake Rotors	•	•							
Electronics Packaging	•			•	•	•		•	
Electronics/Avionics Racks	•			•	•	•			
Engine Cylinder Liners	•	•							
Fastening Equipment in Chemical Environment- Bolts and Screws	•						•		•
Ground Vehicles	•								•
Landing Gear Struts	•		•						•
Medical Implants	•						•		•
Optical/Guidance Systems Structures	•		•	•		•			
Pistons	•	•							
Satellite Antenna Masts	•		•						
Sea Vehicles	•		•				•		
Space Structures	•		•	•				•	
Transmission Components	•	•					•		
Tubing in Nuclear Plants	•						•	•	
Turbine Engine Components	•	•			•				•
Worm Gears	•	•							•

1.11 WEAR

Wear occurs as a natural consequence when two surfaces with a relative motion interact with each other. Wear may be defined as the progressive loss of material from contacting surfaces in relative motion.

We know that one third of our global energy consumption is consumed wastefully in friction. Wear causes an enormous annual expenditure by industry and consumers. Most of this is replacing or repairing equipment that has worn to the extent that it no longer performs a useful function.

For many machine components this occurs after a very small percentage of the total volume has been worn away. For some industries, such as agriculture, as many as 40% of the components replaced on equipment have failed by abrasive wear. So, the effective decrease and control of wear of metals are always desired [1].

1.11.1 Types of Wear [1, 22]

In most basic wear studies where the problems of wear have been a primary concern, the so-called dry friction has been investigated to avoid the influences of fluid lubricants. Dry friction is defined as friction under not intentionally lubricated conditions but it is well known that it is friction under lubrication by atmospheric gases, especially by oxygen. There are generally five types of wear namely abrasive, adhesive, erosive, Surface fatigue and Corrosive.

(i) Abrasive Wear

Abrasive wear can be defined as wear that occurs when a hard surface slides against and cuts groove from a softer surface. It can be account for most failures in practice. Hard particles or asperities that cut or groove one of the rubbing surfaces produce abrasive wear. This hard material may be originated from one of the two rubbing surfaces. In sliding mechanisms, abrasion can arise from the existing asperities on one surface (if it is harder than the other), from the generation of wear fragments which are repeatedly deformed and hence get work hardened for oxidized until they became harder than either or both of the sliding surfaces, such as dirt from outside the system. As shown in Figure 1.2 two body abrasive wear occurs when one surface

(usually harder than the second) cuts material away from the second, although this mechanism very often changes to three body abrasion as the wear debris then acts as an abrasive between the two surfaces.

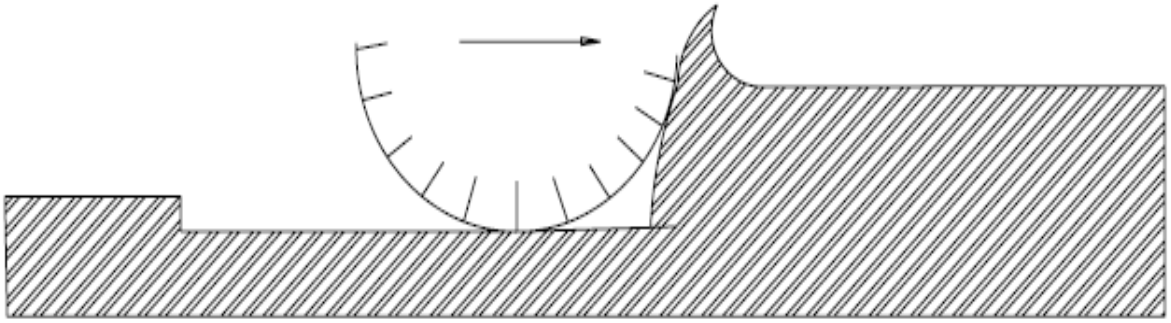

Figure 1.2- Abrasive wear

(ii) Adhesive Wear

Adhesive wear can be defined as wear due to localized bonding between contacting solid surfaces leading to material transfer between the two surfaces or the loss from either surface. As shown in Figure 1.3 for adhesive wear to occur it is necessary for the surfaces to be in intimate contact with each other. Surfaces, which are held apart by lubricating films, oxide films etc. reduce the tendency for adhesion to occur.

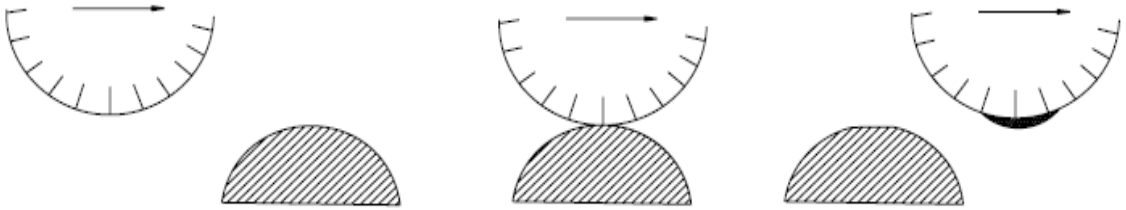

Figure 1.3- Adhesive wear [1]

(iii) Erosive Wear

Erosive wear can be defined as the process of metal removal due to impingement of solid particles on a surface. Erosion is caused by a gas or a liquid, which may or may not carry, entrained solid particles, impinging on a surface. When the angle of impingement is small, the wear produced is closely analogous to abrasion. When the angle of impingement is normal to the surface, material is displaced by plastic flow or is dislodged by brittle failure.

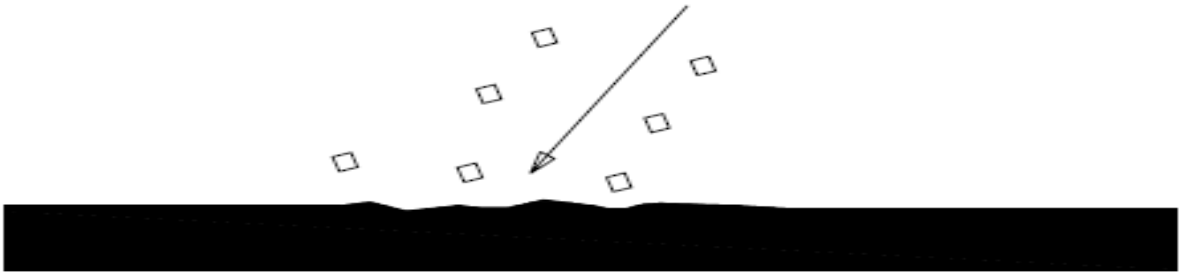

Figure 1.4- Erosive wear [1]

(iv) Surface fatigue wear

Wear of a solid surface caused by fracture arising from material fatigue. The term 'fatigue' is broadly applied to the failure phenomenon where a solid is subjected to cyclic loading involving tension and compression above a certain critical stress. Repeated loading causes the generation of micro cracks, usually below the surface, at the site of a pre-existing point of weakness. On subsequent loading and unloading, the micro crack propagates. Vibration is a common cause of fatigue wear.

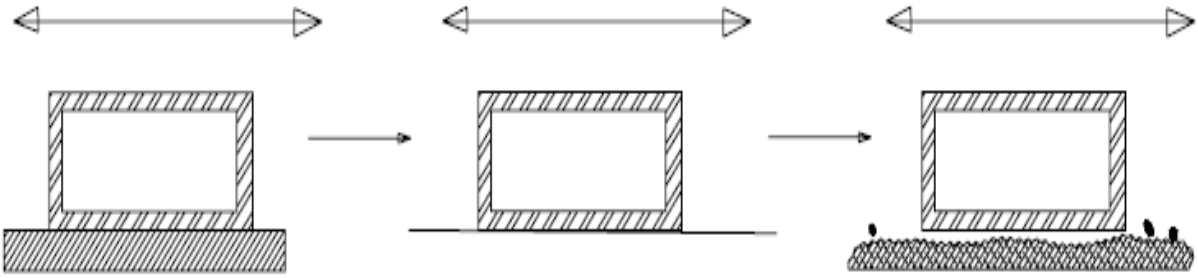

Figure 1.5- Surface Fatigue wear [1]

(v) Corrosive Wear

Most metals are thermodynamically unstable in air and react with oxygen to form an oxide, which usually develop layer or scales on the surface of metal or alloys when their interfacial bonds are poor. Corrosion wear is the gradual eating away or deterioration of unprotected metal surfaces by the effects of the atmosphere, acids, gases, alkalis, etc. This type of wear creates pits and perforations and may eventually dissolve metal parts.

1.11.2 Symptoms of Wear

A summary of the appearance and symptoms of different wear mechanism is indicated in Table 1.2 and the same is a systematic approach to diagnose the wear mechanisms.

Table 1.2- Symptoms and appearance of different types of wear [1]

Types of wear	Symptoms	Appearance of the worn-out surface
Abrasive	Presence of clean furrows cut out by abrasive particles	Grooves
Adhesive	Metal transfer is the prime symptoms	Seizure, catering rough and turnout surfaces.
Erosion	Presence of abrasives in the fast moving fluid and short abrasion furrows	Waves and troughs
Corrosion	Presence of metal corrosion products	Rough pits or depressions
Fatigue	Presence of surface or subsurface cracks accompanied by pits and spalls	Sharp and angular edges around pits

1.12 ALUMINIUM M ATRIX [4, 23, 24]

Aluminium is the most abundant metal in the Earth's crust, and the third most abundant element, after oxygen and silicon. It makes up about 8% by weight of the Earth's solid surface. The chief

source of aluminium is bauxite ore. Its Atomic number is 13. Aluminium is a soft, durable, lightweight, ductile and malleable metal with appearance ranging from silvery to dull gray, depending on the surface roughness. Aluminium is nonmagnetic and non-sparking. Aluminium has about one-third the density and stiffness of steel. It is easily machined, cast, drawn and extruded. Corrosion resistance can be excellent due to a thin surface layer of aluminium oxide that forms when the metal is exposed to air, effectively preventing further oxidation.

1.13 ALUMINIUM ALLOYS [23, 24]

Aluminium alloys are alloys in which Al is the predominant metal. The typical alloying elements are copper, magnesium, manganese, silicon, and zinc. There are two principal classifications, namely cast alloys and wrought alloys.

1.13.1 Wrought alloys

The International Alloy Designation System is the most widely accepted naming scheme for wrought alloys. Each alloy is given a four-digit number, where the first digit indicates the major alloying elements [22, 23, 24].

- 1000 series is essentially pure aluminium with a minimum 99% aluminium content by weight and can be work hardened.
- 2000 series is alloyed with copper, can be precipitation hardened to strengths comparable to steel. Formerly referred to as duralumin, they were once the most common aerospace alloys, but were susceptible to stress corrosion cracking and are increasingly replaced by 7000 series in new designs.
- 3000 series is alloyed with manganese, and can be work-hardened.
- 4000 series is alloyed with silicon. They are also known as silumin.
- 5000 series is alloyed with magnesium.
- 6000 series is alloyed with magnesium and silicon, are easy to machine, and can be precipitation hardened, but not to the high strengths that 2000 and 7000 can reach.
- 7000 series is alloyed with zinc, and can be precipitation hardened to the highest strengths of any aluminium alloy.

1.14 PHYSICAL AND THERMAL PROPERTIES OF ALUMINIUM ALLOY 6061 [25]

(i) Physical properties

- Melting Point: Approx 580°C
- Modulus of Elasticity: 70-80 GPa
- Poisson's Ratio: 0.33
- Density: 2.7 g/ cm^3

(ii) Thermal Properties

- Co-Efficient of Thermal Expansion (20-100°C) is 24.3µm/m°C
- Thermal Conductivity: 173 W/mK

1.15 INTERFACES

Interface between any two phases can be explained as bounding surface where a discontinuity of some kind occurs .The discontinuity may be sharp or gradual. In general the interface is essentially bi- dimensional region through which material parameters, such as concentration of an element, crystal structure elastic modulus, density and coefficient of thermal expansion, change from one side to another. Thus bonding between two phases at interface is termed as interfacial bonding. In case of composites, bonding at particle – matrix interface is called interfacial bonding [4].

1.16 REINFORCEMENT

The role of the reinforcement in a composite material is fundamentally one of increasing the mechanical properties of the neat resin system. All of the different particulates/ fibres used in composites have different properties and so affect the properties of the composite in different ways. The desirable properties of the reinforcements include:

1. High strength
2. Ease of fabrication and low cost
3. Good chemical stability
4. Density and distribution

1.16.1 Red Mud as Reinforcement

Red mud is the caustic insoluble waste residue generated by alumina production from bauxite by the Bayer's process at an estimated annual rate of 66 and 1.7 million tons, respectively, in the World and India [1]. Under normal conditions, when one ton of alumina is produced nearly a ton of red mud is generated as a waste. This waste material has been accumulating at an increasing rate throughout the world.

Figure 1.6- Red Mud as reinforcement

The disposal/utilization of red mud has been an acute problem and a clear cut solution is not available till date. Different avenues of red mud utilization are more or less known but none of them have so far proved to be economically viable or commercially feasible. However, a survey of literature on utilization of red mud published so far, it is revealed that use of red mud is restricted only for recovery of some metal values like Titanium, Vanadium and Zinc; making of ceramics etc. It has also been used for making cement, bricks, pigments and glazed sewer pipes etc. Research and development work on red mud utilization that are under process in India are shown in table no.3. Going through the available information on the utilization of red mud (density 3.05 g/cm^3) [6], it is seen that use of red mud as reinforcement material for preparation of MMC has not been explored till date [1].

1.16.1.1 Need for the reinforcement of Red Mud into Aluminium matrix

To obtain Optimum performance from composite materials there is an advantage to selecting the shape and size of the reinforcement material to fit the application. It is apparent that different material types and shapes will have advantages in different matrices.

There are so many researchers have worked out separately to reinforce SiC, Al_2O_3 (i.e. carbides, Nitrides and oxides) TiC, Boron and Graphite in to the Aluminium matrix to achieve different properties and are expensive [7, 8, 9, 10]. The ever-increasing demand for low cost reinforcement stimulated the interest towards production and utilization of red mud (an industrial waste from Bayer's process) that contains major elements like Al_2O_3, Fe_2O_3, TiO_2, and Na_2O for preparation of a metal matrix composite for different applications such as wear resistant, hardness etc[3, 4]. There are various researches and development works are going on the red mud utilization in India which is shown in Table 1.3.

Table 1.3- Research and Development work on red mud utilization in India [1].

Organization	Investigation
1. Madras Aluminium Company	Red mud as a component in cement
2. Central Building Research Institute (CBRI)	Production bricks with red mud and clay with equal proportions
3. RRL, Bhubaneswar	Recovery of vanadium, chromium &alumna
4. NEITCO	Manufacture of red mud corrugated sheets
5. RRL, Bhopal	Utilization of red mud PVC and lab scale product designed as red mud plastic (RMP)
6. Central glass and ceramic research Institute	Conversion of red mud to ceramics
7. NML, Jamshedpur & RRL, BBSR	Recovery of V_2O_5 and Al_2O_3
8. Metallurgical Dept. B.H.U.	Development of bricks, recovery of titanium and Ferro Titanium
9. Rajasthan Financial Corporation.	Manufacture of pipes and corrugated sheets
10. NALCO, Ltd	Filler to PVC sheets and pipes etc

The chemical analysis showing that Red Mud contains silica, alumina, iron oxide, calcium, titanium as well as an array of minor constituents, namely: Na, K, Cr, V, Ni, Ba, Cu, Mn, Pb, Zn etc. The variation in chemical composition between different red muds worldwide is high. The

chemical composition of red mud in elemental and compound form had found through Energy Dispersive Spectrometer (EDS) which was shown in Table 1.4.

Table 1.4- Chemical Composition of Red Mud in Element and Compound form

Constituents	**%**	**Constituents**	**%**
Na	5.20	Na_2O	7.01
Al	7.67	Al_2O_3	14.49
Si	3.22	SiO_2	6.89
Ca	3.67	CaO	5.13
Ti	12.37	TiO_2	20.63
Fe	30.70	Fe_2O_3	39.49
Cu	2.94	CuO	3.68
Zn	2.14	ZnO	2.68
O	32.09	Total	100
Total	100		

The EDS Spectrum (a) and corresponding Micrograph (b) of Red Mud are shown in Figure 1.7.

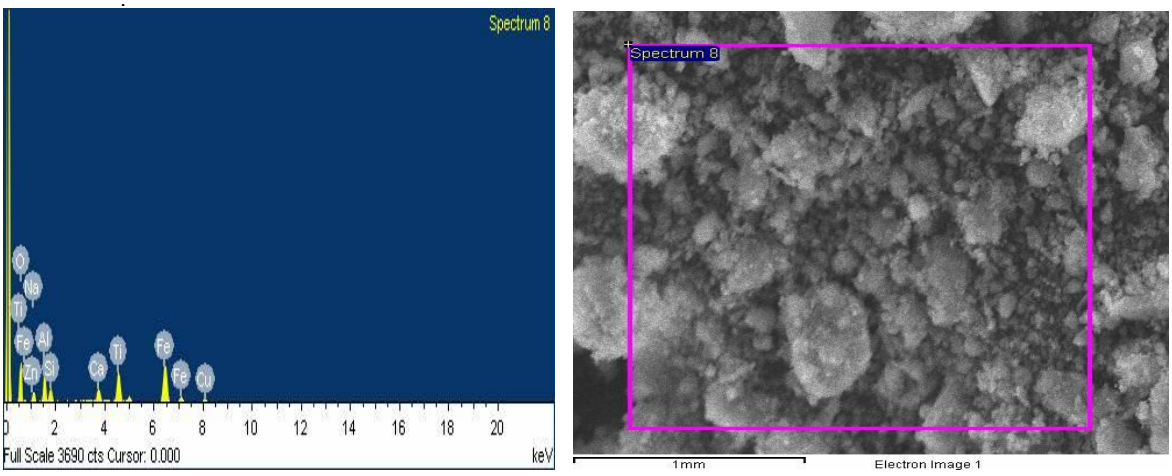

(a) (b)

Figure 1.7- (a) EDS result and (b) corresponding micrograph of Red Mud

1.16.1.2 Applications of Red Mud [26, 27]

Utilization of Red Mud has been a subject of major scientific research. The various uses of red mud include:

1. production of building materials such as constructional bricks, bricks roofing and flooring tiles, cements etc
2. used in road construction
3. use as a filler in rubber and plastic industry
4. as pigment in production of paints
5. Metallurgical ones such as iron and steel production, alumina and minor constituents used for trapping co_2 and so_2 from flue gases.
6. ceramics such as pottery, sanitary ware, tiles and glasses, glazes, ferrites etc
7. Miscellaneous direct uses in waste treatment as a filler and as a fertilizer such as to increase nitrogen and phosphorous removal from sewage effluent, in agricultural situations for use in acidic soils because of its alkaline nature, as a treatment for iron deficient soils etc.

1.16.2 Silicon carbide as Reinforcement

Silicon carbide (SiC), also known as carborundum, is a compound of silicon and carbon with chemical formula SiC. It was originally produced by a high temperature electro-chemical reaction of sand and carbon. Silicon carbide is an excellent abrasive and has been produced and made into grinding wheels and other abrasive products for over one hundred years. Today the material has been developed into a high quality technical grade ceramic with very good mechanical properties [28].

It is used in abrasives, refractories, ceramics, and numerous high-performance applications. The material can also be made an electrical conductor and has applications in resistance heating, flame igniters and electronic components, floor tiles etc. Structural and wear applications are constantly developing. Silicon carbide is composed of tetrahedra of carbon and silicon atoms with strong bonds in the crystal lattice. This produces a very hard and strong material. Figure 1.8 shows the colour of silicon carbide.

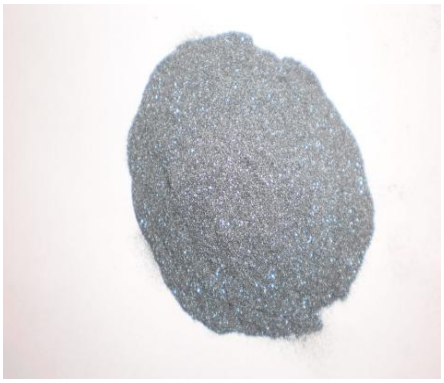

Figure 1.8- Silicon Carbide (SiC)

1.16.2.1 Characteristics of Silicon Carbide

The following are the characteristics of silicon carbide:

- Low density
- High strength and thermal conductivity
- Low thermal expansion
- High hardness

Table 1.5- Properties of Silicon Carbide [28]

Properties	Silicon carbide
Melting Point	2200-2700
Hardness (Kg/mm^2)	2800
Density (g/cm^3)	3.1
Coefficient of Thermal expansion ($\mu m/m^0c$)	4.0
Fracture toughness ($MPa\text{-}m^{1/2}$)	4.6
Poisson's Ratio	0.14
Colour	Black

1.16.3 Aluminium Oxide as Reinforcement

The chemical formula of aluminium oxide is Al_2O_3. It is commonly referred to as alumina, or corundum in its crystalline form, as well as many other names, reflecting its widespread occurrence in nature and industry. Alumina (Al_2O_3) is the most cost effective and widely used material in the family of engineering ceramics. The raw materials from which this high performance technical grade ceramic is made are readily available and reasonably priced,

resulting in good value for the cost in fabricated alumina shapes. With an excellent combination of properties and an attractive price, it is no surprise that fine grain technical grade alumina has a very wide range of applications. Its most significant use is in the production of aluminium metal, although it is also used as an abrasive due to its hardness and as a refractory material due to its high melting point. Figure 1.9 shows the colour of aluminium oxide.

Figure 1.9- Alumina (Al_2O_3)

1.16.3.1 Characteristics of Aluminium Oxide (Alumina)

The following are the characteristics of aluminium oxide:

- Hard and wear-resistant
- Resists strong acid and alkali attack at elevated temperatures
- Good thermal conductivity
- Excellent size and shape capability
- High strength and stiffness

Table 1.6- Properties of Aluminium Oxide [29]

Properties	Aluminium Oxide
Melting Point	2072 °C
Hardness (Kg/mm^2)	1175
Density (g/cm^3)	3.69
Coefficient of Thermal expansion ($\mu m/m^0c$)	8.1
Fracture toughness ($MPa\text{-}m^{1/2}$)	3.5
Poisson's Ratio	0.21
Colour	white

CHAPTER 2 LITERATURE REVIEW

2.1 REVIEW OF LITERATURE

There are several literatures available for aluminium metal-matrix composites and they are as follows:

Naresh Prasad et al. [1] studied the use of red mud as a reinforcing material. Experiments have been conducted under laboratory condition to assess the wear characteristics of the aluminium red mud composite under different working conditions in pure sliding mode on a pin-on-disc machine. This has been possible by fabricating the samples through usual stir casting technique. To enhance the wear properties, the samples were also subjected to heat treatment and different quenching medium. The results indicate that quenching of heat treated samples in water gives better wear resistance than that achieved by air cooling.

Sanjeev Kumar et al. [2] investigated the effects of Thermal Cycling on Cast Aluminium Composites Reinforced with Silicon Carbide and Fly Ash particles. During this investigation, dry fly ash was used with Aluminium reinforced with SiC and a composite was prepared using Liquid metal stir casting route with the reducing quantity of SiC. During the research, Thermal cycling was carried out on the samples prepared and effects on samples before and after thermal cycling were observed.

Narinder Singh et al. [3] studied the effect of age hardening behaviour of Aluminium LM-4/ Zircon sand composite produced by the stir casting technique. During this research, Water and Brine solution has been used as the quenching media and the thermal ageing has been done at different temperature, time and quenching media. Thermal ageing has been done at different temperature, time and quenching media. Microhardness and wear tests were performed on the samples obtained from the stir casting process. The results obtained from this investigation that the ageing demonstrate that the microhardness of the composite depend on the quenching medium in which they are heat treated.

Vishal Sharma et al. [4] investigated the effect of Al-4.5wt%Cu/ zircon sand/ SiC hybrid composite by stir casting route by controlling various casting parameters. The as-cast samples were observed under optical and scanning electron microscope. Micro structural observations of the as-cast hybrid composite, shows uniform distribution of reinforcement particles and also good interfacial bonding between the particles and the matrix. Micro hardness tester is employed to evaluate the interfacial bonding between the particles and the matrix by indenting the micro hardness indenter on the particle with the varying load (100 gm, 200 gm, and 300 gm) and time (10 sec, 15 sec, 20 sec and 25 sec). It has been concluded that by the variation in hardness at constant load varying time or at constant time varying load, the bond strength can be compared.

Shailove Kumar et al. [5] studied the age hardening behaviour of Aluminium alloy (6351) - 9%wt SiC composite produced by the stir casting technique. Water and Brine solution has been used as the quenching media. Thermal ageing has been done at different temperature, time and quenching media. Micro hardness and wear tests were performed on the samples obtained from the stir casting process. The results of ageing demonstrate that the micro hardness of the composite depend on the quenching medium in which they are heat treated and peak hardness depends on quenching media and ageing time durations. X-ray Diffraction was performed to know the presence of the phases of reinforced material. Optical micrography was done to know the distribution of SiC particles in aluminium alloy.

Vladimir Cablik et al. [6] studied the characterization of red mud which is a waste generated by the Bayer process in the aluminium industry – which causes environmental problems. Residue of the alumina leaching from bauxite was analyzed for mineral compositions of the mineral ore and its residue for chemical composition, density, and grain-size composition. The residue was calcinated and finally tested as a pigment for use in the building material industry.

M.Ramachandra and K. Radhakrishna [7] had presented that aluminium based metal matrix composite containing up to 15% weight percentage of Silicon carbide particles are synthesized using stir-cast method. Macrostructural studies have shown near uniform distribution of SiC particulates in the longitudinal direction. Microstructure also showed uniform distribution along the cross section of the specimen. Friction and wear behavior is studied by using computerized pin on disc wear testing machine. Resistance to wear has increased with increase in silicon

carbide particles. But wear has increased with increase in normal load and sliding velocity. Hardness has increased with increase in SiC particles.

S. Sawla and S. Das [8] examined the abrasive wear behaviour of LM13 alloy and LM13–15 wt. % SiC composite, in cast and heat-treated conditions, as a function of applied load. The wear constant (K) was calculated based on the wear rate data. It was observed that the wear constant decreases with load. In the case of cast alloy the value of wear constant was higher than that of the heat-treated alloy and composite. The wear surface and the subsurface were studied using scanning electron microscope (SEM).

G. B. Veeresh Kumar et al. [9] this paper deals with the mechanical properties such as hardness, tensile strength and wear resistance etc. of Al6061-SiC and Al7075-Al_2O_3 composites. The composites are prepared using the liquid metallurgy technique, in which 2-6 wt. % of particulates was dispersed in the base matrix in steps of 2. The SiC and Al_2O_3 resulted in improving the hardness and density of their respective composites. Further, the increased %age of these reinforcements contributed in increased hardness and density of the composites. The microphotographs of the composites studied revealed the uniform distribution of the particles in the matrix system. The dispersed SiC in Al6061 alloy and Al_2O_3 in Al7075 alloy contributed in enhancing the tensile strength of the composites. The wear factor K obtained using computerized pin on disc wear tester with counter surface as EN31 steel disc (HRC60) and the composite pin as specimens, demonstrated the superior wear resistance property of the composites.

N. R. PRABHU SWAMY et al. [10] the aim of this paper is to investigate the Al6061–SiCp composites was fabricated by liquid metallurgy route with percentages of SiCp varying from 4 wt% to 10 wt% in steps of 2 wt%. The cast matrix alloy and its composites have been subjected to solutionizing treatment at a temperature of 530°C for 1 h followed by quenching in different media such as air, water and ice. The quenched samples are then subjected to both natural and artificial ageing. In this paper microstructural studies have been carried out to understand the nature of structure. Mechanical properties such as microhardness, tensile strength, and abrasive wear tests have been conducted both on matrix Al6061 and Al6061–SiCp composites before and after heat treatment. However, under identical heat treatment conditions, adopted Al6061–SiCp

composites exhibited better microhardness and tensile strength reduced wear loss when compared with Al matrix alloy.

Adem Kurt et al. [11] investigated the two stages. In the first stage, bronze-based break linings were produced and friction-wear properties of them were investigated. In the second stage, 0.5%, 1%, 2% and 4% alumina (Al_2O_3) powders were added to the bronze-based powders and Al_2O_3 reinforced bronze-based break linings were produced. Friction–wear properties of the Al_2O_3 reinforced samples were also investigated and compared to those of plain bronze-based ones. For this purpose, friction coefficient and wear behaviour of the samples were tested on the grey cast iron disc. The hardness and density of the samples were also determined. With increase in Al_2O_3 content, a reduction in mass loss of the samples was also observed. Overall, the samples reinforced with 2% and 4% Al_2O_3 exhibited the best results.

M.K. Surappa et al. [12] studied the tribological behaviour of stir-cast Al–Si/ SiCp composites against automobile brake pad material was studied using Pin-on-Disc tribotester. The Al-metal matrix composite (Al-MMC) material was used as disc, whereas the brake pad material forms the pin. It has been found that both wear rate and friction coefficient vary with both applied normal load and sliding speed. With increase in the applied normal load, the wear rate was observed to increase whereas the friction coefficient decreases. However, both the wear rate and friction coefficients were observed to vary proportionally with the sliding speed. I this during the wear tests, formation of a tribolayer was observed, presence of which can affect the wear behavior, apart from acting as a source of wear debris. Tribolayer formed over the worn disc surfaces was found to be heterogeneous in nature. It has also investigated the morphology and topography of worn surfaces and debris were studied using scanning electron microscope (SEM).

Soner Buytoz et al. [13] was investigated that Al6061 alloy and Al6061/Al_2O_3 metal matrix composites (MMCs) were fabricated by stir casting. The MMCs were prepared by addition of 5, 10and 15 wt% Al_2O_3 particulates and the size of particulates was taken as 16 μm. The effect of Al_2O_3 particulate content, thermal properties and stir casting parameters on the dry sliding wear resistance of MMCs were investigated under 50–350 N loads. It was observed that, the increase in Al_2O_3 vol% decreased both thermal conductivity and friction coefficient and hence increased the transition load and transition temperature for mild to severe wear during dry sliding wear test.

Sanjeev Das et al. [14] observed the effect of alumina and Zircon sand particles of different size and amount have been incorporated in Al-4.5 wt% Cu alloy by stir casting route. It is basically a comparative study on abrasive wear behavior of aluminum metal matrix composite reinforced with alumina and zircon sand particles has been carried out. Microstructures of the composites in as-cast condition show uniform distribution of particles and reveal better bonding in the case of zircon particles reinforced composite compared to that in alumina particles reinforced composite also studied in this. Abrasive wear resistance of both the composites improves with the decrease in particle size. It is observed that the alumina particle reinforced composite shows relatively poor wear resistance property compared to zircon-reinforced composite.

Kamalpreet Kaur and O. P. Pandey [15] have studied the dry sliding wear behaviour of zircon sand as a reinforcement and Al–Si alloy as a base material. In the present study composite has been developed via spray forming technique. The wear behaviour of Al–Si/zircon sand composite and base Al–Si alloy at various applied loads and constant sliding velocity of 1.6 m/s. The wear rate and volume loss showed the two stages of wear for all the applied loads. At the initial stage run-in wear occur up to 1 km sliding distance and in later stage wear approaches a steady state. The results confirmed that spray formed Al–Si/zircon sand composite is clearly superior to base Al–Si alloy in delaying the transition to severe wear at higher loads as well as showing greater resistance to wear at lower loads also.

Jaykant Gupta et al. [16] investigated the mechanical properties and wear behaviour of mild steels carburized at different temperature range of 850, 900 and 950^0C and found that the simple heat treatment greatly improves the hardness, tensile strength and wear resistance of the mild steels. It also examined the effects of these different carburization temperatures and conditions on the mechanical and wear properties of the carburized mild steels. For this purpose the mild steels are carburized under the different temperature range as stated above and then it is tempered at 2000 C for half an hour after this the carburized and tempered mild steels are subjected for different kind of test such as abrasive wear test, hardness test, tensile test and the toughness test. The results of these experiment shows that the process of carburization greatly improves the mechanical and wear properties like hardness, tensile strength and wear resistance and these properties increases with increase in the carburization temperature but apart from this

the toughness property decreases and it is further decreases with increase in carburization temperature.

Ashutosh Sharma et al. [17] had investigated the age hardening behavior of Al–4.5%Cu alloy composite reinforced with zircon sand particulates and produced by stir casting route in different quenching media viz, water, oil, and salt brine solution (7 wt%). Optical microscopy of the as cast alloy composite indicates that the matrix of the composite has the cellular structure. The results of ageing demonstrate that the micro hardness of age hardenable Al–Cu based alloy composites depend on the quenching medium in which they are heat treated. Salt brine quenching is faster as compared to water and oil, even if higher strength is obtained but cannot be used for complex shapes and thin sections where oil quenching is the alternative due to minimum distortion and cracking problems. Thermal cycling studies of the composite at 25 – 540 ^{0}c have been also carried out to determine the extent of quenching of the matrix after each solution heat treatment cycle while varying the quenching media.

S.K. VARMA et al. [18] studied the grain growth during an isothermal treatment at a solutionizing temperature of 540°c in a composite containing 6061 aluminium alloy matrix with $A1_20_3$ particles. The grain growth law is generally applicable to the composites containing 0.10, 0.15, and 0.20 volume fraction of the $A1_20_3$ particles (VFAP). The dislocation densities at these two locations in the composites increase with an increase in VFAP and the particle size. From this paper we find that the grain size increases with increase in solutionizing time in all the three composites.

Murphy et al. [19] studied the average chemical composition of red mud (dry weight). The red mud slurry resulting from the alkaline digestion of bauxite and consisting of finely divided red mud particles dispersed in an aqueous medium. Murphy et al. also investigated the process for improving the settling rate and filterability of aqueous red mud slurries resulting from the aluminiferous ores.

A.R. Daud et al. [20] was investigated the role of fly ash. In this study, Al alloys were reinforced with different solid fly ash particles. The X-ray diffraction (XRD), scanning electron microscopy (SEM) and X-ray fluorescence (XRF) analyses were used to identify the fly ash

particles, and they were also applied to the composite alloys. The X-ray diffraction (XRD) results indicated that the crystalline phase of the fly ash was an effective reinforced phase. The SEM and optical micrographs of the composite samples indicated that fly ash could be reacted or settled in the matrix of the aluminium. The microhardness analyses were also used to study the Al–fly ash composites.

2.2 SUMMARY AND GAP IN LITERATURE REVIEW

It was observed from the review of available literature following gaps are identified:

A lot of work has been done on aluminium based metal matrix composite with different types of reinforcements, different sizes and manufactured techniques either by stir casting or by spray casting technique and then subjected to study the wear behaviour. Alloy composition and its condition influence the wear rate. With increase in weight % of reinforcement in the matrix the wear resistance of composite increases. The hardness will also increase with increase in weight % of reinforcement.

A major research work has been reported on alloy 6061 by taking different reinforcements such as zircon sand, alumina etc. but none of them had made attempt for Al alloy 6061 and red mud as reinforcement and secondly limited data is available related to red mud which is used as reinforcement in matrix so far.

Now from last few decades interest has been increased on composites containing low density and low cost reinforcement. Red mud is one of the best example of this type of reinforcement. Such reinforced composites are likely to overcome the cost barrier for wide spread applications in automotive and small engine applications and also control the environmental condition because this waste material has been accumulating at an increasing rate throughout the world.

In this thesis, the combination of red mud as reinforcement and matrix is Al alloy 6061 was used with the help of simple and cheaper technique called stir casting technique. Other reinforcements are also used in place of red mud such as silicon carbide and aluminium oxide varying from 2.5 to 10% by wt. in Al alloy 6061 and studied the effect of all these combinations on macroscopic and microscopic behaviour such as wear rate, wear loss, hardness, microstructure and XRD etc.

CHAPTER 3 PROBLEM FORMULATION

3.1 PROPOSED WORK

The problem is associated with the study of Wear behaviour of Al-Red Mud, SiC and Al_2O_3 metal matrix composites (MMCs) of aluminium alloy of grade 6061 with addition of varying percentage composition of Red Mud, SiC and Al_2O_3 by stir casting technique. The wear behaviour and the change in physical and mechanical properties were taken into consideration.

For the achievement of the above, an experimental set up was prepared to facilitate the preparation of required MMCs. The aim of the experiment was to study the effect of variation of the percentage composition to predict the wear rate as well as to measure the microhardness. The experiment was carried out by preparing the samples of different percentage composition by stir casting technique and then subjected to computerized Pin on disc wear testing machine under dry sliding condition and Vicker's Microhardness Tester. A brief analysis of microstructure had been conducted by Optical Microscope and SEM to verify the dispersion of reinforcement in the matrix and presence of different phases through XRD technique.

3.2 OBJECTIVES

1. To study the effect of different weight percentage of reinforcement on wear rate, microhardness and micro structure of metal matrix composites.
2. To analyze the microstructure for study the change in material properties.

The tests performed on different types of specimens are as follows:

1. Wear Test (computerized Pin on Disc Machine)
2. Micro Hardness Test (Vicker's Micro Hardness Tester)
3. X-Ray Diffraction Test
4. The Microstructure Test (Microscope)
5. Scanning Electron Microscope Test (SEM)

CHAPTER 4 EXPERIMENTAL DETAILS

4.1 EXPERIMENTAL SETUP

For performing the experiment and testing of composites the following machines/equipments were used:

- Sieve Shaker
- Weighing Machine
- Matrix (Al alloy 6061)
- Reinforcements (Red Mud, SiC, Al_2O_3)
- Digital control Muffle Furnace
- Radial Drilling Machine
- Crucible (Graphite)
- Mould (Mild Steel)
- Stirrer (Graphite)
- Stainless steel rod (SS3l6) of diameter 12mm, Length 600mm
- Power Hacksaw
- Lathe Machine
- Belt Grinder
- Laser Gun
- Computerized Pin on Disc Machine
- Micro Hardness Testing Machine
- Energy Dispersive Spectrometer (EDS)
- Optical Microscope
- Scanning Electron Microscope (SEM)
- X-Ray Diffraction (XRD)

4.2 WORK PLAN FOR EXPERIMENTS

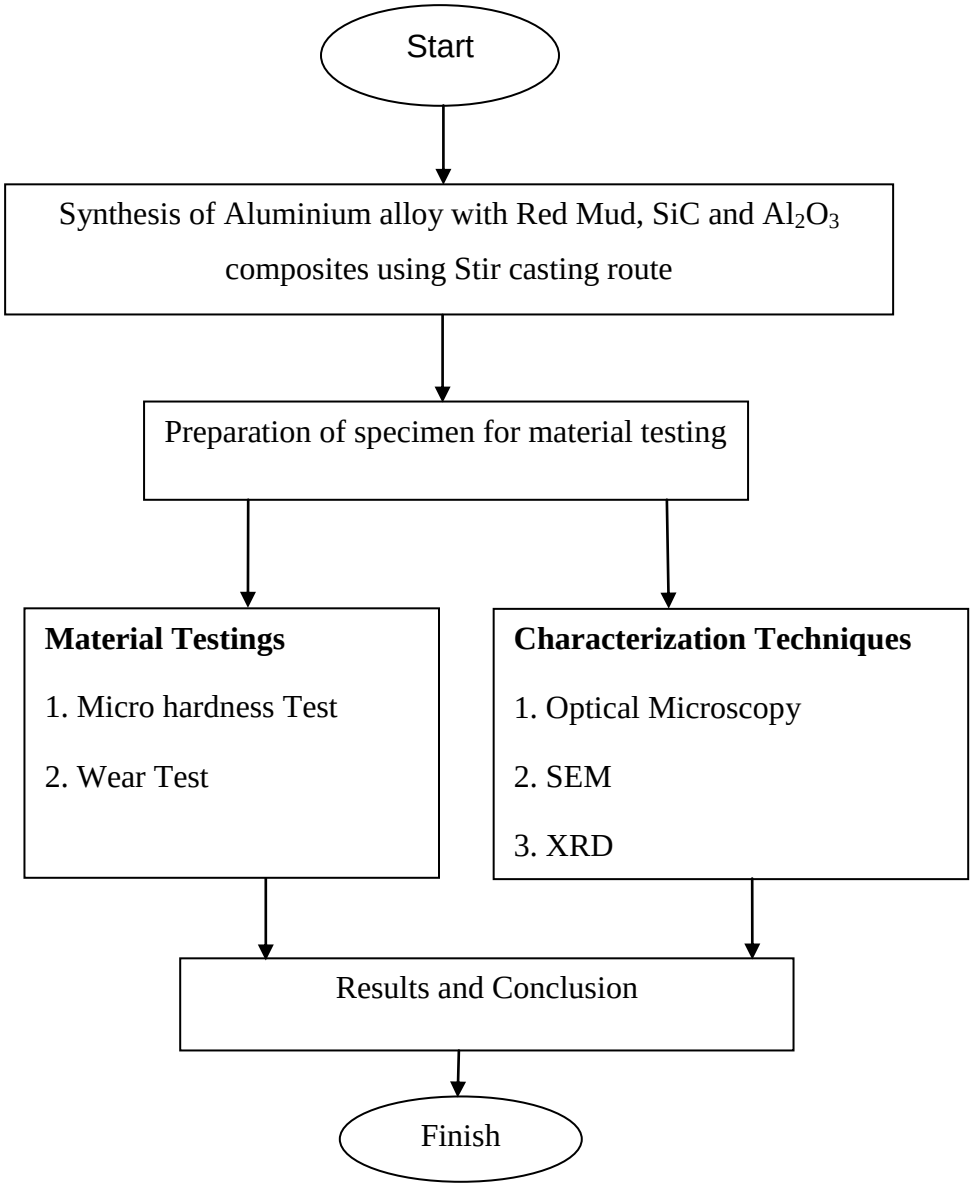

Figure 4.1- Flow chart of work plan for Experiments

4.3 FLOW CHART SHOWING STEPS INVOLVED IN STIR CASTING

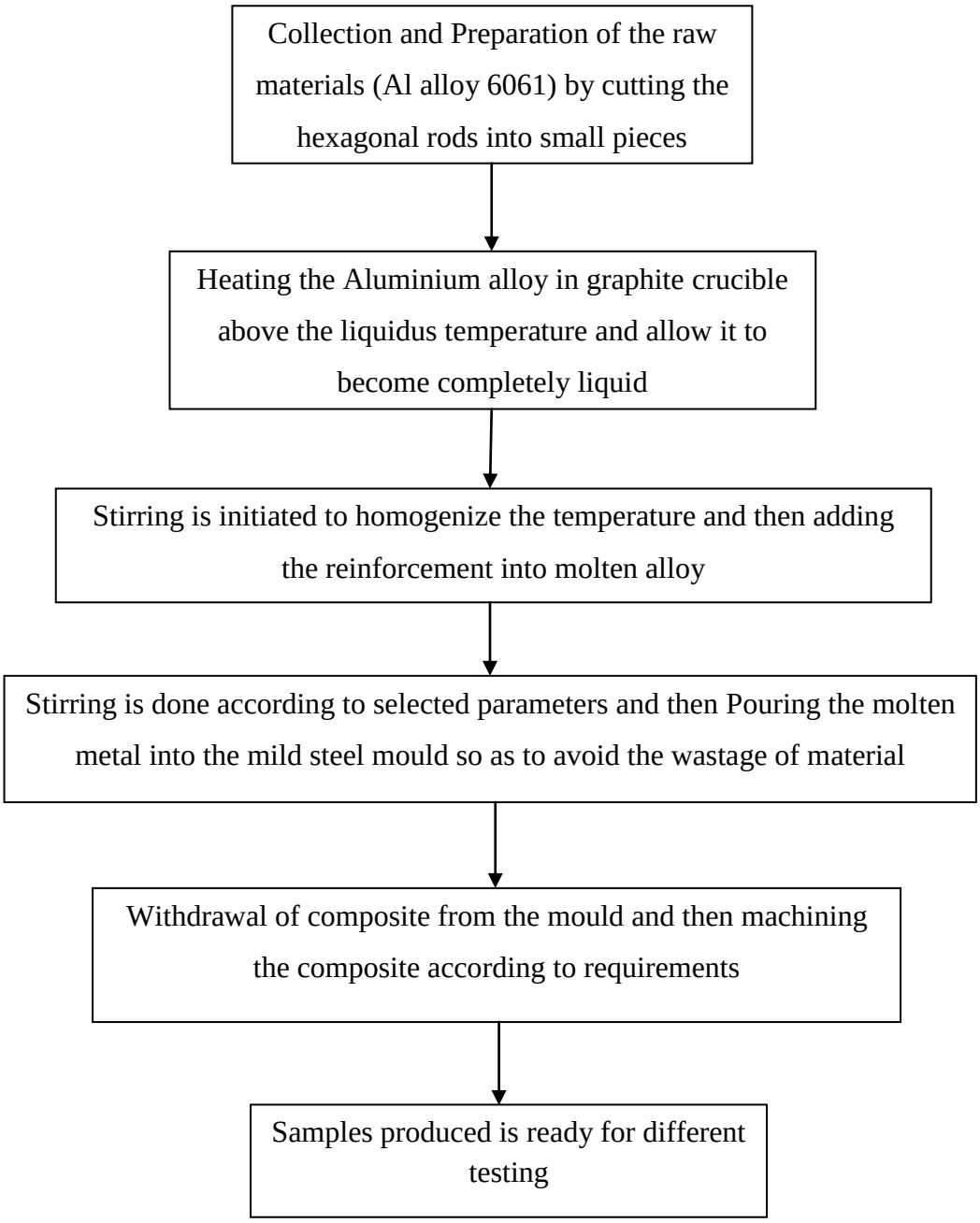

Figure 4.2- Flow Chart Showing Steps in Involved in Stir Casting

4.4 SYNTHESIS OF Al ALLOY 6061 WITH RED MUD, SILICON CARBIDE AND ALUMINIUM OXIDE COMPOSITES

A brief description of the raw material as well as reinforcement materials used in synthesis of composites is as follows:

4.4.1 Matrix Alloy

Aluminium alloy 6061 was used as matrix in the synthesis of composite. Aluminium alloy was taken from the Hindalco Industries Limited, in the form of hexagonal rod and then cut into smaller pieces with the help of power hacksaw in order to keep the alloy inside the crucible properly.

Composition of matrix alloy was analyzed and the chemical composition of the matrix alloy is given in Table 4.1.

Table 4.1- Chemical Composition of Al6061 alloy

Element	Si	Fe	Mn	Mg	Cu	Zn	Ti	Cr	Al
Wt%	0.76	0.14	0.29	0.84	0.33	0.004	0.02	0.006	97.61

4.4.2 Reinforcement Material

Red Mud, silicon carbide (SiC) and Alumina (Al_2O_3) was used as reinforcement material. Initially red mud was received in solid form like small stones then these solid particles were crushed and grinded in the mixer grinder in order to achieve the required particle size of Red Mud i.e. range varies between 103-150 µm. This is achieved with the help sieve shaker. SiC and Al_20_3 was already in the form of powder whose size varies between 60– 90 µm and 30- 50 µm. The reinforced particles of different size was shown in the Table 4.2

Table 4.2- Particle size range of Red Mud, SiC and Al_2O_3 [1, 4, 11]

Reinforcement	**Particle size range (μm)**
Red Mud	103- 150
Silicon Carbide (SiC)	60- 90
Alumina (Al_2O_3)	30- 50

4.5 Al BASED MMC PREPARATION BY STIR CASTING ROUTE

A stir casting setup as shown in Figure 4.3, Consisted of a resistance Muffle Furnace and a stirrer assembly, was used to synthesize the composite. The stirrer assembly consisted of a graphite stirrer, which was connected to a variable speed vertical drilling machine with range of 80 to 890 rpm by means of a steel shaft. The stirrer was made by cutting and shaping a graphite block to desired shape and size manually. The stirrer consisted of three blades at an angle of 120° apart. Figure 4.5- 4.7 shows the photograph of the stirrer, mould and crucible. Clay graphite crucible of 1.5 Kg capacity was placed inside the furnace. The graphical representation of stir casting was shown in Figure 4.3.

Approximately 1Kg of alloy in solid form (hexagonal rod) was melted at 820°C in the resistance furnace. Preheating of reinforcement (Red Mud at 400°C, silicon carbide and Alumina at 800°C) was done for one hour to remove moisture and gases from the surface of the particulates. The reinforcement particles were sieved by sieve shaker as shown in Figure 4.4. The stirrer was then lowered vertically up to 3 cm from the bottom of the crucible (total height of the melt was 9 cm). The speed of the stirrer was gradually raised to 800 rpm and the preheated reinforced particles were added with a spoon at the rate of 10- 20g/min into the melt [4, 5].

The speed controller maintained a constant speed of the stirrer, as the stirrer speed got reduced by 50-60 rpm due to the increase in viscosity of the melt when particulates were added into the melt. After the addition of reinforcement, stirring was continued for 8 to 12 minutes for proper

mixing of prepared particles in the matrix. The melt was kept in the crucible for approximate half minute in static condition and then it was poured in the mould.

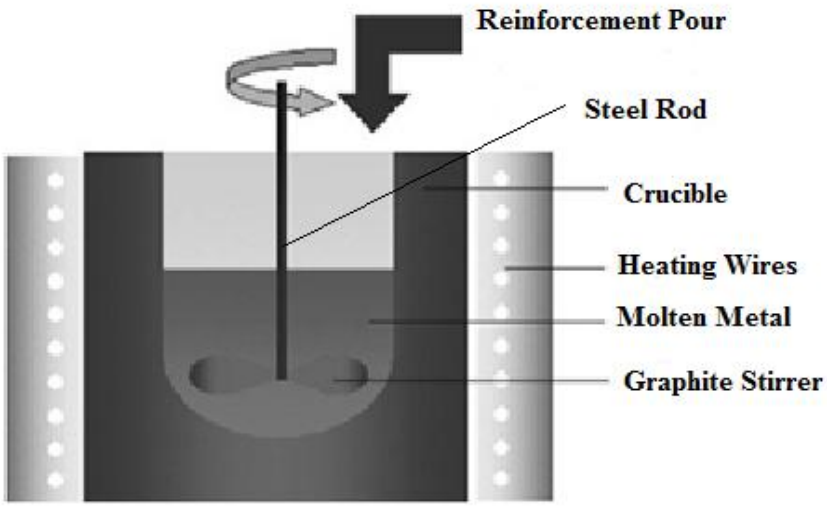

Figure 4.3- Graphical representation of Stir Casting [3]

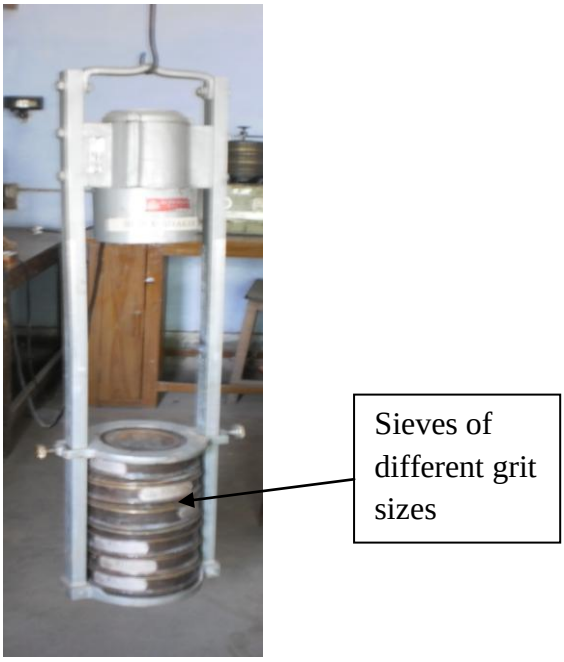

Figure 4.4- Sieve Shaker

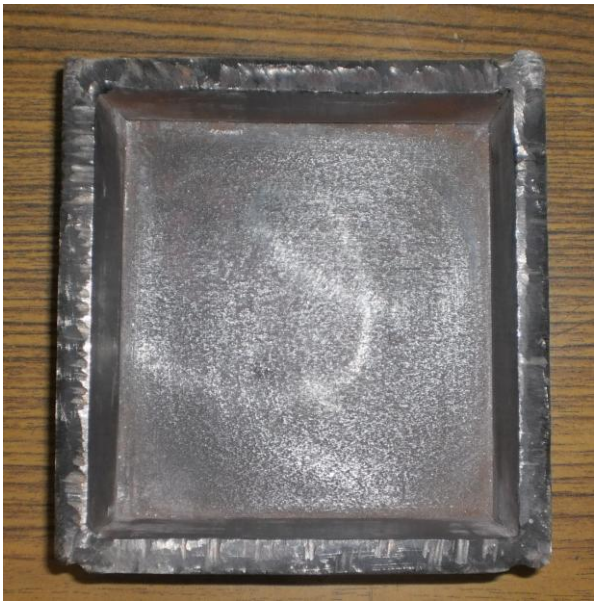

Figure 4.5- Mould (Mild Steel)

Figure 4.6- Crucible (Graphite)

Figure 4.7- Graphite stirrer

Figure 4.8- Stir casting set up

Figure 4.9- Muffle Furnace

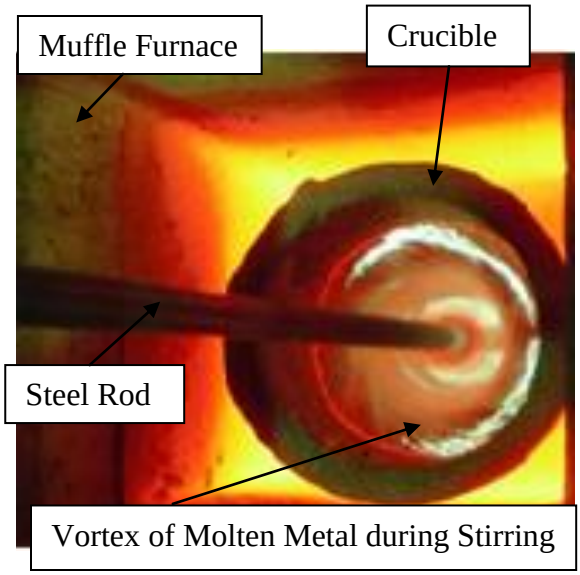

Figure 4.10- Preparation of Samples in Muffle furnace

4.6 SPECIMEN PREPARATION FROM BASE METERIAL TO POLISHED SAMPLES (MMC)

Matrix Al alloy 6061 (Extrusion form)

Synthesis of Al alloy with Red Mud, SiC and Al_2O_3 composites using Stir casting route

Centre Lathe

Sample preparation for Wear Testing

Pin (50X8 mm)

Sample Preparation for Micro- Hardness, Micro-structure, XRD and SEM

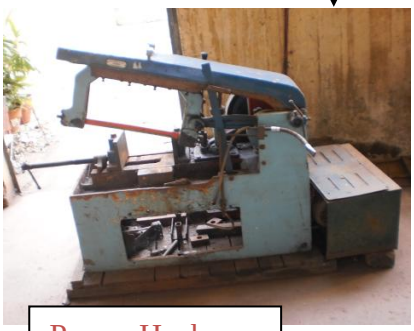

Power Hacksaw

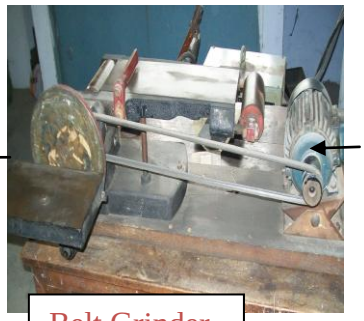

Belt Grinder

Figure 4.11- Specimen Preparation from Base Material to polished samples

4.7 IMPORTANT PARAMETERS USED IN STIR CASTING [5]

Synthesis of composite was done by stir casting route. The parameters used in this work were stirrer design, preheating temperature for particulate and stirring speed and time. These parameters are discussed below:

(i) Particulate Preheating Temperature

Preheating of particulate is necessary to avoid moisture from the particulate otherwise chances of agglomeration of particulate occurs due moisture and gases. The red mud was preheated in a furnace up to 400^{o}C and maintained at that temperature before mixing with Aluminium melt. Along this SiC and Al_2O_3 particles were heated at 800ºC to form a oxide layer on the SiC and Al_2O_3 particles which make it chemically more stable and by the oxide layer formation wet ability will increase so particles will effectively embedded in aluminium matrix and will result in less number of porosities in casting.

(ii) Stirring Speed

In stir casting process stirring speed is very important parameter for consideration. In the process stirring speed was 540 rpm which was effectively producing vortex without any spattering [3]. Stirring speed is decided by fluidity of metal if metal having more fluidity then stirring speed will be low. It is also found that at less speed, dispersion of particulates is not proper because of ineffective vortex.

(iii) Stirrer Design

It is also one of the important parameter for stir casting process. It is essentially requires for vortex formation for the uniformly dispersion of particles. There is different type of stirrer some 90º form the shaft and some are bent at 45º. There is a no uniform dispersion of particles in case of no vortex formation.

4.8 MATERIAL CHARRACTERIZATION

Micro hardness was measured with the help of micro hardness tester .Wear rate was calculate with the help of volume loss technique.

4.8.1 Microhardness Measurement

Micro hardness testing is a method for measuring the hardness of a material on a microscopic scale. Micro hardness was calculated by using MVH-II digital micro hardness tester as shown in Figure 4.12. A precision diamond indenter is impressed into the material at loads from a few grams to 1 kilogram. The impression length, measured microscopically, and the applied load are used to calculate a hardness value as shown in Figure 4.13.

The indentations are typically made using either a square-based pyramid indenter (Vickers hardness scale) or an elongated, rhombohedral-shaped indenter. The tester applies the selected test load using dead weights. The length of the hardness impressions was precisely measured with a light microscope using either a filar eyepiece or a video image and computer software. A hardness number is then calculated using the test load, the impression length, and a shape factor for the indenter type used for the test [3].

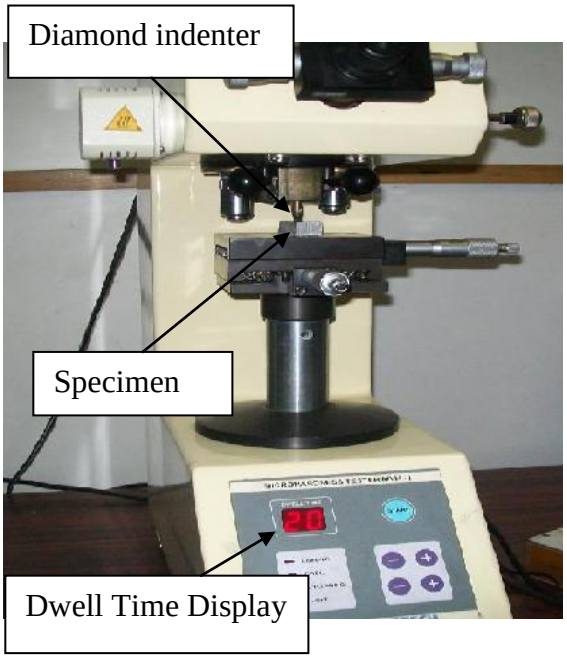

Figure 4.12- Vicker's Microhardness Tester

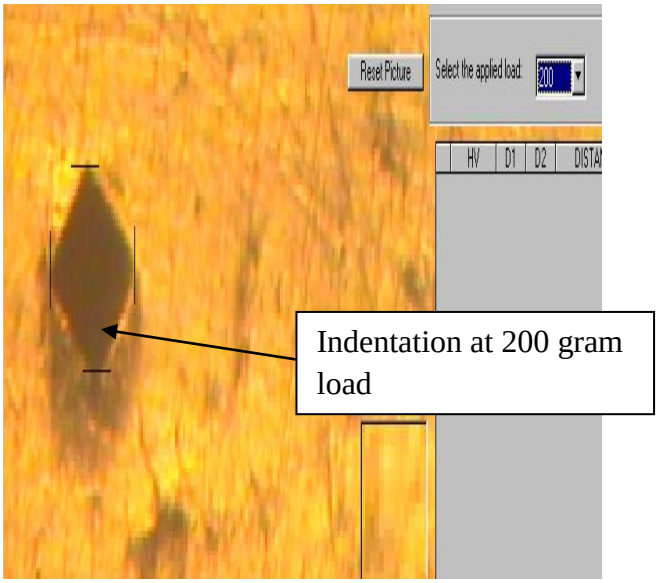

Figure 4.13- Micro indentation at 10X optical zoom

4.8.2 Wear Testing Measurement

4.8.2.1 Sliding Wear

Wear is a process of removal of material from one or both of two solid surfaces in solid state contact. As the wear is a surface removal phenomenon and occurs mostly at outer surfaces, it is more appropriate and economical to make surface modification of existing alloys than using the wear resistant alloys.

4.8.2.2 Experimental procedure of wear test

Dry sliding wear tests for different number of specimens was conducted by using a pin-on-disc machine (Model: Wear & Friction Monitor TR-20) supplied by DUCOM, was shown in Figure 4.14.

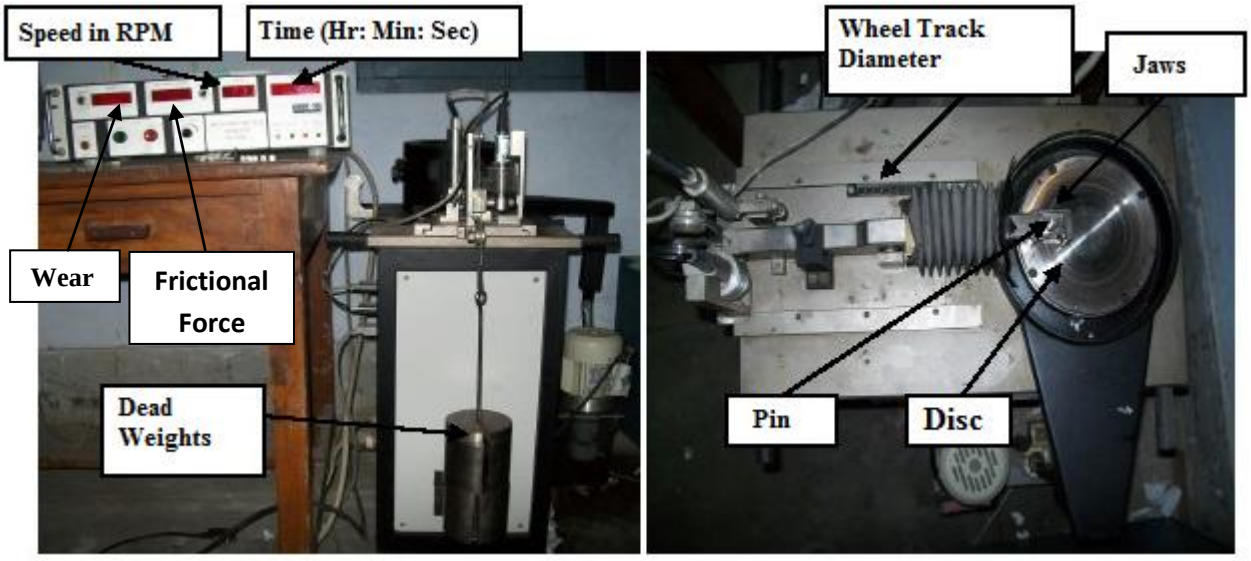

Figure 4.14- Wear Testing Machine

The pin was held against the counterface of a rotating disc (EN32 steel disc) with wear track diameter 60mm. The pin was loaded against the disc through a dead weight loading system. The wear test for all specimens was conducted under the normal loads of 2kg and a fixed sliding velocity of 1.6 m/s. Wear tests were carried out for a total sliding distance of approximately 2900 m under similar conditions as discussed above. The pin samples were 50 mm in length and 8 mm in diameter. The surfaces of the pin samples was slides using emery paper (80 grit size) prior to test in ordered to ensure effective contact of fresh and flat surface with the steel disc. The

samples and wear track were cleaned with acetone and weighed (up to an accuracy of 0.0001 gm using microbalance) prior to and after each test. The wear rate was calculated from the height loss technique and expressed in terms of wear volume loss per unit sliding distance.

In this experiment the test was conducted with the following parameters:

(1) Load

(2) Speed

(3) Time

In the present experimental, the parameters such as speed, time and load kept constant through out for all the experiments. These Parameters are given in Table 4.3.

Table 4.3- Parameter taken constant during sliding wear test

Load	2 kg
Speed (V)	1.6 m/s
Total Time	30 min

4.8.2.3 Pin-on-disc test:

In this study, Pin-on-Disc testing method was used for tribological characterization. The test procedure is as follows:

- Initially, pin surface was made flat such that it will support load over its entire cross-section called First Stage. This was achieved by the surfaces of the pin sample ground using emery paper (80 grit size) prior to test.
- Run-in-wear was performed in the next stage/ Second stage. This stage avoids initial turbulent period associated with friction and wear curves.
- Final stage/ Third stage is the actual testing called constant/ steady state wear. This stage is the dynamic competition between material transfer processes (transfer of material from pin onto disc and formation of wear debris and their subsequent removal). Before the test, both the pin and disc were cleaned with ethanol soaked cotton [12, 13, 14].

Before the start of each experiment, precautionary steps were taken to make sure that the load applied was in normal direction. Figure 4.15 represents a schematic view of Pin-on-Disc set up.

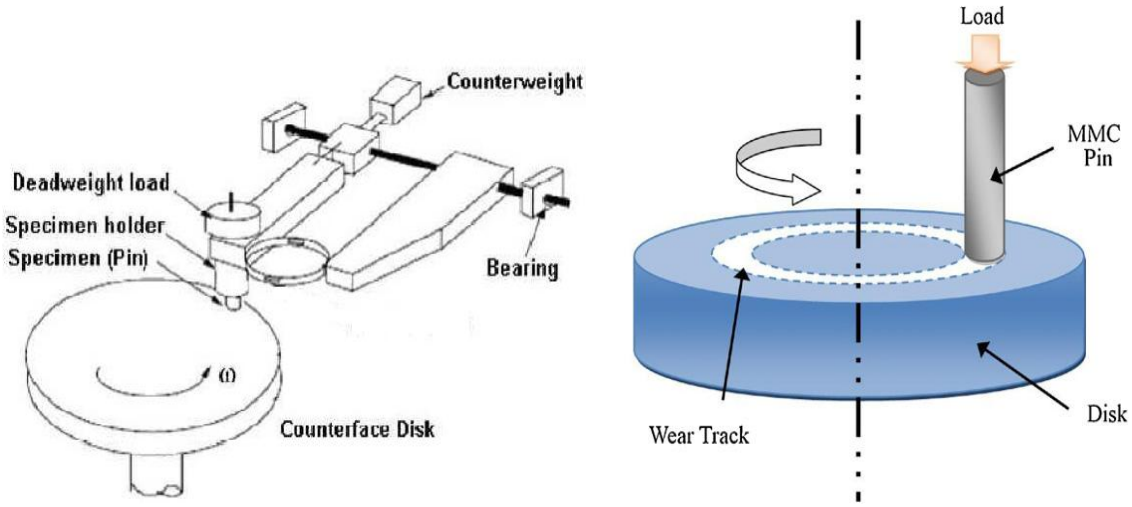

Figure 4.15- Schematic views of the pin-on-disk apparatus [5]

4.9 CHARACTERIZATION TECHNIQUE

Particles distribution was evaluated with the help of optical microscope. XRD studies were carried out to confirm the presence of reinforcement in the alloy matrix. Scanning electron microscopy of the specimens was studied.

4.9.1 Optical Microscopy

The casting procedure was examined under the optical microscope to determine the reinforcement pattern and cast structure. A section was cut from the castings. They were grinded using 100 grit silicon carbide paper followed by 220, 400, 600 and 1000 grades of emery paper. Before optical observation the samples were mechanically polished and etched by Keller's reagent to obtain better contrast.

Figure 4.16- Optical microscope

CHAPTER 5 RESULTS AND DISCUSSIONS

MICROSCOPIC BEHAVIOUR:

5.1 MICRO HARDNESS MEASUREMENT

A micro hardness tester MVH-1is used for the micro hardness measurement. The surface being tested generally requires a metallographic finish and it was done with the help of 100, 220, 400, 600 and 1000 grit size emery paper. Load used on Vicker's micro hardness tester was 200 grams at 10X optical zoom with dwell time 20 seconds for each sample.

The result of Vicker's Micro hardness test for alloy 6061 without reinforcement (Sample No.1) and the wt.% variation of different reinforcements such as SiC, Al_2O_3 and Red Mud in Al alloy 6061 MMCs (Sample No. 2-13) are shown in Table 5.1.

Table 5.1- Micro hardness Measurement

Sample No.	Sample Name (Al alloy 6061+)	Mean Micro Hardness No. (VHN)
1	Pure (Base Alloy)	49.7431675
2	2.5% Sic	57.30065
3	5% SiC	65.7694
4	7.5% SiC	92.7731
5	10% SiC	100.206025
6	2.5% Al_2O_3	90.45515
7	5% Al_2O_3	99.4015
8	7.5% Al_2O_3	109.699925
9	10% Al_2O_3	110.8675
10	2.5 % Red Mud	60.2283575
11	5% Red Mud	76.6930125
12	7.5% Red Mud	114.2908
13	10% Red Mud	104.01875

5.1.1 Bar Charts showing the trend of micro hardness of alloy and different MMCs

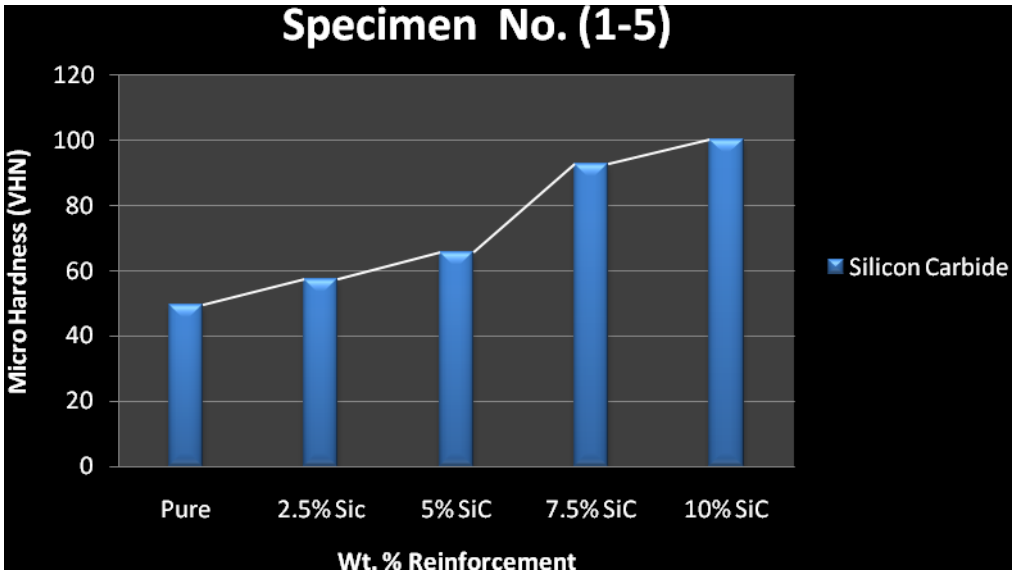

Figure 5.1- Comparison the Microhardness of alloy and MMCs with wt. % variation of SiC

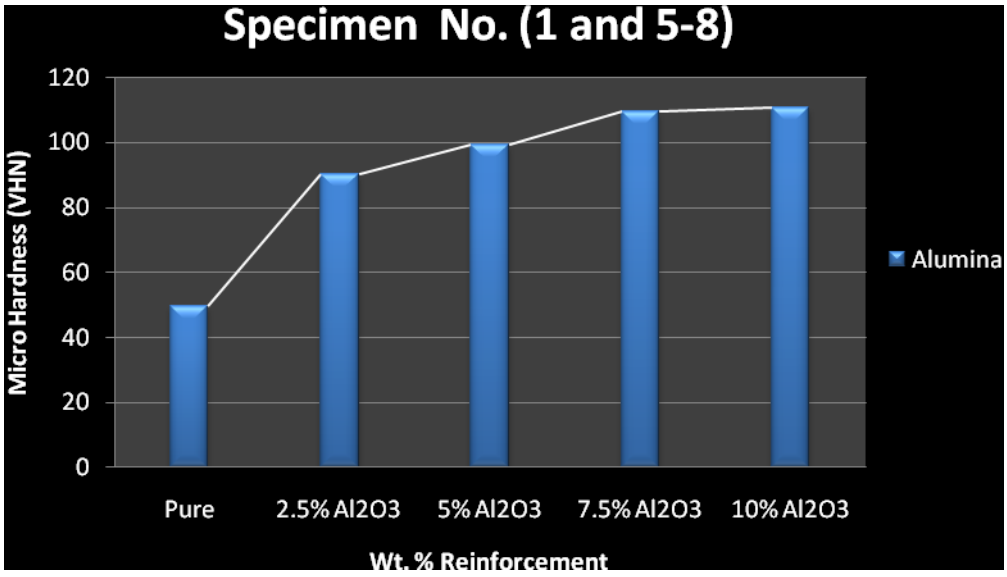

Figure 5.2- Comparison the Microhardness of alloy and MMCs with wt. % variation of Al_2O_3

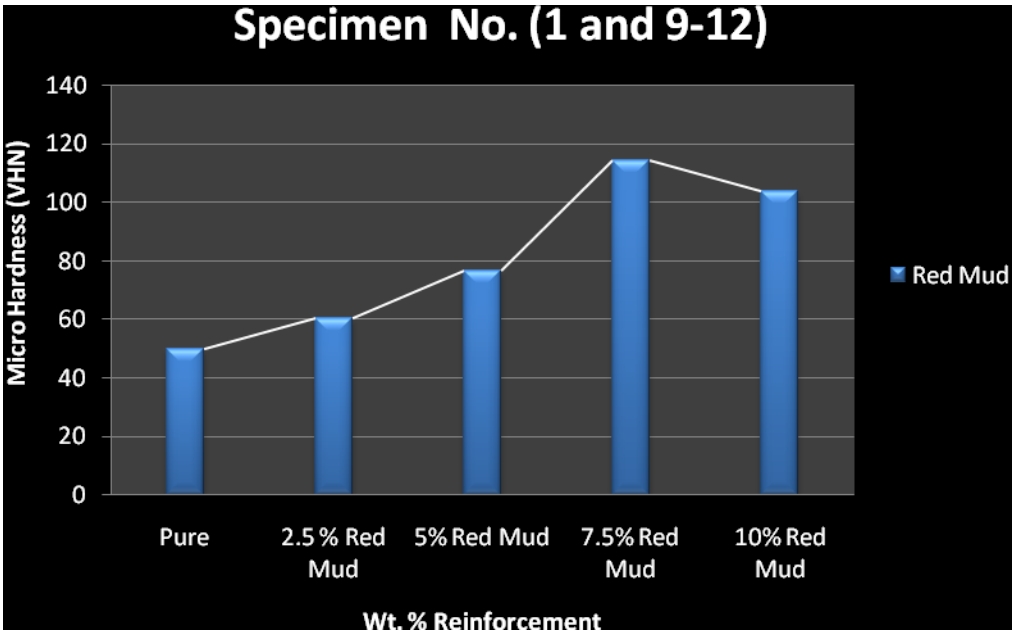

Figure 5.3- Comparison the Microhardness of alloy and MMCs with wt. % variation of Red Mud

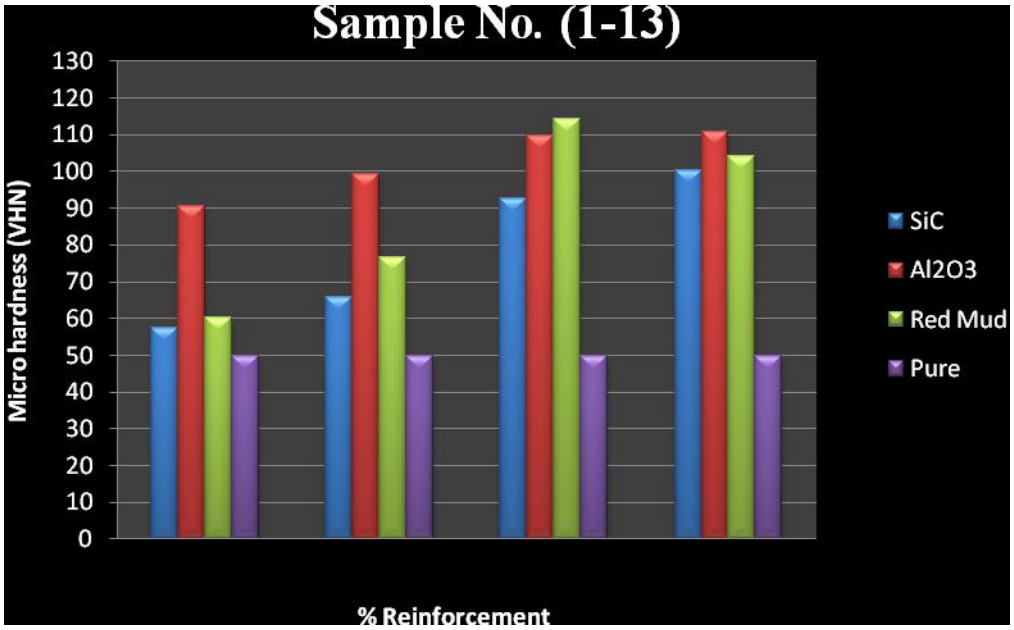

Figure 5.4- Comparison the Micro hardness of alloy and all different MMCs

5.1.2 Result and discussion of Micro-hardness number of samples (1-13):

Figure 5.1- 5.4 shows the micro hardness of Al alloy and Al based MMCs reinforced with SiC, Al_2O3 and Red Mud. It is observed that hardness of alumina and Red Mud reinforced composite is more than that of SiC reinforced composite. It can be attributed to the higher hardness of red mud and alumina compared to SiC particles.

Hardness of composite depends on the hardness of the reinforcement and the matrix. As the Coefficient of thermal expansion (CTE) of ceramic particles (SiC: 4.03µm/m°C, Al_2O3: 8.103µm/m°C) is less than that of aluminium alloy 6061 (24.3µm/m°C), an enormous amount of dislocations are generated at the particle–matrix interface during solidification process, which further increases the matrix hardness. The higher the amount of particle–matrix interface, the more is the hardening due to dislocations. Smaller ceramic particle reinforced composite have more particle–matrix interface as in case of alumina reinforcement compared to larger particle reinforced (red mud, SiC) composite for same amount. Hence, the hardness of the composite increases with the decrease in particle size and increase the volume fraction of the reinforcement. These results are analogous to Abrasive wear of zircon sand and alumina reinforced Al–4.5 wt% Cu alloy matrix composites – A comparative study observed by Sanjeev Das, Siddhartha Das and Karabi Das [14].

From the graphs (Figure 5.1 and 5.2) it is clear thar as the reinforcement percentage increses the microhardness also increses.

But in the case of Red Mud reinforcement (Figure 5.3) the value of microhardness increses upto 7.5 wt. % then decreses. The reason for this may be either the improper mixing due to high viscosity of molten composites or poor interfacial bonding beween the the particle– matrix interfaces .

From the Figure 5.4 it is clearly shows that the maximum value of micro hardness number amongs the MMCs for sample number 9 (Al alloy 6061 + 7.5% Red Mud) which is approximately double from the sample number 1 (Al alloy 6061 + 2.5% SiC) and mimimum value of micro hadrness number amongs the MMCs for ample number 1 (Al alloy 6061 + 2.5% SiC) which is still heiger than sample number 13 (Al alloy 6061).

MACROSCOPIC BEHAVIOUR

5.2 EFFECT OF DIFFERENT REINFORCEMENTS ON WEIGHT LOSS OF MMCs UNDER DRY SLIDING CONDITION

A pin-on-disc tribometer is used to perform the wear experiment. The wear track, alloy and composite specimens are cleaned thoroughly with acetone prior to test. Each specimen is then weighed using a digital balance having an accuracy of ±0.0001 gm. After that the specimen is mounted on the pin holder of the tribometer ready for wear test. For all experiments, the sliding speed is adjusted to 1.6 m/s, track diameter 60mm, load 2kg and total time is 30 minute under room temperature.

Table 5.2- Weight loss of Sample no. (1-13) under dry sliding condition

Length (mm)	**Diameter (mm)**	**Velocity (m/s)**	**Track Diameter (mm)**	**Weight (Kg)**	**Time (Sec)**
50	8	1.6	60	2	1800

Sample No.	**Specimen Name** **Al alloy 6061+**	**Initial Weight (gm)**	**Final Weight (gm)**	**Weight Loss(gm)**
1	2.5% Sic	6.71898	6.70330	0.01568
2	5% SiC	6.86166	6.84660	0.01506
3	7.5% SiC	6.62918	6.61820	0.01098
4	10% SiC	6.30940	6.29884	0.01056
5	2.5% Al_2O_3	5.84633	5.82111	0.02522
6	5% Al_2O_3	6.16840	6.15064	0.01776
7	7.5% Al_2O_3	5.50940	5.49290	0.01650
8	10% Al_2O_3	5.89106	5.87688	0.01418
9	2.5 % Red Mud	6.15920	6.13370	0.0255
10	5% Red Mud	5.82509	5.80113	0.02396
11	7.5% Red Mud	6.17206	6.15246	0.0196
12	10% Red Mud	5.71050	5.68728	0.02322
13	Base alloy (Al alloy 6061)	6.64630	6.62088	0.02542

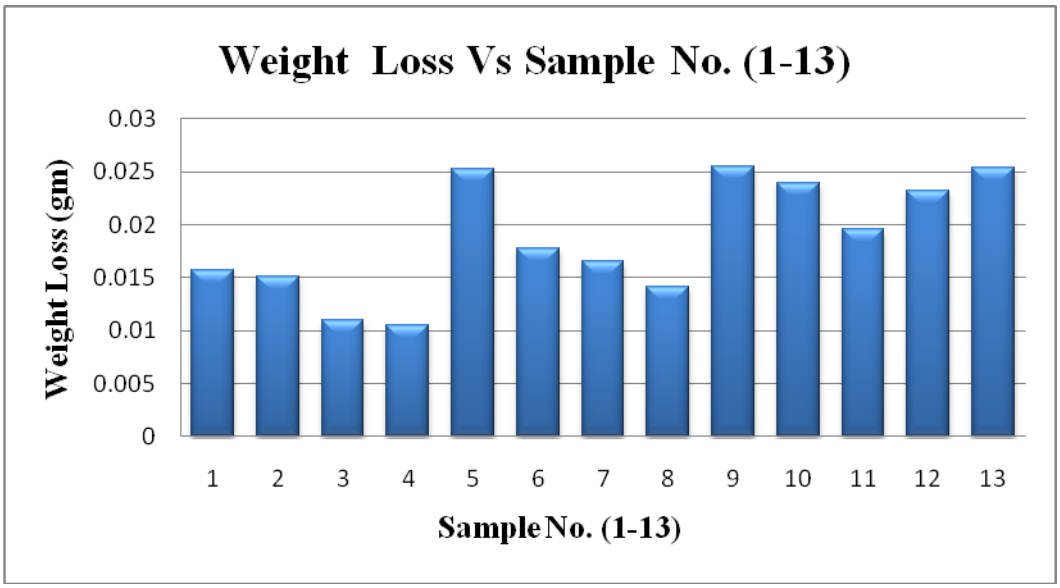

Figure 5.5- Weight Loss of alloy and composites

5.2.1 Result and discussion of graph between the Weight loss and MMCs:

As shown in Bar Chart (Figure 5.5) results predict that as the reinforcement wt.% increses, the weight loss of MMCs decreases.

But in the case of red mud reinforcement, the weight loss decrease upto 7.5 wt.% then increses. This happens may be due to either the improper dispersion of red mud into the matrix due to high viscosity of molten composites or weak interfacial bonding in between the Al alloy 6061 and red mud interfaces.

Comparing the weight loss properties of composites reinforced with silicon carbide, alumina and red mud, it is observed that despite their higher hardness, composites reinforced with alumina and red mud particles show greater weight loss as compared to composites reinforced with SiC particles. It can be attributed to the comparatively poor bonding between red mud-matrix and in alumina-matrix. There might be particle pull out, in the case of composite reinforced alumina and red mud particles during wear test, which enhances weight loss.

It is clear from Figure 5.5, the maximum weight loss for Sample No. 9 (Al alloy 6061 + 2.5% Red Mud) and minimum weight loss for Sample No.4 (Al alloy 6061 + 10% SiC).

5.3 SLIDING WEAR LOSS AND WEAR RATE PERFORMANCE OF DIFFERENT SPECIMENS WITH AND WITHOUT REINFORCEMENT INTO THE MATRIX (1-13) UNDER DRY SLIDING CONDITION AT AMBIENT TEMPERATURE

A pin-on-disc apparatus was used to perform the wear experiment. The wear track, alloy and composite specimens are cleaned thoroughly with acetone prior to each test. After that the specimen is mounted on the pin holder of the tribometer ready for wear test. For all experiments, the sliding speed is adjusted to 1.6 m/s, wear track diameter 60mm, load 2kg and total time is 30 minute.

5.3.1 Wear loss of the MMCs of sample number 1-12 and sample number 13 for aluminium alloy 6061 (pure) is shown in Table 5.3.

Table 5.3- Wear loss of MMCs and alloy Vs Time

Time (seconds) / **Wear loss (µm)**	**300**	**600**	**900**	**1200**	**1500**	**1800**
Sample 1(alloy + 2.5% SiC)	75.75	107.21	136.70	166.24	195.92	222.73
Sample 2 (alloy + 5% SiC)	67.85	96.79	113.55	130.80	146.75	167.59
Sample 3 (alloy + 7.5% SiC)	42.58	64.08	87.22	106.8	125.13	145.31
Sample 4 (alloy + 10% SiC)	38.31	57.99	78.86	101.57	101.57	140.38
Sample 5 (alloy + 2.5% Al_2O_3)	106.38	140.48	170.43	201.33	229.99	257.79
Sample 6 (alloy + 5% Al_2O_3)	102.75	144.87	171.64	193.91	224.99	262.86
Sample 7 (alloy + 7.5% Al_2O_3)	78.48	124.67	159.76	199.03	228.99	255.7
Sample 8 (alloy + 10% Al_2O_3)	66.91	100.93	131.48	163.01	193.39	218.24
Sample 9 (alloy + 2.5% RM)	64.88	132.98	189.86	235.48	281.78	308.5

Sample 10 (alloy + 5% RM)	138.55	163.41	189.14	215.17	243.84	270.19
Sample 11 (alloy + 7.5% RM)	44.24	78.68	124.76	174.44	217.43	269
Sample 12 (alloy + 10% RM)	88.2	129.77	174.54	227.77	266.96	302.99
Sample 13 (alloy)	68.98	142.66	192.01	232.02	268.04	302.2

5.3.1.1 Graphs showing the trend of Wear Performance of different MMCs and alloy with Time:

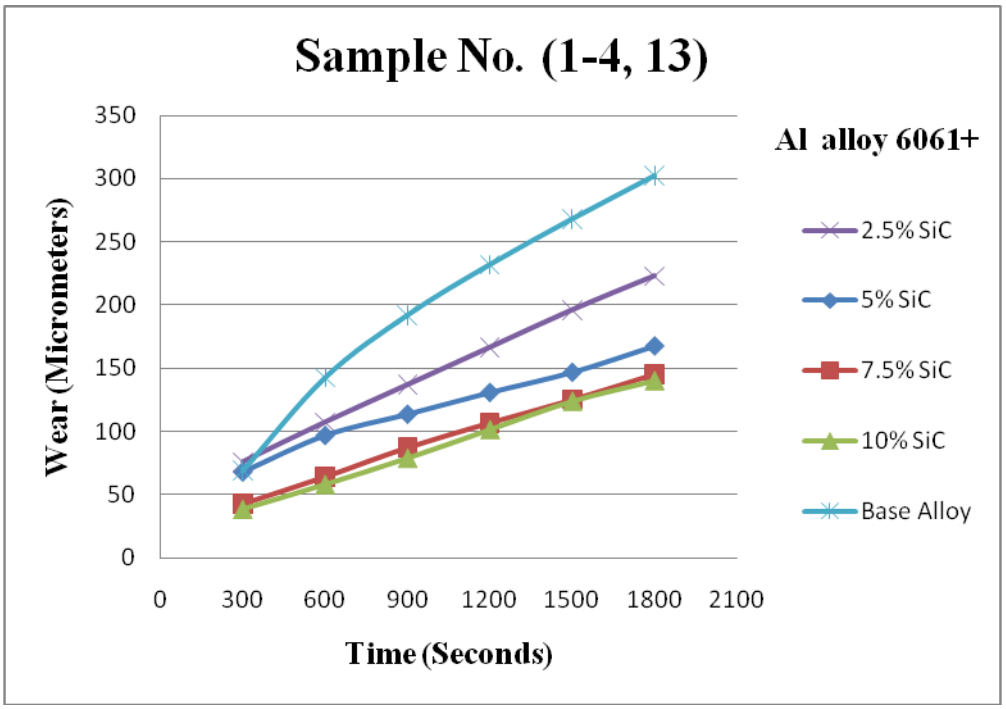

Figure 5.6- Wear in Micrometers Vs Time in seconds of Samples (1-4, 13)

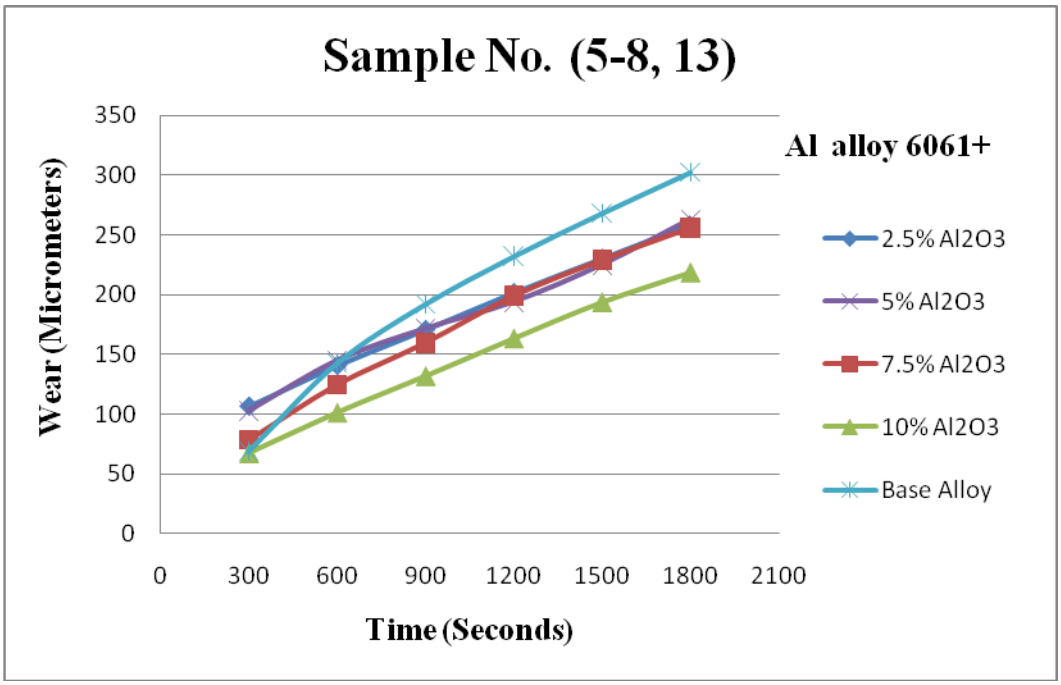

Figure 5.7- Wear in Micrometers Vs Time in seconds of Samples (5-8, 13)

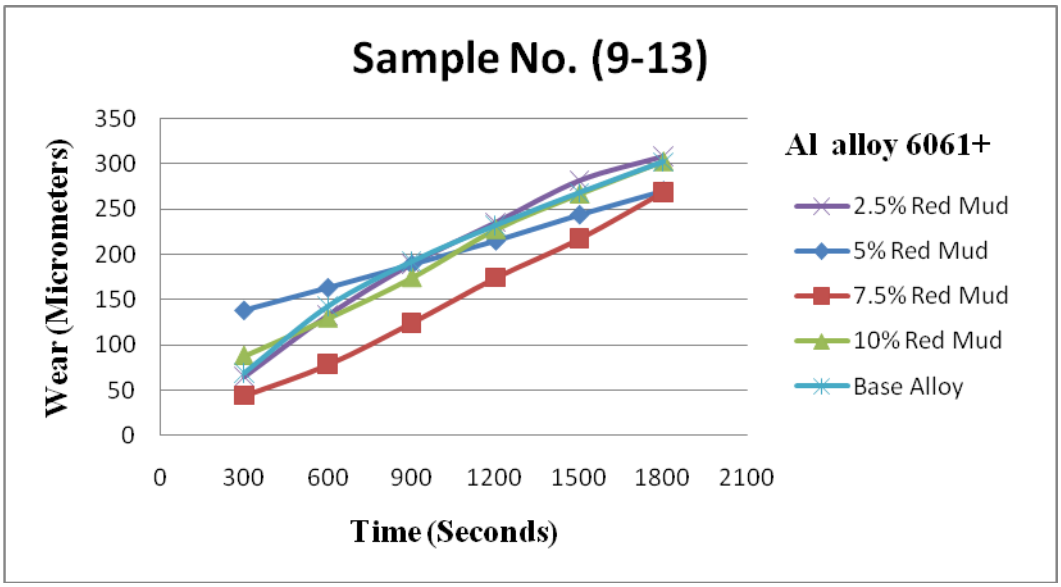

Figure 5.8- Wear in Micrometers Vs Time in Seconds of Samples (9-13)

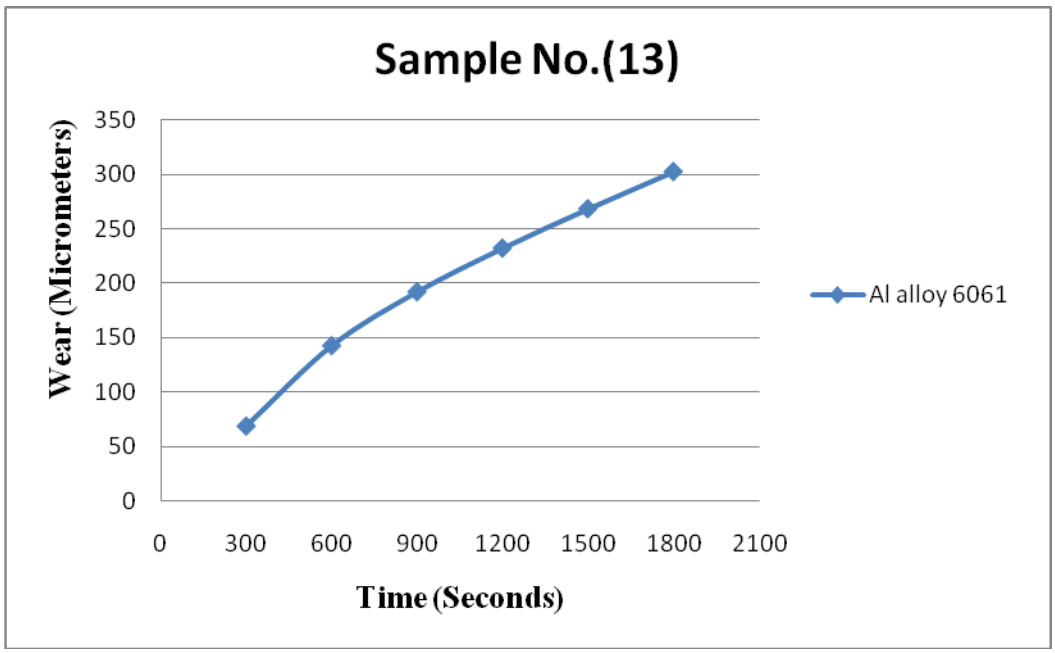

Figure 5.9- Wear in Micrometers Vs Time in Seconds of Sample (13)

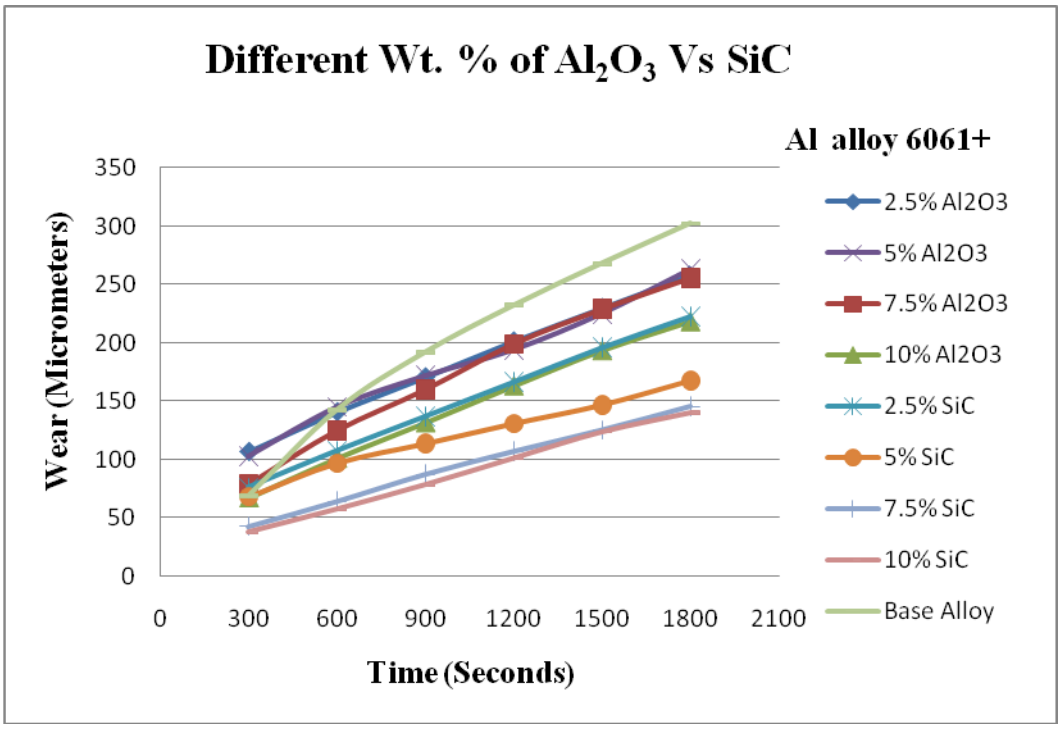

Figure 5.10- Wear in Micrometers Vs Time in Seconds of Samples (1-8, 13)

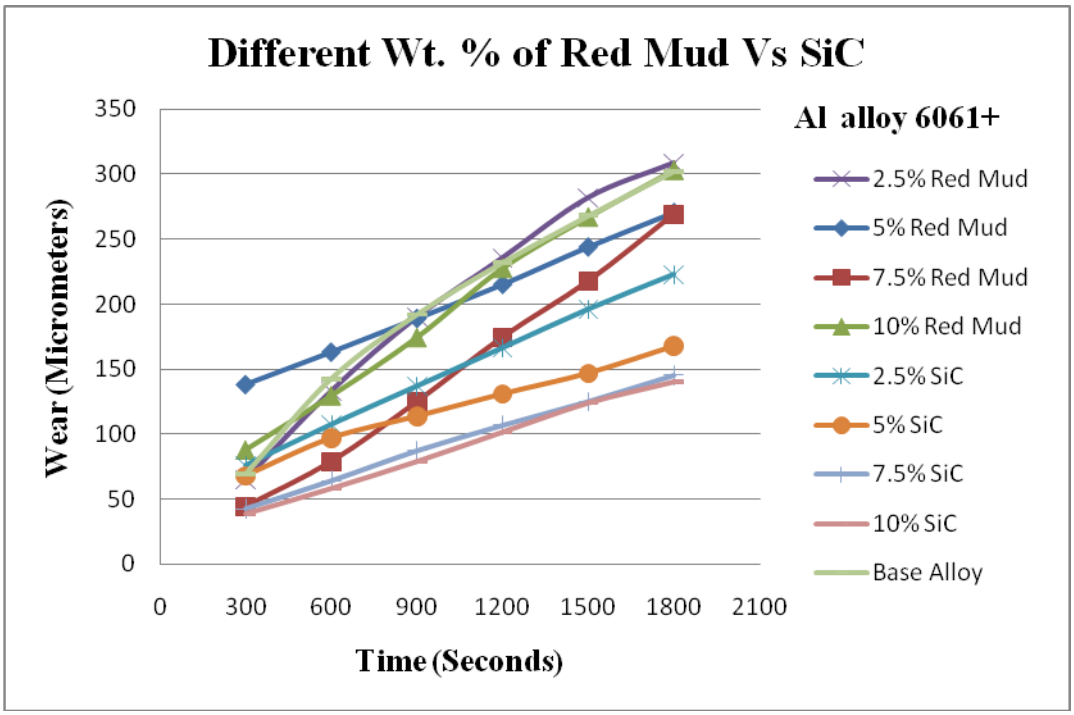

Figure 5.11- Wear in Micrometers Vs Time in Seconds of Samples (1-4 and 9-13)

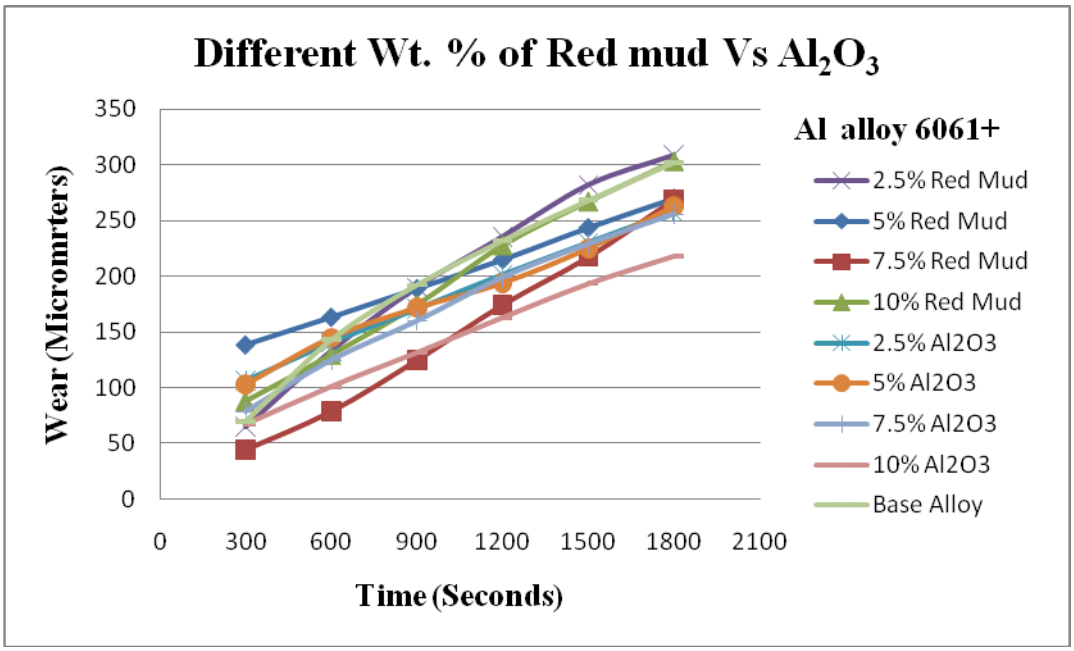

Figure 5.12- Wear in Micrometers Vs Time in Seconds of Samples (5-13)

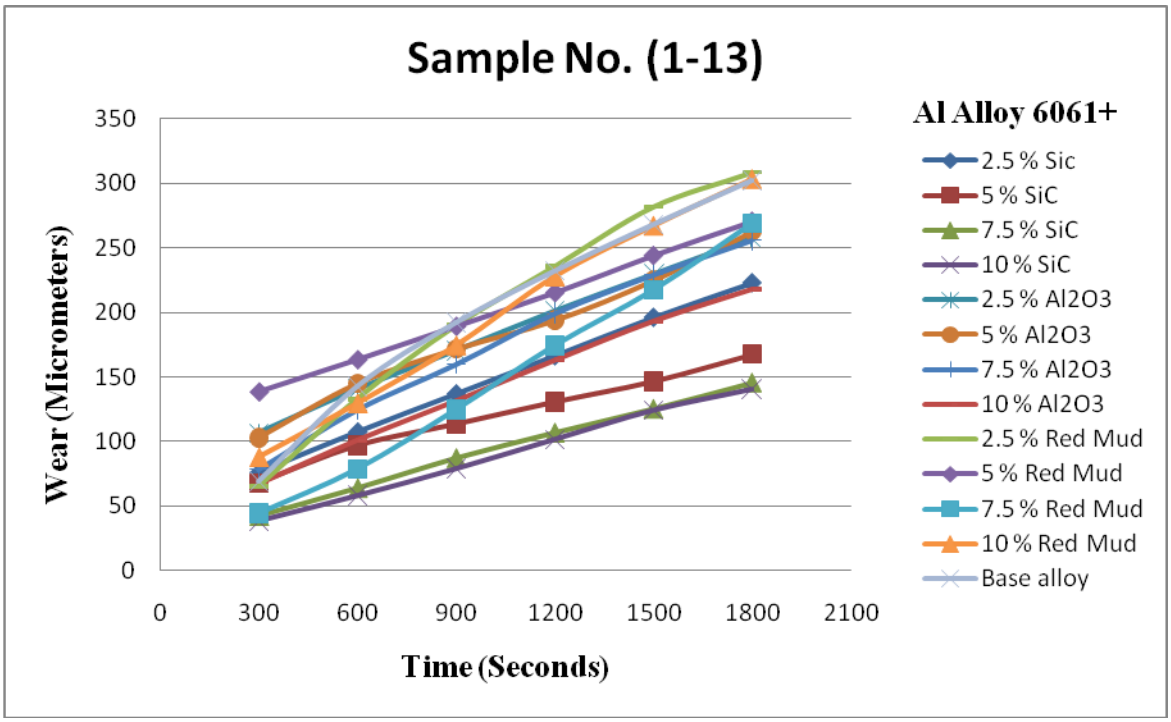

Figure 5.13- Wear in Micrometers Vs Time in Seconds of Samples (1-13)

5.3.1.2 Result and discussion of graphs between wear loss and time:

Figure 5.13 shows the wear loss (commutative wear height loss) as a function of time for the Al alloy 6061 and composites reinforced with silicon carbide, alumina and red mud particles of different size ranges (60- 90 µm, 30-50 µm and 103- 150 µm) at a constant load of 20 N and total time is 30 minute. It is observed that wear loss of Al alloy 6061 decreases after addition of SiC, Al_2O_3 and red mud particles. It can be attributed to the increase in hardness of the material due to the presence of hard ceramic particles. Material removal in a ductile material such as aluminium alloy matrix is due to the indentation and ploughing action of the sliding disc which is made from hard steel material (EN32 steel disc). Incorporation of hard silicon carbide, aluminium oxide and red mud particles in the Al alloy 6061 restricts such ploughing action of hard steel counterpart and improves the wear resistance.

Comparing the wear properties of composites reinforced with silicon carbide, alumina and red mud, it is observed that despite their higher hardness, composites reinforced with alumina and red mud particles show poor wear resistance as compared to composites reinforced with SiC

particles. It can be attributed to the comparatively poor bonding between the red mud-matrix and in alumina-matrix. There might be particle pull out, in the case of composite reinforced alumina and red mud particles during wear test, which enhances wear loss. These results are analogous to Abrasive wear of zircon sand and alumina reinforced Al–4.5 wt% Cu alloy matrix composites – A comparative study observed by Sanjeev Das, Siddhartha Das and Karabi Das [14].

Moreover, the fracture toughness of alumina is inferior compared to SiC, which leads to breakage of alumina particles prior to SiC particles causing an increase in wear loss (Fracture toughness: SiC = 4.6 MPa $m^{1/2}$ [28], Alumina = 3.5 MPa $m^{1/2}$ [29]).

Figure (5.6 to 5.9) shows the variation of wear loss with time (total time is taken to be 30 min) for constant load 2 Kg at 510 rpm. It can be observed from the plots that with addition of SiC, Al_2O_3 and Red Mud Particulates in the matrix the wear loss of composites was decreased. Also as the time increses the wear loss increses.

The results as indicated from Figure 5.6 the decreasing trend of wear loss with increase in weight percentage of SiC up to 10% weight fraction.

Similarly, the results as indicated from Figure 5.7 the decreasing trend of wear loss with increase in weight percentage of Al_2O_3 up to 10% weight fraction.

But the results from Figure 5.8 shows the decreasing trend of wear loss with increase in weight percentage of Red Mud up to 7.5% by weight. Beyond this weight % the wear loss trend started increasing. This is because when red mud is added beyond 7.5% by wt. in the matrix the viscosity of MMC increased and stirrer was not rotated properly, thereby poor interfacial bonding takes place between the red mud and Al alloy matrix.

From the comparison graph i.e. different wt. % of SiC Vs Al_2O_3 in Figure 5.10 shows that 10% SiC has the superior wear resistance property over the other different wt. % of reinforcements in the case of wear loss.

Similarly, from the comparison graph i.e. different wt. % of SiC Vs Red Mud in Figure 5.11 shows that 10% SiC has superior wear resistance property over the other different wt. % of reinforcements in the case of wear loss.

But from the comparison graph i.e. different wt. % of Red Mud Vs Al_2O_3 in Figure 5.12 shows that 7.5% Red Mud has superior wear resistance property over the 7.5% of alumina reinforcement in the case of wear loss. It is clear from the plots that at the same wt. % of red mud and alumina, we can replace alumina by red mud in case of wear loss calculations. Thereby we can save the money and environment up to some amount by utilization of waste residue i.e. red mud.

5.3.2 Sliding Wear Rate performance of different samples with and without reinforcement into the matrix (1-13) at ambient temperature

Wear rate and wear resistance for the MMCs were obtained by:

Wear Rate:- It is defined as wear volume per unit distance travelled [16].

Wear Rate = Wear Volume (mm^3) / Sliding distance (m)

Sliding distance can be calculated as:

Sliding distance = Sliding Speed X Time

$= (\pi D N / 60) t$

Wear Volume= $\pi r^2 h$

Where, D = Diameter of wheel track (60mm),
r= radius of pin (4 mm),
h= commulative wear height loss (mm),
N= R.P.M (510),
ΠI= 3.14 (constant),
t= Time duration in seconds and
V= Sliding Speed (1.6 m/s).

Wear Resistance:- wear resistance is a reciprocal of wear rate.

wear resistance = 1 / wear rate

5.3.2.1 Wear rate of MMCs (sample number 1-12) and Al alloy (sample 13) is shown in Table 5.4.

Table 5.4- Wear rate of MMCs and alloy Vs Sliding Distance

Sliding Distance (m) / **Wear rate $X10^{-3}$ (mm^3/m)**	**500**	**1000**	**1500**	**2000**	**2500**	**3000**
Sample 1(alloy + 2.5% SiC)	7.7742	5.5025	4.755	4.2921	4.0716	3.9014
Sample 2 (alloy + 5% SiC)	6.9822	4.9230	3.9333	3.3814	3.0046	2.9210
Sample 3 (alloy + 7.5% SiC)	4.4500	3.3910	2.9194	2.7913	2.6250	2.5378
Sample 4 (alloy + 10% SiC)	4.0741	3.0055	2.6963	2.6527	2.5345	2.4532
Sample 5 (alloy + 2.5% Al_2O_3)	10.7155	7.1947	5.8094	5.1872	4.7109	4.5122
Sample 6 (alloy + 5% Al_2O_3)	10.4351	7.3611	5.9394	5.0725	4.6791	4.5912
Sample 7 (alloy + 7.5% Al_2O_3)	8.12142	6.4943	5.5803	5.1816	4.7187	4.4628
Sample 8 (alloy + 10% Al_2O_3)	7.0314	5.2639	4.5573	4.2382	3.9646	3.8340
Sample 9 (alloy + 2.5% RM)	13.5954	8.0395	6.6942	6.0082	5.5602	5.6087
Sample 10 (alloy + 5% RM)	14.0122	8.3382	6.4671	5.5008	5.0136	4.7181
Sample 11 (alloy + 7.5% RM)	5.4440	4.6935	4.5838	4.4732	4.2424	4.1593
Sample 12 (alloy + 10% RM)	7.8969	7.4129	6.625	6.2136	5.6657	5.4069
Sample 13 (alloy)	15.2882	8.7967	6.3692	5.0981	4.8193	4.7103

5.3.2.2 Graphs showing the trend of Wear rate Performance of different MMCs and base alloy with Sliding Distance

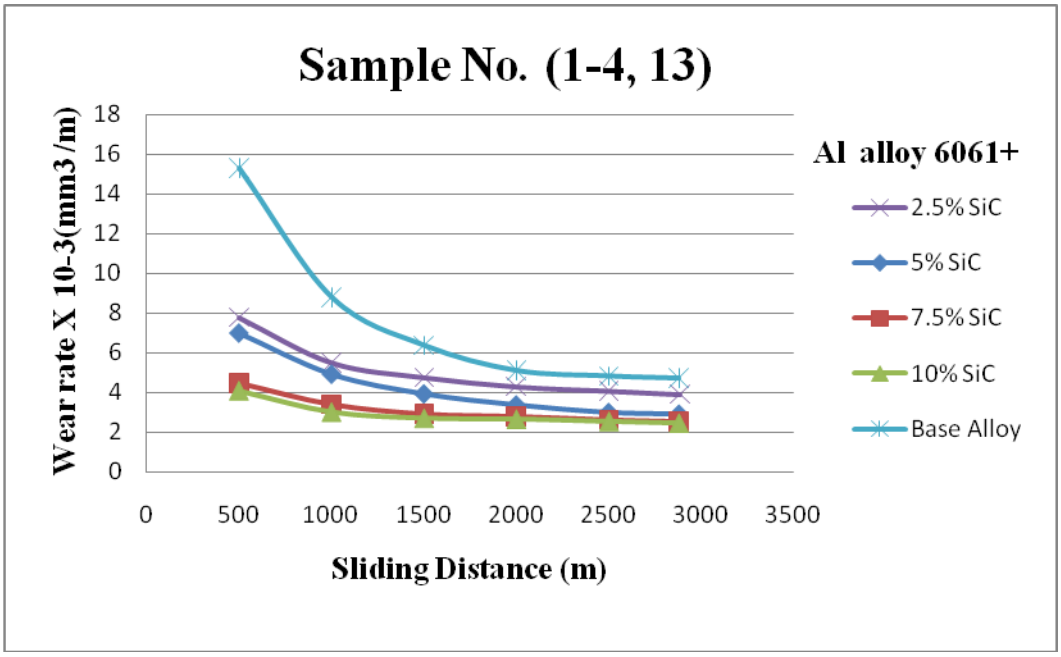

Figure 5.14- Wear rate in 10^{-3} X mm^3/m Vs Sliding Distance in m of samples (1-4, 13)

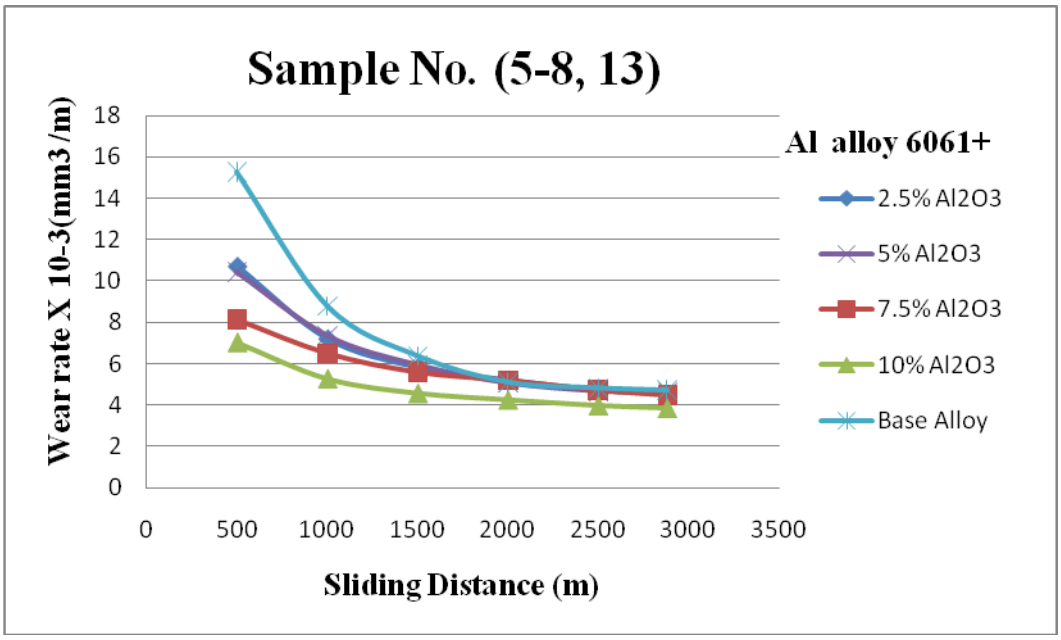

Figure 5.15- Wear rate in 10^{-3} X mm^3/m Vs Sliding Distance in m of samples (5-8, 13)

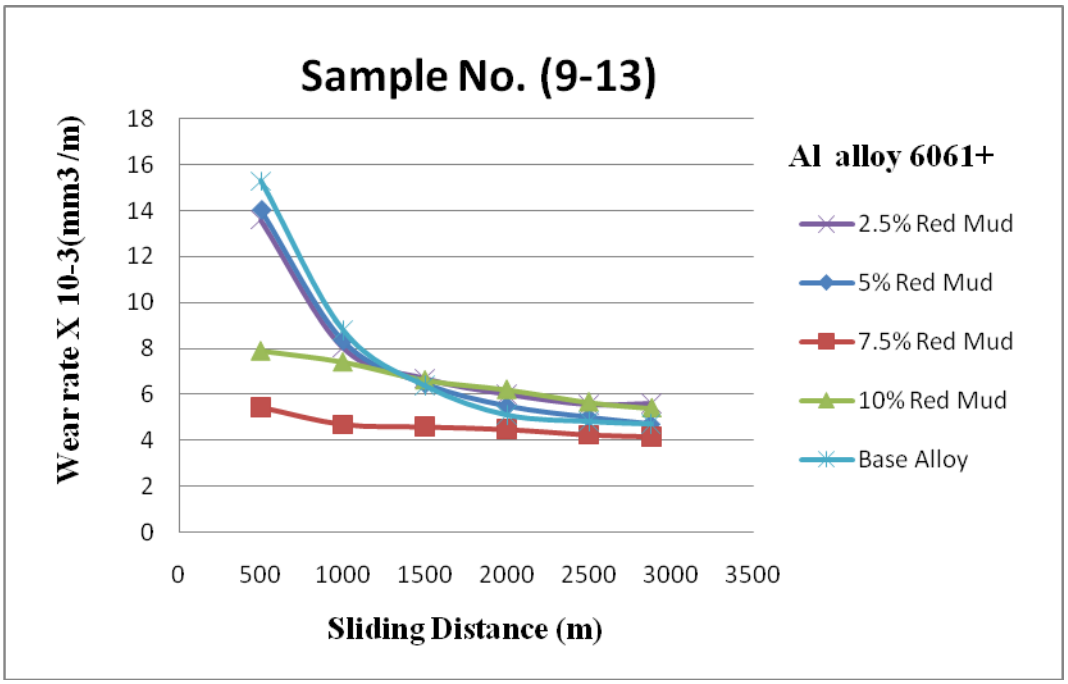

Figure 5.16- Wear rate in 10^{-3} X mm^3/m Vs Sliding Distance in m of samples (9-13)

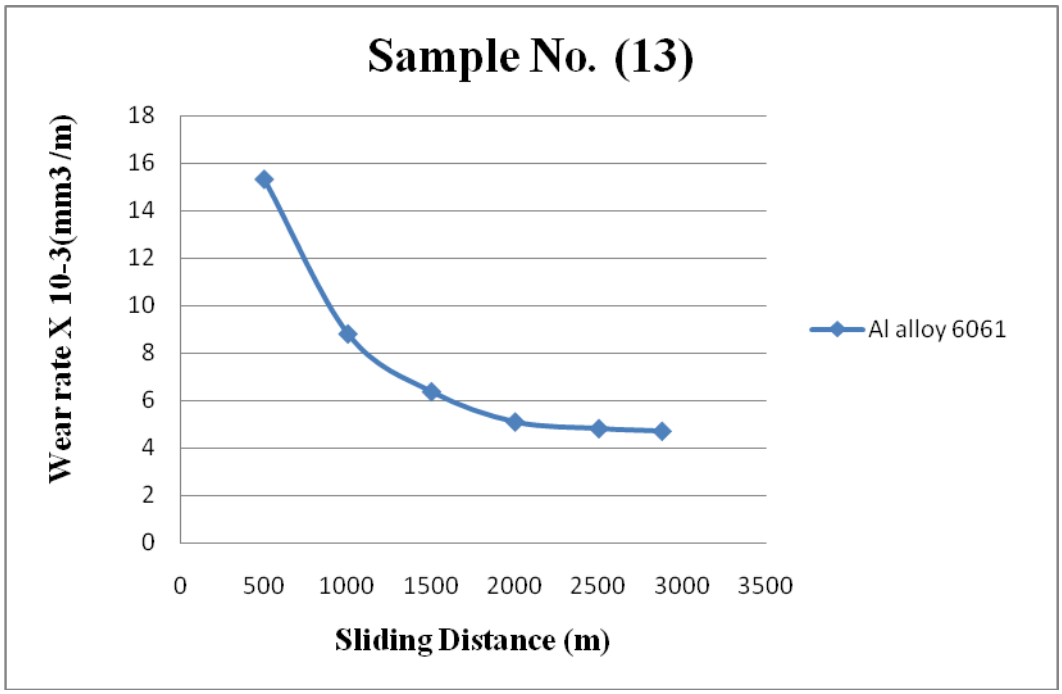

Figure 5.17- Wear rate in 10^{-3} X mm^3/m Vs Sliding Distance in m of sample (13)

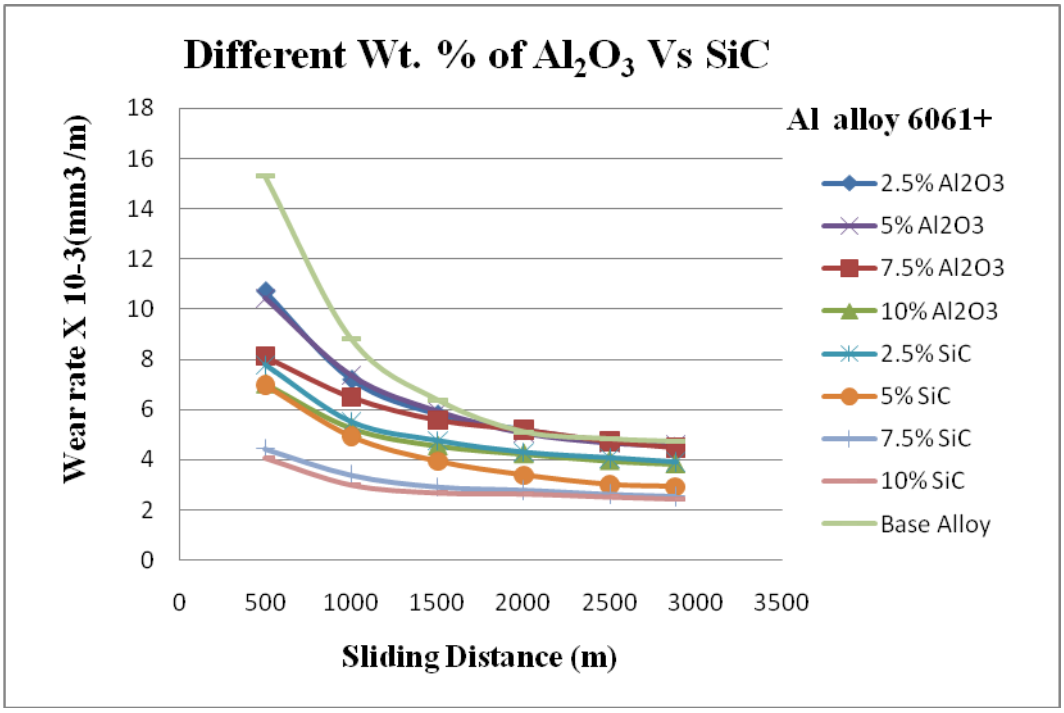

Figure 5.18- Wear rate in 10^{-3} X mm^3/m Vs *Sliding* Distance in m of samples (1-8, 13)

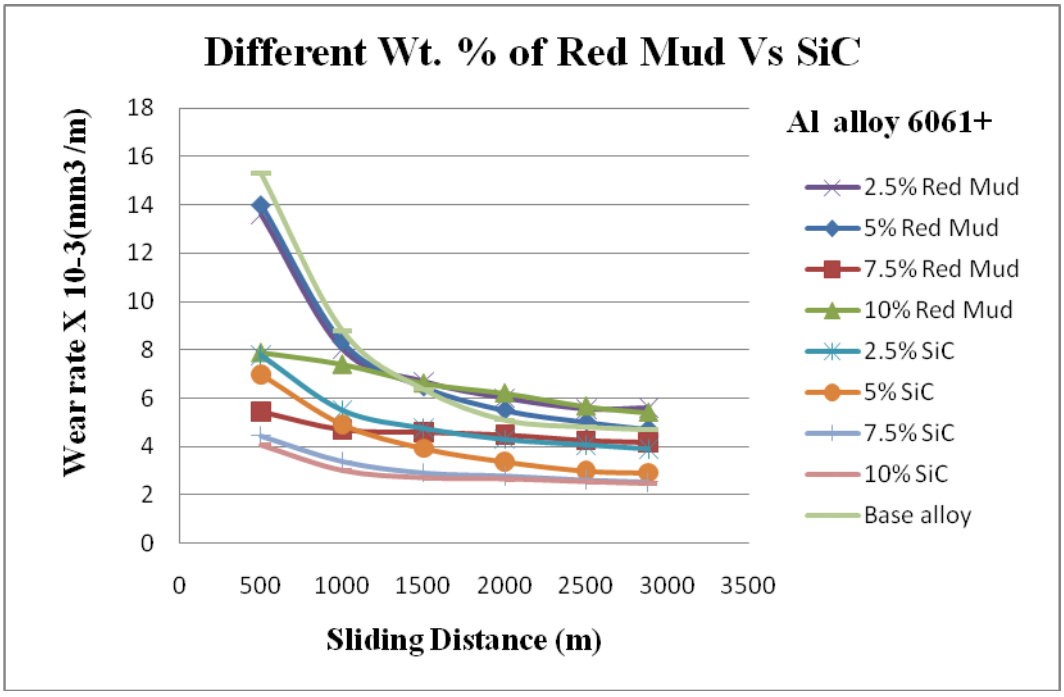

Figure 5.19- Wear rate in 10^{-3} X mm^3/m Vs Sliding Distance in m of samples (1-4 and 9-13)

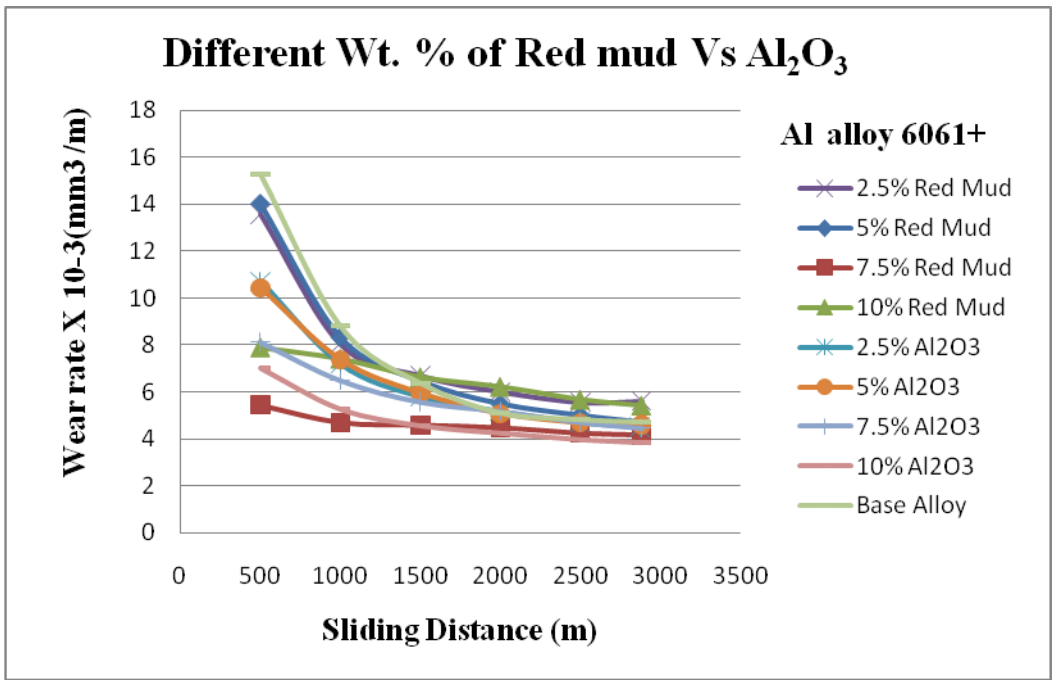

Figure 5.20- Wear rate in 10^{-3} X mm^3/m Vs Sliding Distance in m of samples (5-13)

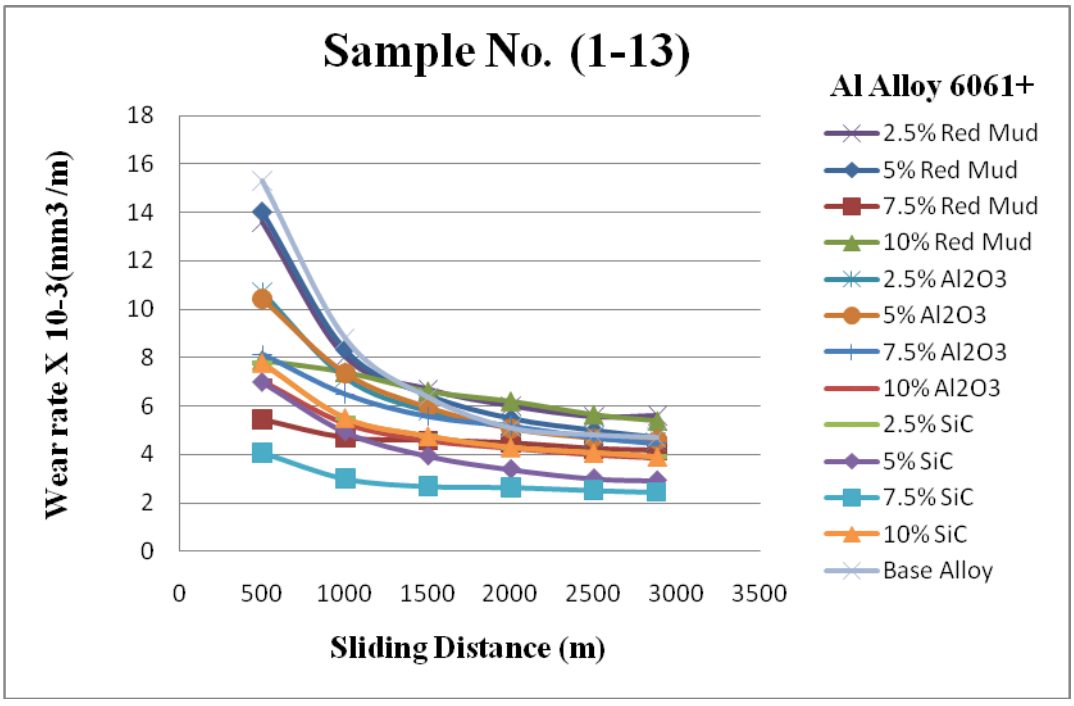

Figure 5.21- Wear rate in 10^{-3} X mm^3/m Vs Sliding Distance in m of samples (1-13)

5.3.2.3 Result and discussion of graphs between wear rate and sliding distance:

Figure 5.21 shows the variation of wear rate with sliding distance for the Al alloy 6061 and composites reinforced with Silicon Carbide, aluminium oxide and red mud particles of various size ranges (50- 75 µm, 30- 50 µm and 103- 150µm) at a load of 20 N and total distance is approximately 2900m.

The wear rates of the composite did not increase linearly through the entire applied load range. The wear rate curves show that the change of wear volume with sliding distance is in the form of polynomial function. These results are analogous to relationship between thermal and sliding wear behaviour of Al 6061/ Al_2O_3 metal matrix composites observed by Serdar Osman Yılmaz and Soner Buytoz [13].

Under an applied load two different type of wear behaviour can be predicted from the curves. Fluctuating, unstable and greater wear at the initial stage corresponds to the run-in wear which avoids initial turbulent period associated with friction [12, 15]. This may be due to adhesive nature of sample to the sliding disc at the initial stage of wear. It is observed that wear rate increases initially and then gradually decreases with sliding distance in the case of alloy and composites. At the initial stage of sliding, the MMC is softer compared to at the later stage, as the MMCs gets strain hardened due to continuous sliding under an applied load after a certain sliding distance. These results are analogous to Abrasive wear of zircon sand and alumina reinforced Al–4.5 wt% Cu alloy matrix composites – A comparative study observed by Sanjeev Das, Siddhartha Das and Karabi Das [14].

On the other hand, constant wear rate has been obtained at later stage corresponding steady state wear. This is the final stage of actual testing. For both reinforced and unreinforced materials, a steady state is approachable approximately after 1 km sliding distance for the given applied load. These results are analogous to dry sliding wear behaviour of Zircon sand reinforced Al- Si alloy observed by Kamalpreet Kaur and O. P. Pandey [15].

Figure (5.14 to 5.17) shows the variation of wear rate with sliding distance (total sliding distance appx. 2900 m) for constant load 2 Kg at 510 rpm. It is seen from the plots that with addition of

SiC, Al_2O_3 and Red Mud Particles in the matrix the wear rate of composites was decreased. Also as the sliding distance reached upto 500 m the wear rate first decreses and then almost remains same for the entire test period.

The results as indicated from Figure 5.14 the decreasing trend of wear rate with increase in weight percentage of SiC up to 10% weight fraction.

Similarly, the results as indicated from Figure 5.15 the decreasing trend of wear rate with increase in weight percentage of Al_2O_3 up to 10% weight fraction.

But the results from Figure 5.16 shows the decreasing trend of wear rate with increase in weight percentage of Red Mud up to 7.5% weight fraction. Beyond this wt. % the wear rate trend starts increasing.

This is because when red mud is added beyond 7.5% by wt. in the matrix the viscosity of MMC increased and stirrer was not rotated properly, thereby improper dispersion and poor interfacial bonding takes place between the red mud and Al alloy matrix. MMC with 7.5% red mud reinforcement have approximately constant wear rate throughout the test.

From the comparison graph i.e. different wt. % of SiC Vs Al_2O_3 in Figure 5.18 shows that 10% SiC has the superior wear resistance property over the other different wt. % of reinforcements in the case of wear rate.

Similarly, from the comparison graph i.e. different wt. % of SiC Vs Red Mud in Figure 5.19 shows that 10% SiC has superior wear resistance property over the other different wt. % of reinforcements in the case of wear rate.

But from the comparison graph i.e. different wt. % of Red Mud Vs Al_2O_3 in Figure 5.20 shows that 7.5% Red Mud has superior wear resistance property over the 7.5% of alumina reinforcement. It is clear from the plots that at the same wt. % of red mud and alumina, we can replace alumina by red mud in case of wear rate. Thereby we can save the money and environment up to some amount by utilization of waste residue i.e. red mud.

5.4 MICROSTRUCTURAL OBSERVATION OF DIFFERENT SPECIMENS BEFORE WEARING

Microstructure was visualized with the help of optical microscope. For the specimen preparation, first of all specimen were cut down into small cuboids shapes after that the different samples were grinded on different grit size papers sequencelly by 100, 220, 400, 600 and 1000. After grinding, the specimens were mechanically polished by alumina paste and then etched by kellar's reagant to obtain better contrast. The specimens were visualized on different magnifications (50X and 100X) to show the presence of reinforcement and its distribution on the metal martix. Different elements/ compounds which were present in the red mud are difficult to distinuish by optical micrograpy. The microstructure of all the samples was shown in Figure 5.22 to 5.34.

Optical microstruucture of Al alloy 6061 as matrix

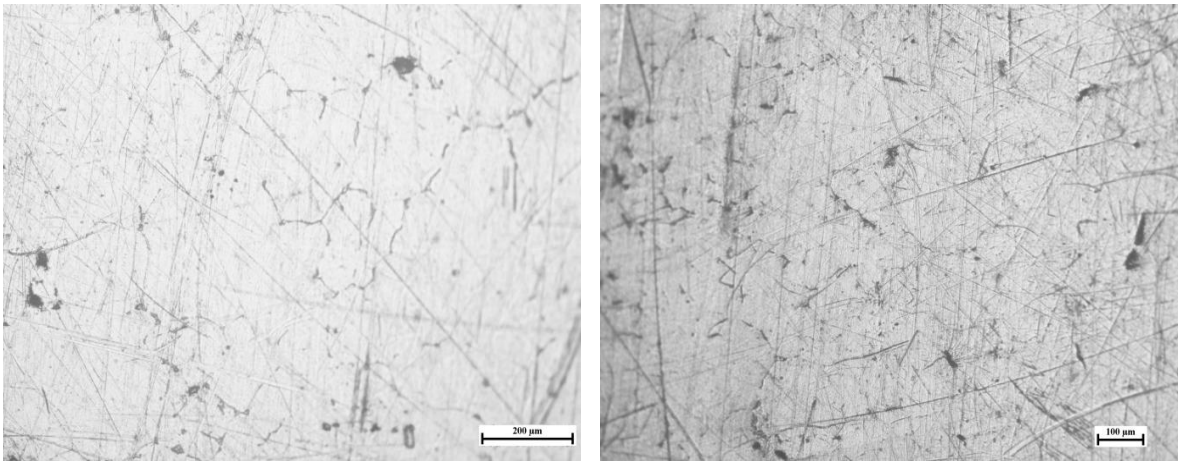

(a) (b)

Figure 5.22- Optical micrographs of Al alloy 6061 at (a) 50X, (b) 100X

Optical Microstructure of MMCs with Alumina as a reinforcement

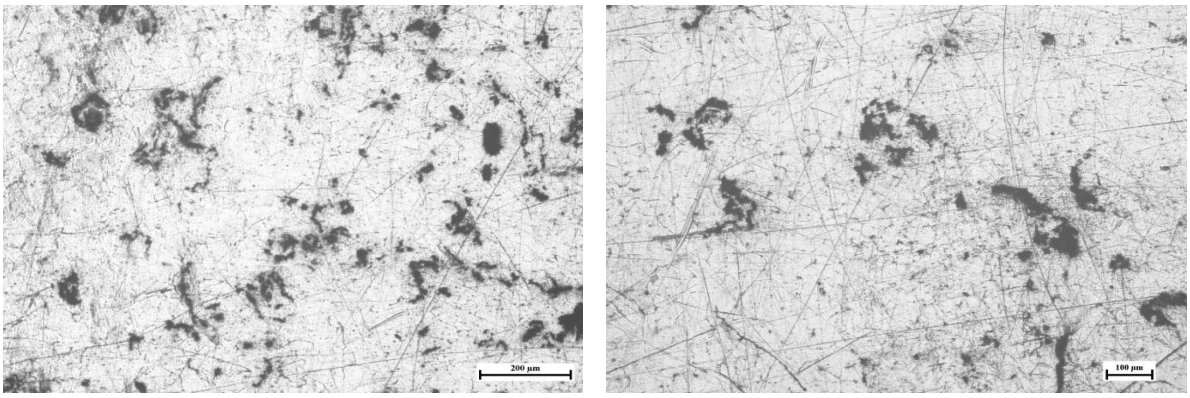

(a) (b)

Figure 5.23- Optical micrographs of MMC with 2.5 wt. % Al_2O_3 at (a) 50X, (b) 100X

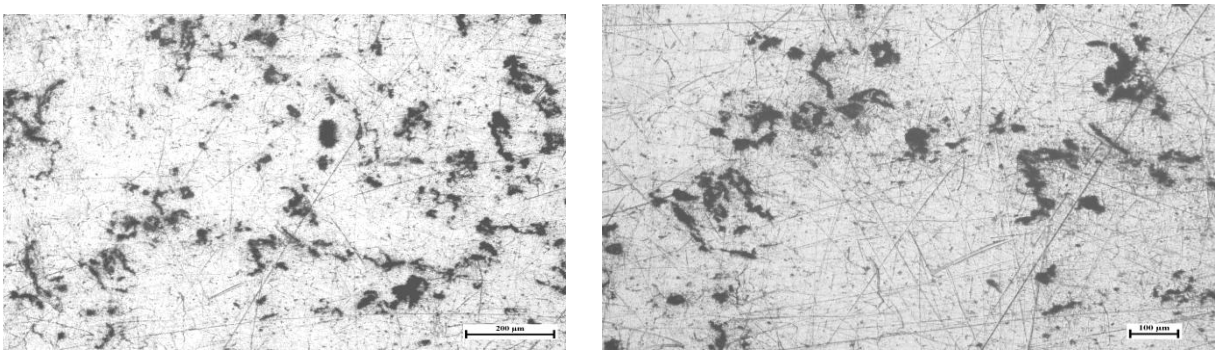

(a) (b)

Figure 5.24- Optical micrographs of MMC with 5 wt. % Al_2O_3 at (a) 50X, (b) 100X

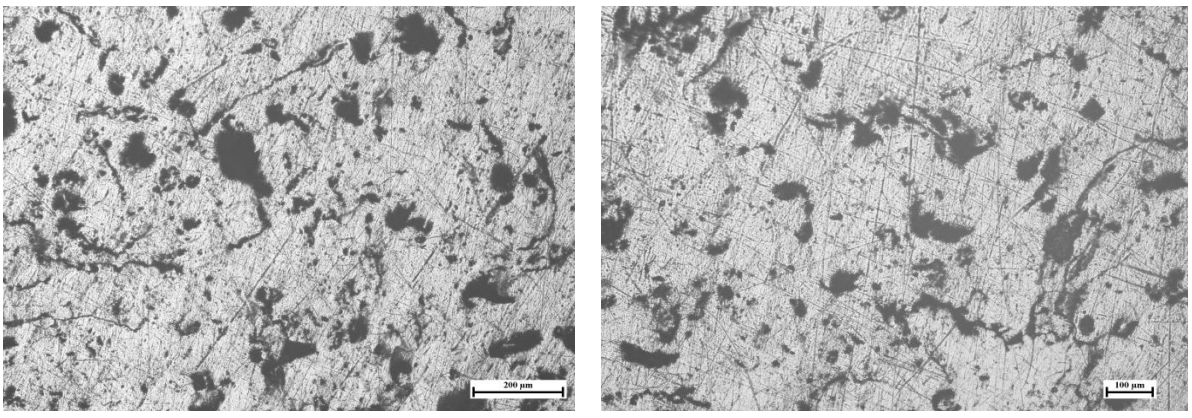

(a) (b)

Figure 5.25- Optical micrographs of MMC with 7.5 wt. % Al_2O_3 at (a) 50X, (b) 100X

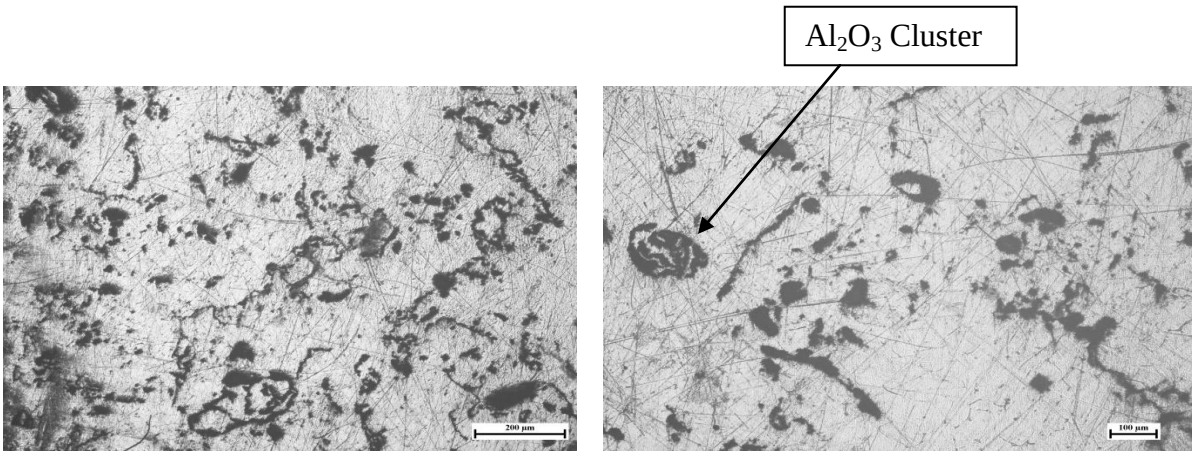

(a) (b)

Figure 5.26- Optical micrographs of MMC with 10 wt. % Al_2O_3 at (a) 50X, (b) 100X

It is clear from the Figure 5.23- 5.26 that the distribution of Al_2O_3 particles in a matrix alloy is fairly uniform. The average size of Al_2O_3 particles is around 30µm-50µm.The shape of most Al_2O_3 particles is irregular in nature. Irregular shape of aluminium oxide particles may be due to the breakage of particles during ball milling.

It is found that as the percentage of reinforcement increases the area fraction also increases as shown in optical micrograph. It also observed that there is increase in hardness and wear resistance this can be attributed to the increase in interfacial bonding of reinforcement with the aluminium matrix alloy. Good interfacial bonding can be obtained by pre-heating of Al_2O_3 particulates before adding in the matrix. It is also found that at some places there was clustering of Al_2O_3 particulates as shown in Figure 5.26.

Optical Microstructure of MMCs with SiC as a reinforcement

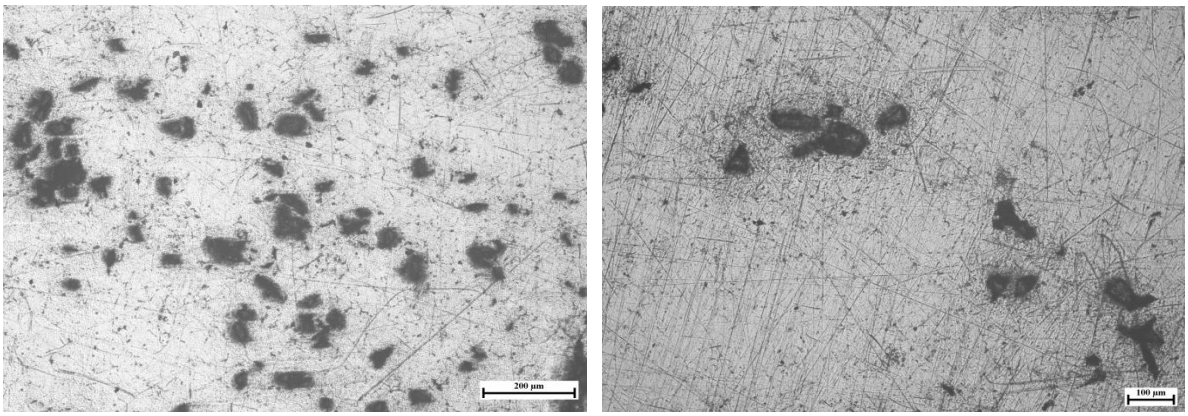

(a) (b)

Figure 5.27- Optical micrographs of MMC with 2.5wt. % SiC at (a) 50X, (b) 100X

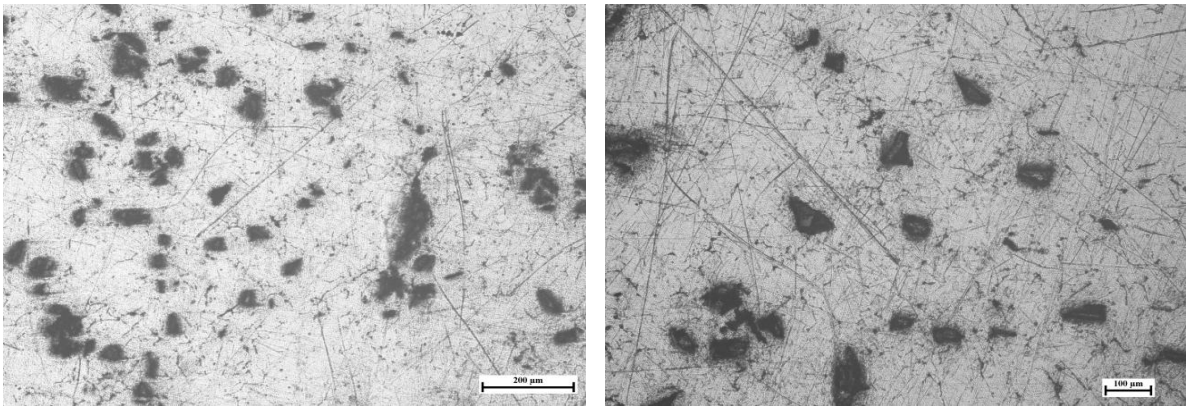

(a) (b)

Figure 5.28- Optical micrographs of MMC with 5 wt. % SiC at (a) 50X, (b) 100X

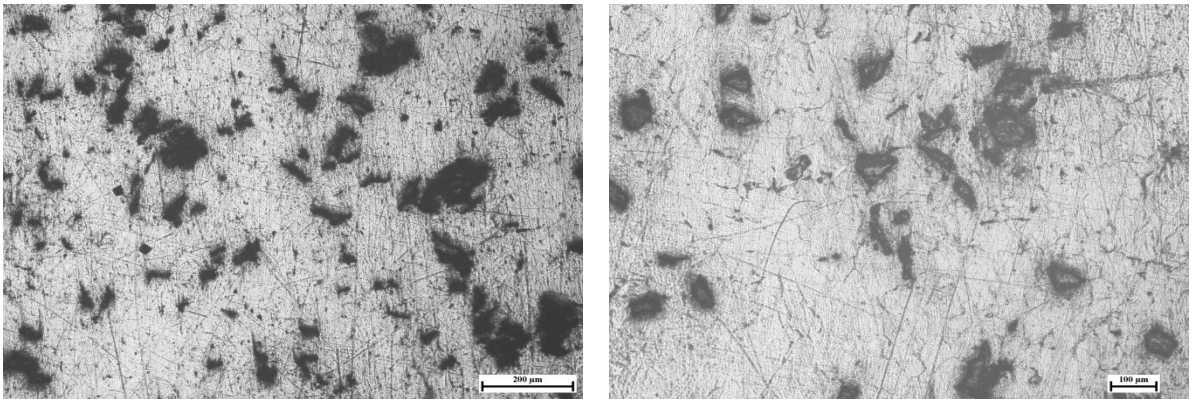

(a) (b)

Figure 5.29- Optical micrographs of MMC with 7.5 wt. % SiC at (a) 50X, (b) 100X

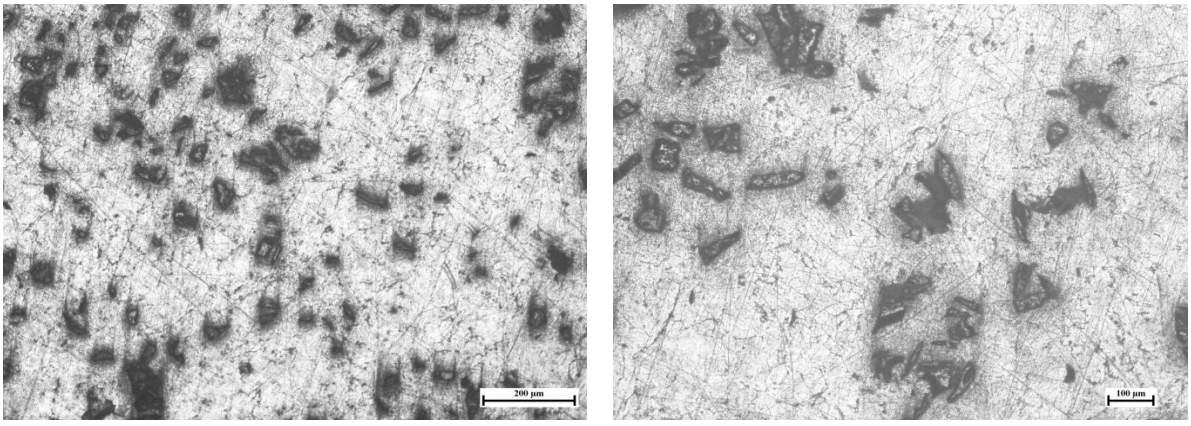

(a) (b)

Figure 5.30- Optical micrographs of MMC with 10 wt. % SiC at (a) 50X, (b) 100X

It is clear from the Figure 5.27- 5.30 that the distribution of SiC particles in a matrix alloy is nearly uniform. The average size of SiC particles is around 60µm- 90µm. The shape of most SiC particles is angular and sub-angular in nature.

It is found that as the percentage of reinforcement increase the area fraction also increases as shown in optical micrograph. It also observed that there is increase in hardness and wear resistance this can be attributed to the increase in interfacial bonding of reinforcement with the aluminium matrix alloy. Good interfacial bonding can be obtained by pre-heating of SiC particulates before adding in the matrix.

Optical Microstructure of MMCs with Red Mud as a reinforcement

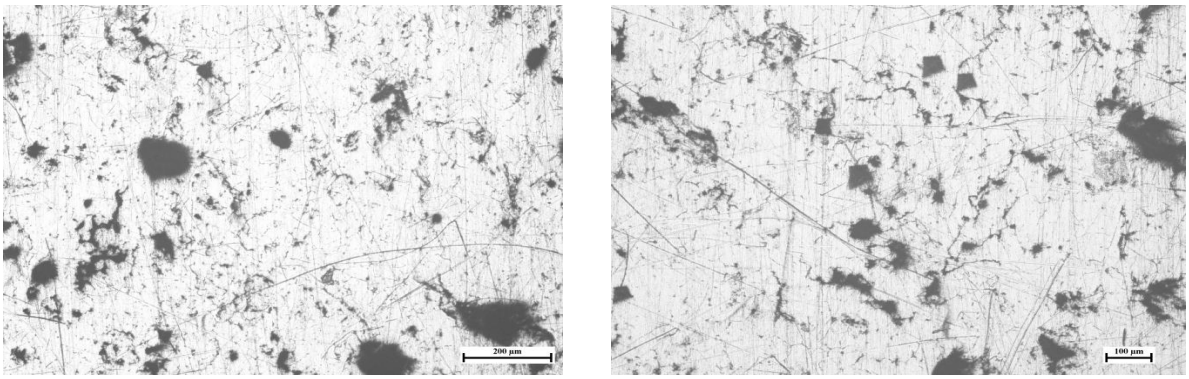

(a) (b)

Figure 5.31- Optical micrographs of MMC with 2.5 % Red Mud at (a) 50X (b) 100X

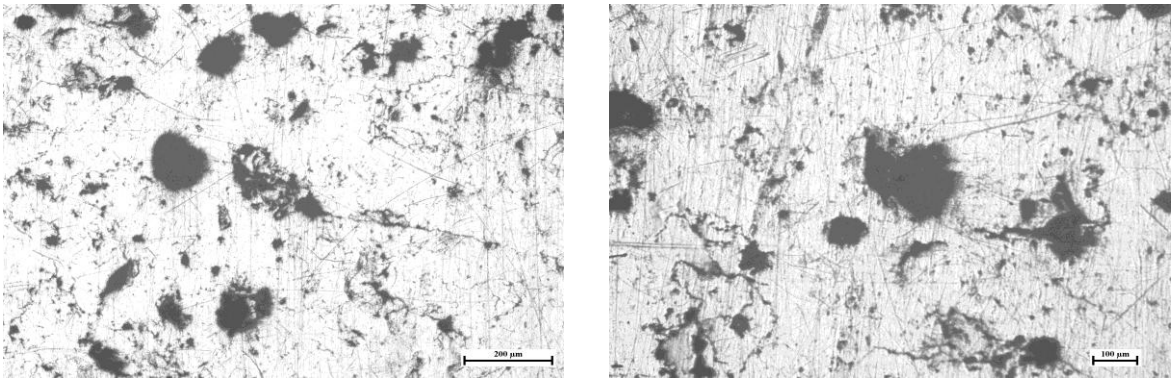

(a) (b)

Figure 5.32- Optical micrographs of MMC with 5 % Red Mud at (a) 50X (b) 100X

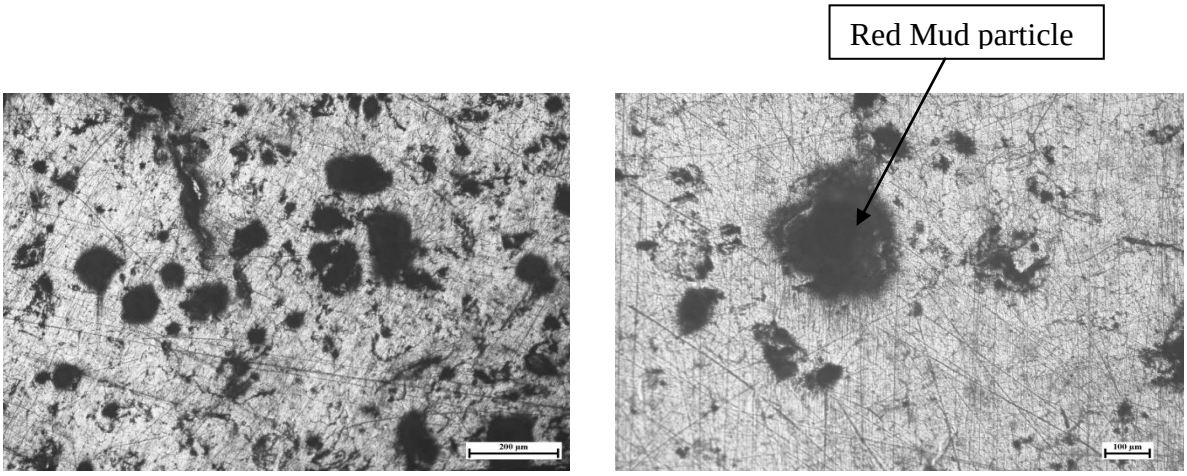

(a) (b)

Figure 5.33- Optical micrographs of MMC with 7.5 % Red Mud at (a) 50X, (b) 100X

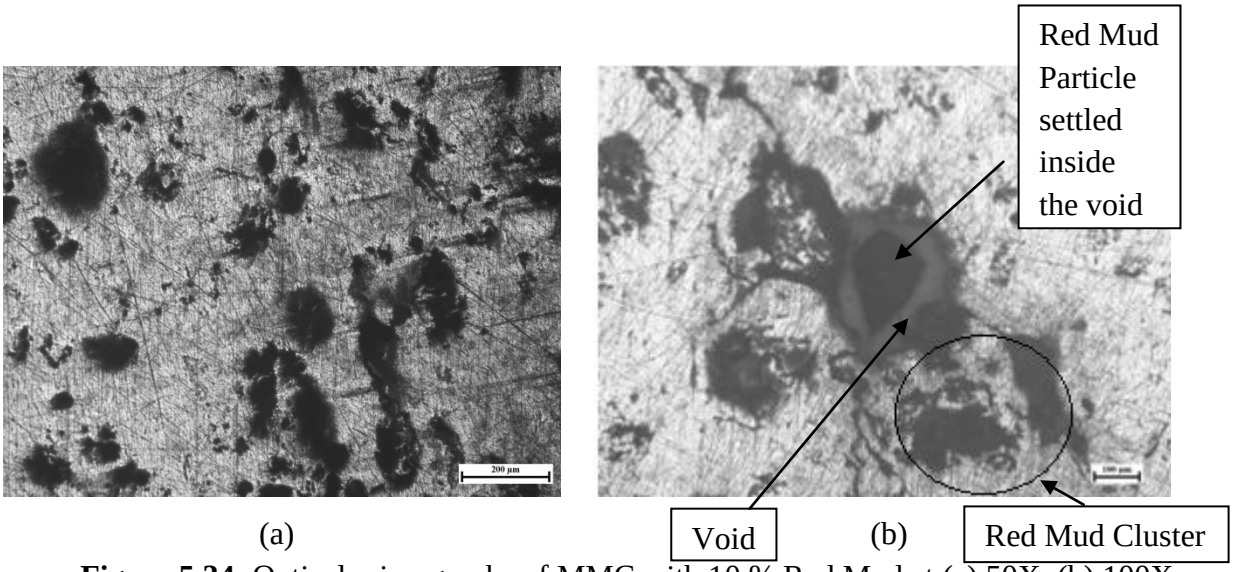

(a) (b)

Figure 5.34- Optical micrographs of MMC with 10 % Red Mud at (a) 50X, (b) 100X

It is clear from the Figure 5.31- 5.34 that the distribution of Red Mud particles in a matrix alloy is fairly uniform. The average size of Red Mud particles is around 103µm-150µm. The shape of most Red Mud particles is round in nature. Different elements/ compounds which were present in the red mud are difficult to distinuish by optical micrograpy.

It is found that as the percentage of reinforcement increase the area fraction also increases as shown in optical micrograph. It also observed that there is increase in hardness and wear resistance this can be attributed to the increase in interfacial bonding of reinforcement with the aluminium matrix alloy. Good interfacial bonding can be obtained by pre-heating of Red Mud particulates before adding in the matrix. It is also found that at some places there was voids and clustering of Red Mud particulates as shown in Figure 5.34.

5.5 SCANNING ELECTRON MICROSCOPY (SEM) ANALYSIS

The cleaned, dried and etched specimens is prepared and subsequently mounted on specially designed aluminium stubsusing (holder). The specimens thus mounted were viewed under Jeol, JSM 6510 LV scanning electron microscope at an accelerating voltage of 20 kV. Figure 5.35-5.40 shows the SEM micrograph of the different Aluminium matrix composites at different magnifications (100X, 250X, 500X and 1000X).

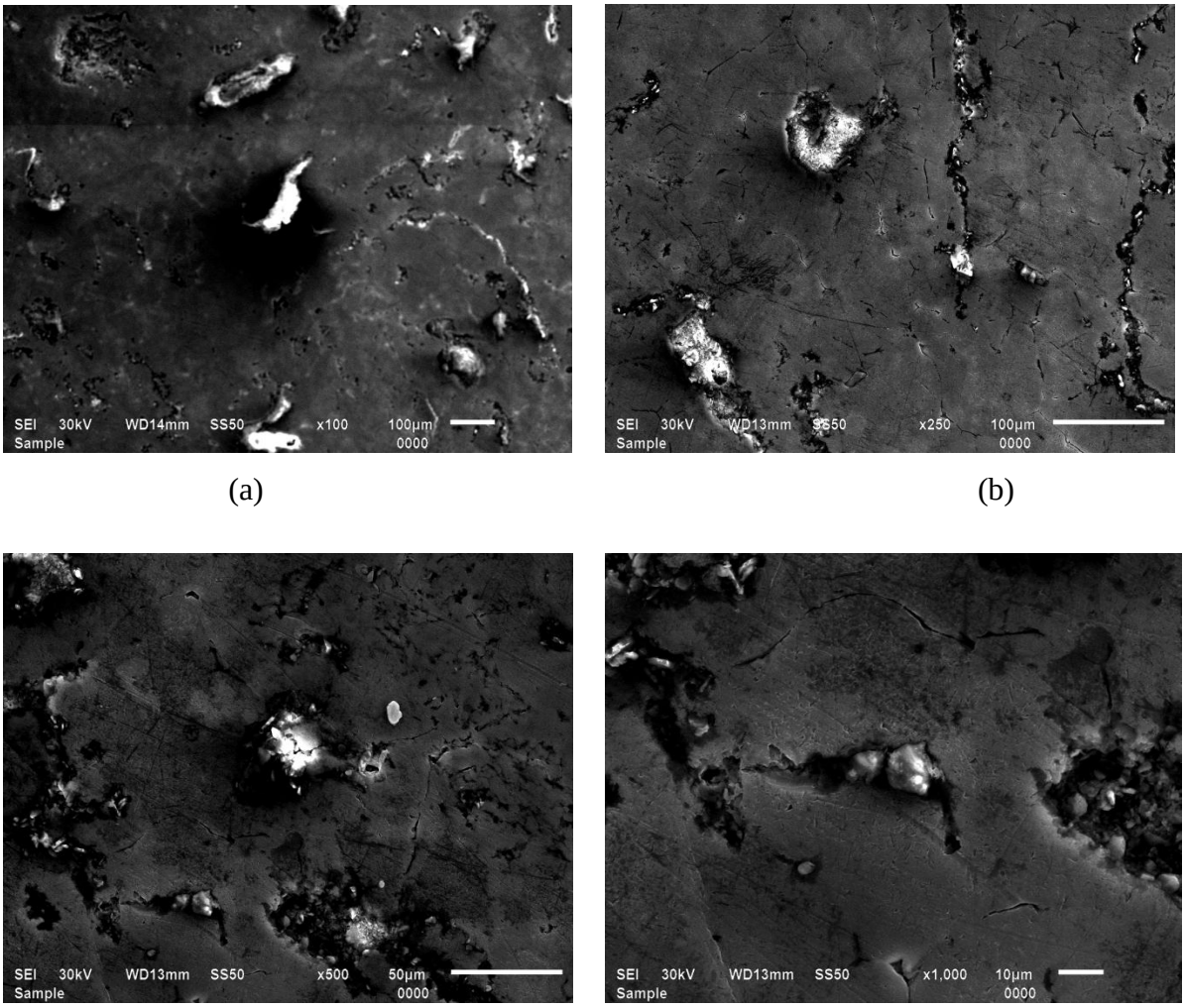

Figure 5.35- SEM of MMC with 7.5 wt.% Al_2O_3 at (a) 100X, (b) 250X, (c) 500X, (d) 1000X

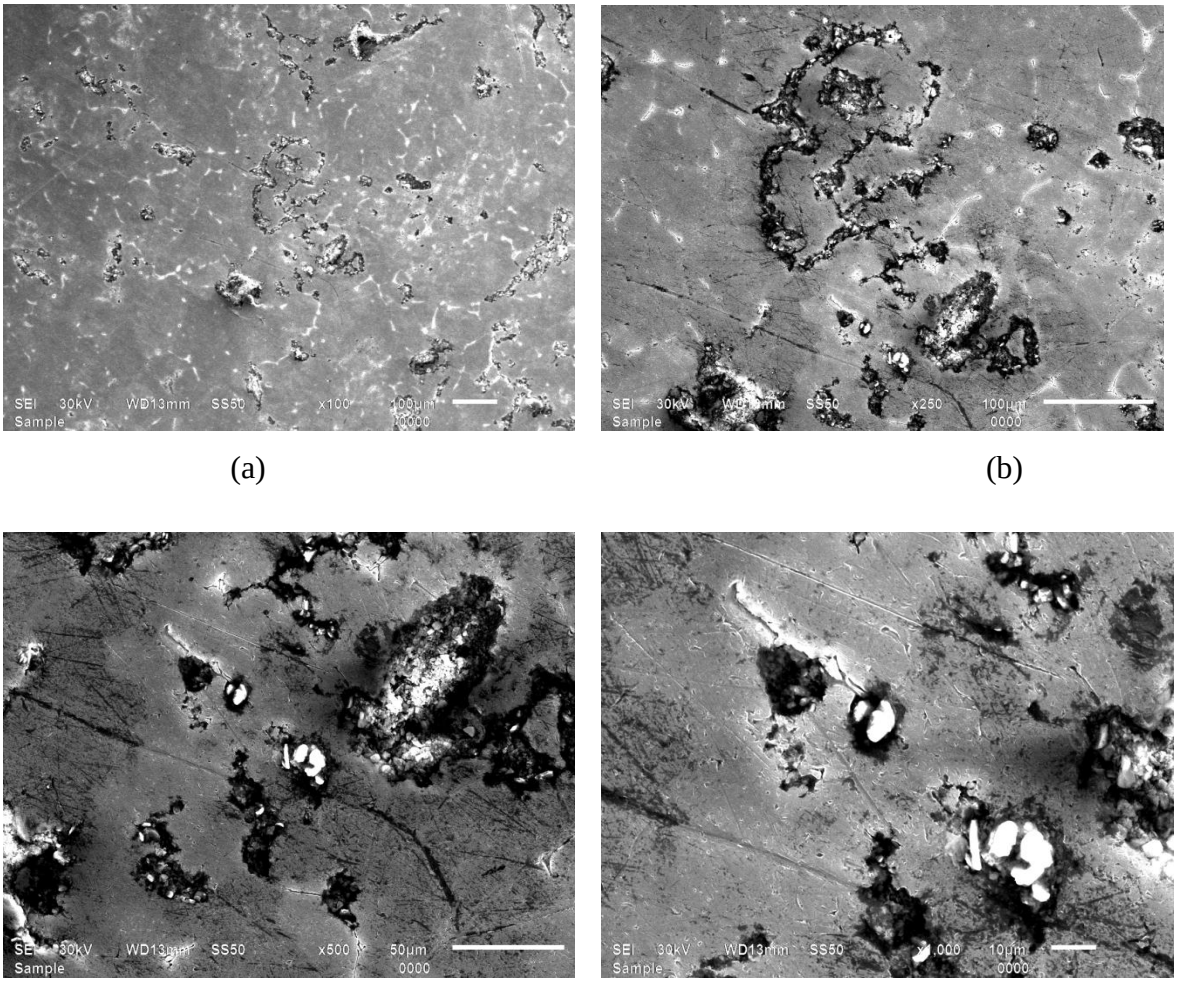

Figure 5.36- SEM of MMC with 10 wt.% Al_2O_3 at (a) 100X, (b) 250X, (c) 500X, (d) 1000 X

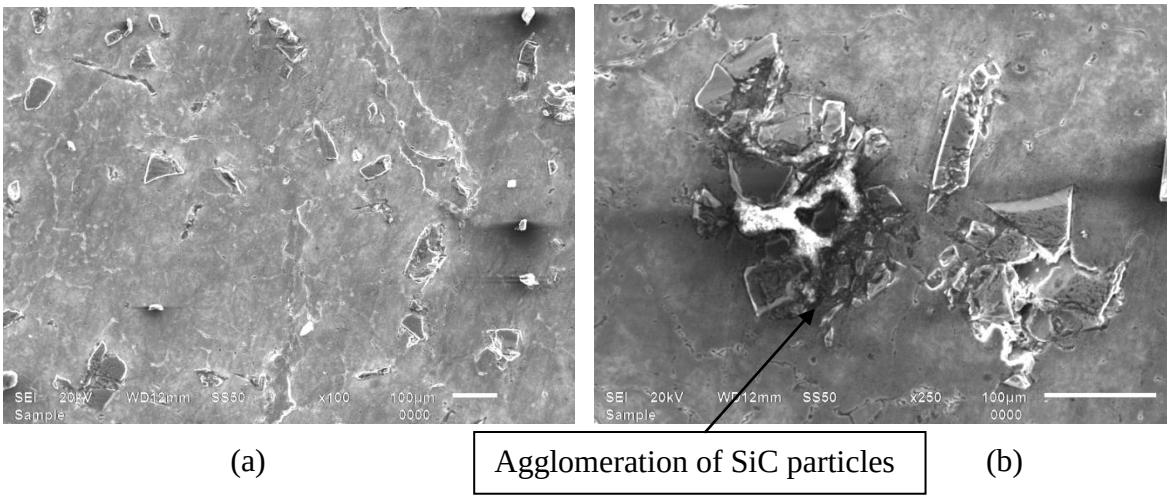

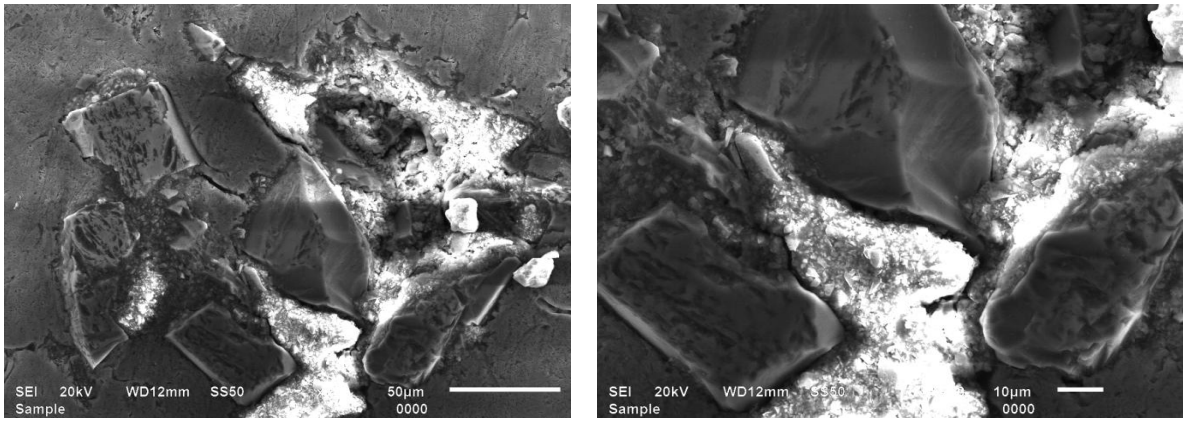

(c) (d)

Figure 5.37- SEM of MMC with 7.5 wt. % SiC at (a) 100X, (b) 250X, (c) 500X, (d) 1000 X

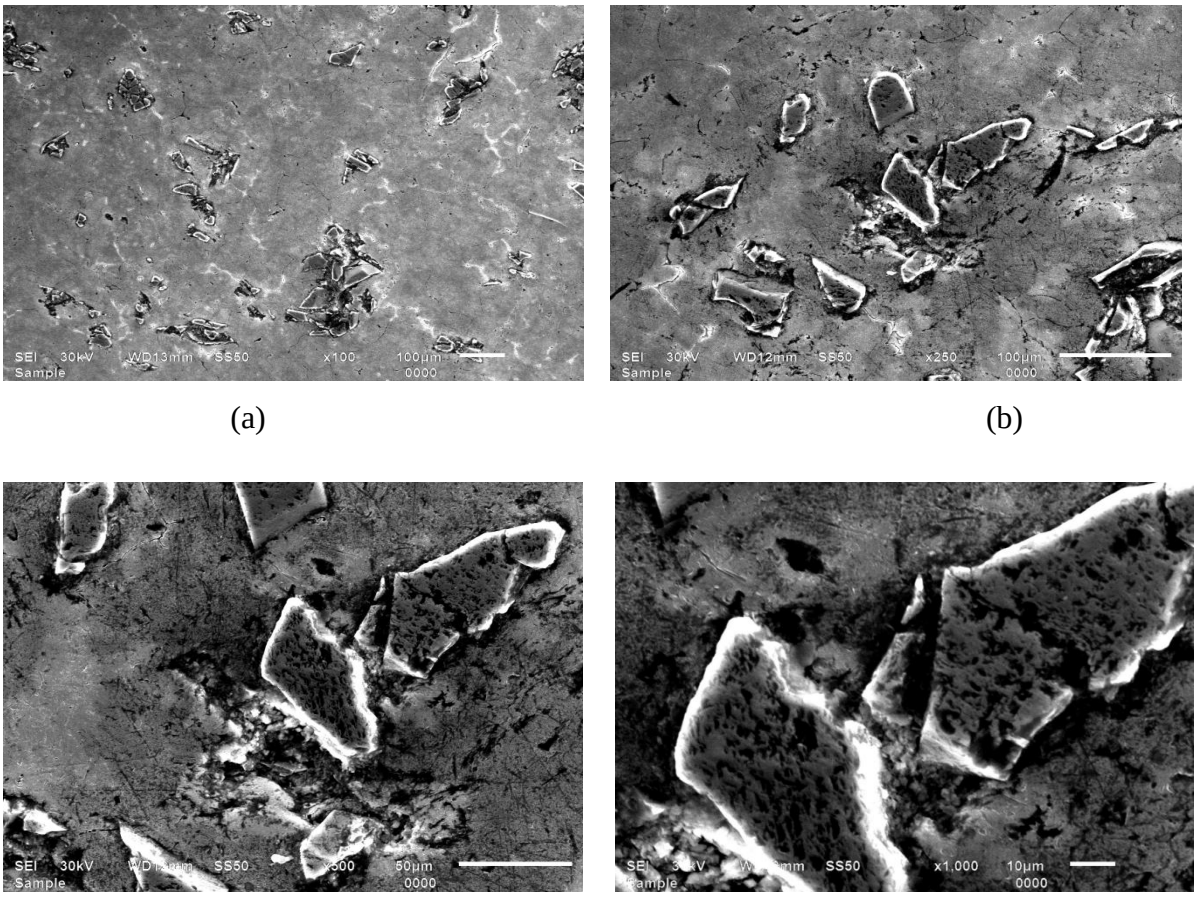

(a) (b)

(c) (d)

Figure 5.38- SEM of MMC with 10 % SiC at (a) 100X, (b) 250X, (c) 500X, (d) 1000 X

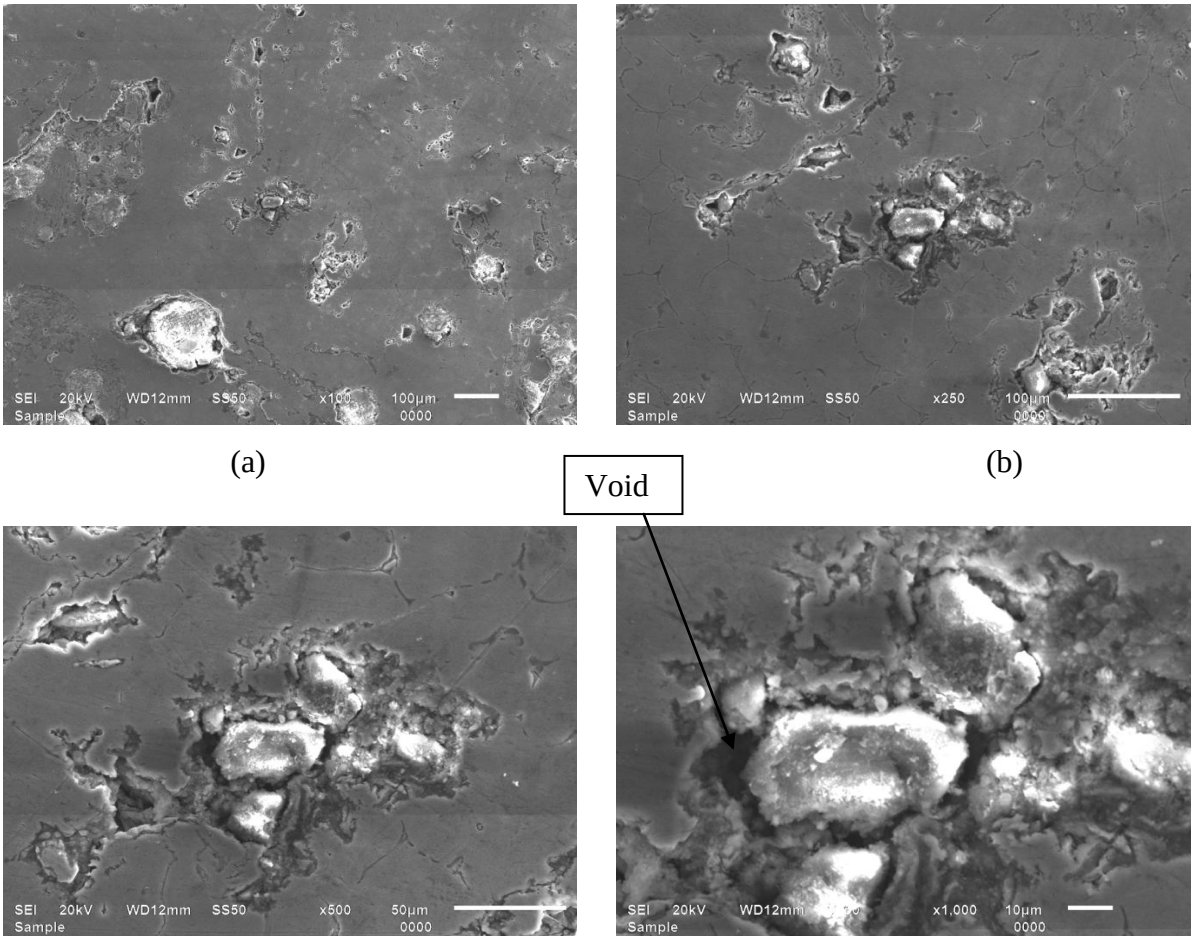

Figure 5.39- SEM of MMC with 7.5 wt. % Red Mud at (a) 100X, (b) 250X, (c) 500X, (d) 1000 X

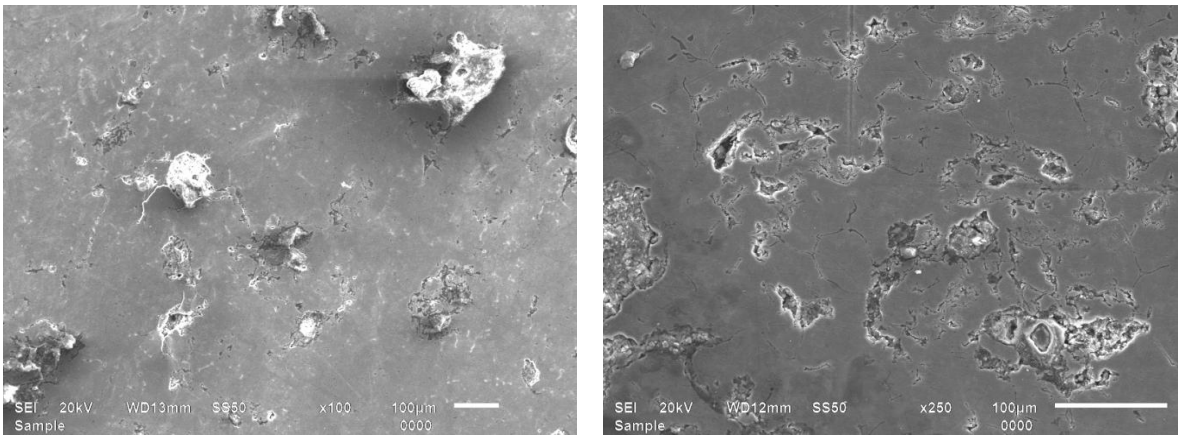

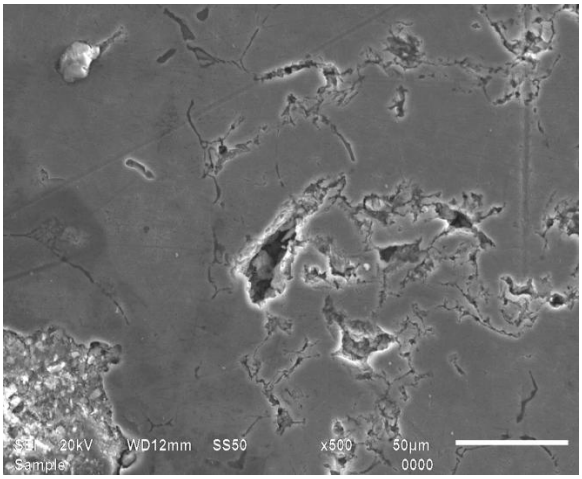

(c)

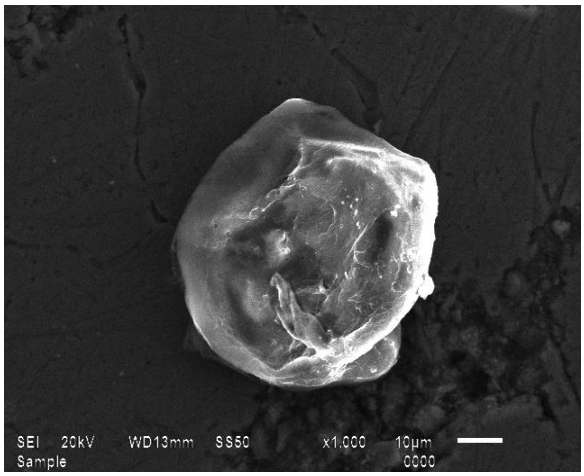

(d)

Figure 5.40- SEM of MMC with 10 wt. % Red Mud at (a) 100X, (b) 250X, (c) 500X, (d) 1000 X

Scanning electron micrographs at lower magnification shows that the distribution of SiC, Al_2O_3 and Red Mud particulate throughout the MMCs. Scanning electron micrographs at higher magnification shows the particle–matrix interfaces.

Figure 5.37 and 5.38 shows the homogeneous distribution of SiC reinforced particles in alloy matrix. Homogeneous distribution of particles is desired for achieving better wear behaviour and mechanical properties. Homogeneous distribution of particles in a molten alloy is achieved due to the high shear rate caused by stirring which also minimize the particles settling.

However, agglomeration of particles in some regions is clearly visible in all cases; this is due to the presence of porosity associated to it. Presence of entrapped air and moisture in the reinforcement particles results in the voids/ porosity after casting.

It is observed that the particle–matrix interface of Al_2O_3 and Red Mud reinforced composite is not as smooth as that of SiC reinforced composite, which indicates relatively poor bonding between the alumina-Al alloy 6061 alloy matrix and Red Mud-Al alloy 6061 alloy matrix.

Figure 5.39 and 5.40 shows the scanning electron micrographs of Red Mud composite at different magnification. At higher magnification SEM shows the shape of most Red Mud particles exhibits globular morphology. Other different types of particle are also visible in red mud MMCs but still it is not possible to distinguish these different particles types.

Further the SEM reveal an excellent bond between the matrix alloy and SiC reinforcement particles as shown in Figure 5.37 (c and d) and 5.38 (c and d).

5.6 X-RAY DIFFRACTION ANALYSIS

An X-ray diffraction (XRD) pattern of aluminium alloy matrix composites and aluminium alloy were shown in given Figure 5.41- 5.53. X-ray diffraction of different samples was carried out by X'PERT PRO of PAN ANALYTICAL using CuKα radiation. In XRD, the physical content of the constituents present in the samples are indicated in the form of a graphs and tables shows the name and percentage of elements/ compounds present in respective Samples.

Sample 1: X-ray diffraction pattern of the alloy with 2.5% Silicon Carbide as a reinforcement

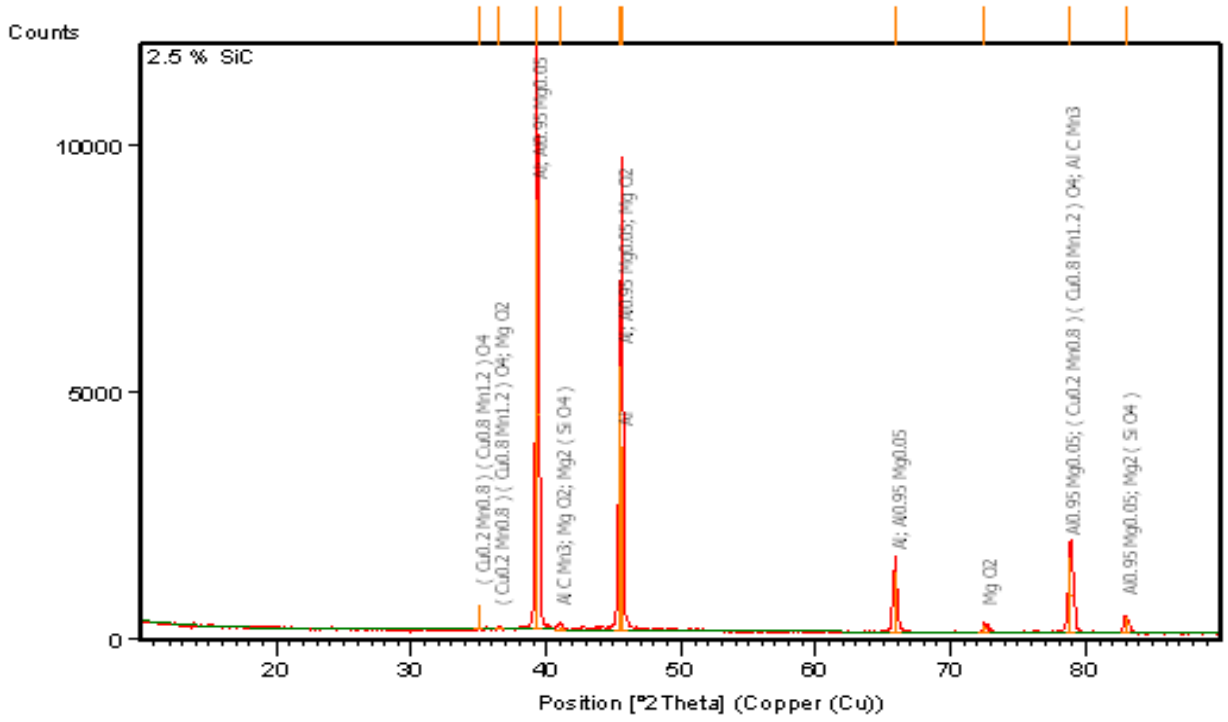

Figure 5.41- X-ray diffraction pattern of the alloy with 2.5 wt. % SiC (Sample No.1)

Table 5.5- XRD results of alloy reinforced with 2.5% SiC

Ref.Code	Score	Compound Name	Chemical Formula	Weight Fraction (%)

01-071-4622	52	Aluminium	Al	68.0
01-074-5237	39	Aluminium Magnesium	$Al_{0.95}Mg_{0.05}$	19.0
01-074-2847	13	Copper Manganese Oxide	$(Cu_{0.2}Mn_{0.8})(Cu_{0.8}Mn_{1.2})O_4$	2.0
03-065-8481	12	Aluminium Carbon Manganese	$AlCMn_3$	1.0
01-076-1363	10	Magnesium Oxide	MgO_2	7.0
01-087-2031	11	Magnesium Silicate	$Mg_2(SiO_4)$	3.0

Table 5.5 shows the X-ray diffraction pattern of the MMC (Sample No.1), which show the presence of Al and many other compounds. This confirms the presence of SiC in the aluminium alloy 6061.

In X-ray difrracetion (Figure 5.41), Ten peaks have been obtained in 2θ span ranging from 10 to 100. From these peaks the maximum value of reletive intensity [%] is 100.00 at the position [^{0}2 Th.] of 39.3059 gives two assignments i.e. Al and $Al_{0.95}Mg_{0.05}$. The peaks in the pattern can be indexed to a mixture of different compounds and other remaining minor peaks attributed to impurity.

Sample 2: X-ray diffraction pattern of the alloy with 2.5% Alumina as a reinforcement

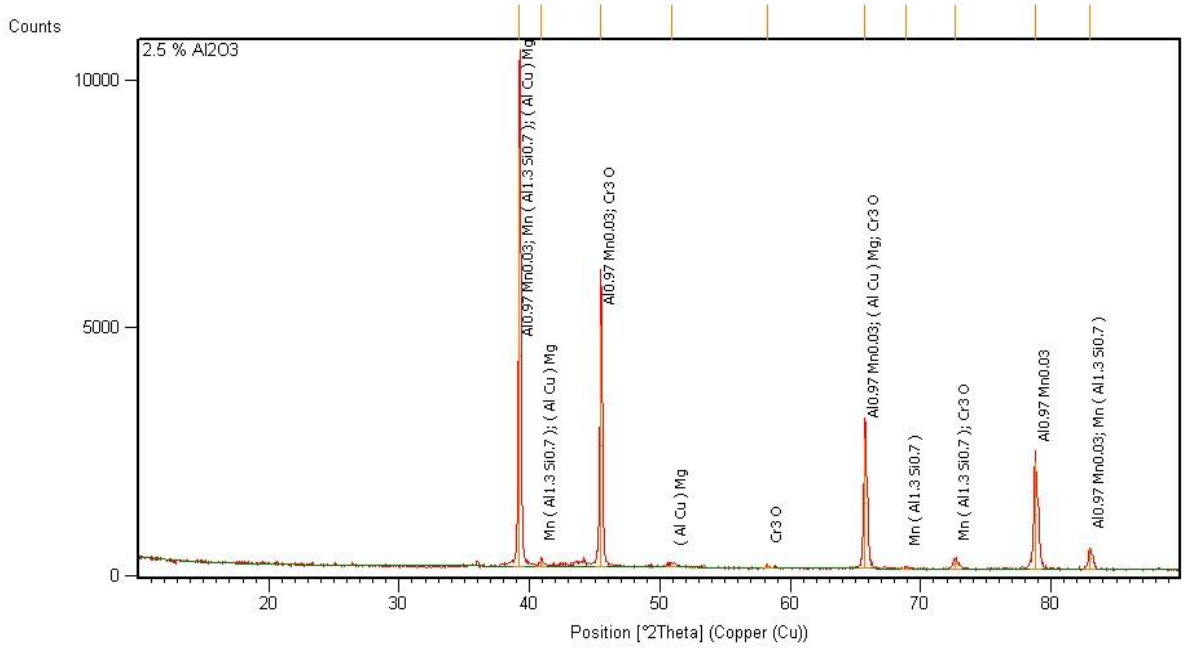

Figure 5.42- X-ray diffraction pattern of the alloy with 2.5 wt. %Al_2O_3 (Sample No.2)

Table 5.6- XRD results of alloy reinforced with 2.5% Al_2O_3

Ref.Code	Score	Compound Name	Chemical Formula	Weight Fraction (%)
01-074-5245	76	Aluminium Manganese	$Al_{0.97}Mn_{0.03}$	77.0
01-071-4023	13	Manganese Aluminium Silicon	$Mn(Al_{1.3}Si_{0.7})$	2.0
01-074-6460	9	Aluminium Copper Magnesium	(AlCu)Mg	6.0
01-072-0528	22	Chromium Oxide	Cr_3O	16.0

Table 5.6 shows the X-ray diffraction pattern of the MMC (Sample No.2), which show the presence of Al and many other compounds. This confirms the presence of Al_2O_3 in the aluminium alloy 6061.

In X-ray difrracetion (Figure 5.42), Ten peaks have been obtained in the 2θ span ranging from 10 to 100. From these peaks the maximum value of reletive intensity [%] is 100.00 at the position [^{0}2Th.] of 39.2248 gives three assignments i.e. $Al_{0.97}Mn_{0.03}$, $Mn(Al_{1.3}Si_{0.7})$ and (AlCu)Mg. The peaks in the pattern can be indexed to a mixture of different compounds and other remaining minor peaks attributed to impurity.

Sample 3: X-ray diffraction pattern of the alloy with 2.5% Red Mud as a reinforcement

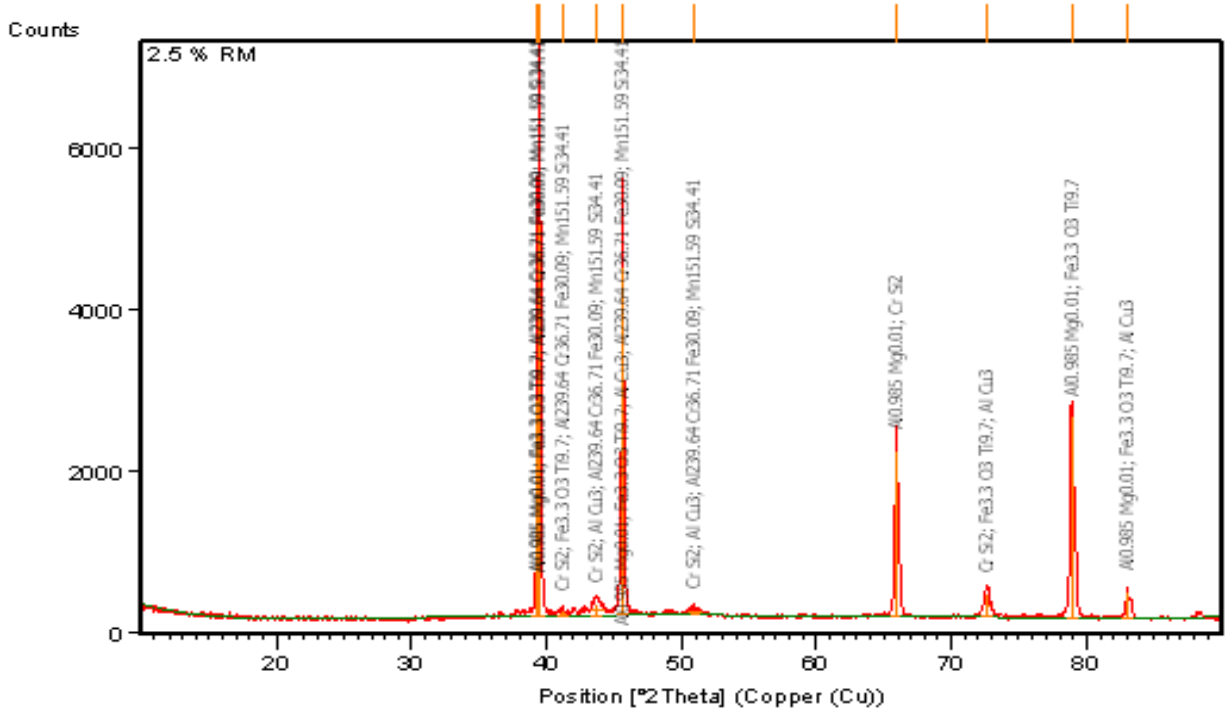

Figure 5.43- X-ray diffraction pattern of the alloy with 2.5 wt. % Red Mud (Sample No.3)

Table 5.7- XRD results of alloy reinforced with 2.5% Red Mud

Ref.Code	Score	Compound Name	Chemical Formula	Weight fraction (%)
01-074-5175	57	Aluminium Magnesium	$Al_{0.985}Mg_{0.01}$	14.0
03-065-9705	27	Chromium Silicide	$CrSi_2$	2.0
01-078-0473	4	Titanium Iron Oxide	$Ti_{9.7}Fe_{3.3}O_3$	18.0

01-074-6895	27	Aluminium Copper	$AlCu_3$	12.0
01-073-7530	11	Aluminium Chromium Iron	$Al_{239.64}Cr_{36.71}Fe_{30.09}$	52.0
01-071-0632	3	Manganese Silicon	$Mn_{151.59}Si_{34.41}$	2.0

Table 5.7 shows the X-ray diffraction pattern of the MMC (Sample No.3), which show the presence of Al and many other compounds. This confirms the presence of Red Mud in the aluminium alloy 6061.

In X-ray difrracetion (Figure 5.43), Ten peaks have been obtained in the 2θ span ranging from 10 to 100. From these peaks the maximum value of reletive intensity [%] is 100.00 at the position [^{0}2 Th.] of 39.426 gives four assignments i.e. $CrSi_2$, $Ti_{9.7}Fe_{3.3}O_3$, $Al_{239.64}Cr_{36.71}Fe_{30.09}$, $Mn_{151.59}Si_{34.41}$. The peaks in the pattern can be indexed to a mixture of different compounds and other remaining minor peaks attributed to impurity.

Sample 4: X-ray diffraction pattern of the alloy with 5% Silicon Carbide as a reinforcement

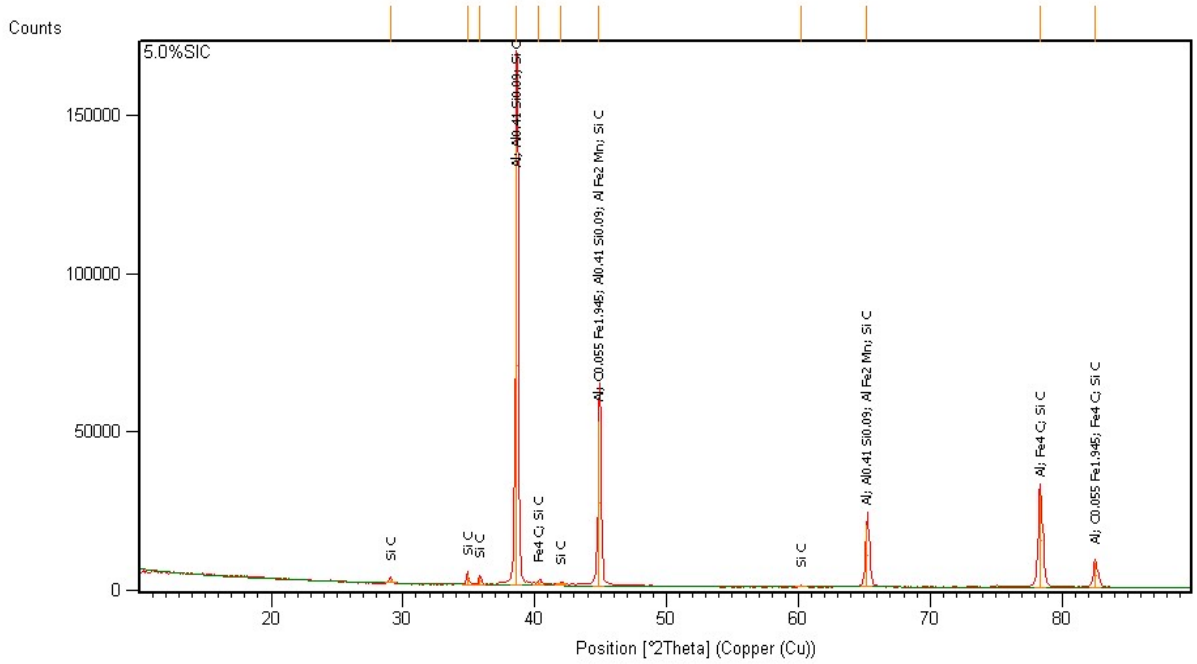

Figure 5.44- X-ray diffraction pattern of the alloy with 5 wt. % SiC (Sample No.4)

Table 5.8- XRD results of alloy reinforced with 5% SiC

Ref.Code	Score	Compound Name	Chemical Formula	Weight fraction (%)
01-072-3440	80	Aluminium	Al	65.0
00-044-1290	21	Carbon Iron	$C_{0.055}Fe_{1.945}$	2.0
01-074-5273	53	Aluminium Silicide	$Al_{0.41}Si_{0.09}$	19.0
01-073-8855	34	Aluminium Iron Manganese	$AlFe_2Mn$	11.0
01-089-4053	9	Iron Carbide	Fe_4C	1.0
01-073-6302	13	Silicon Carbide	SiC	2.0

Table 5.8 shows the X-ray diffraction pattern of the MMC (Sample No.4), which show the presence of Al and many other compounds. This confirms the presence of SiC in the aluminium alloy 6061.

In X-ray difrracetion (Figure 5.44), Eleven peaks have been obtained in the 2θ span ranging from 10 to 100. From these peaks the maximum value of reletive intensity [%] is 100.00 at the position [^{0}2 Th.] of 38.6315 gives three assignments i.e. Al, $Al_{0.41}Si_{0.09}$ and SiC. The peaks in the pattern can be indexed to a mixture of different compounds and other remaining minor peaks attributed to impurity.

Sample 5: X-ray diffraction pattern of the alloy with 5% Alumina as a reinforcement

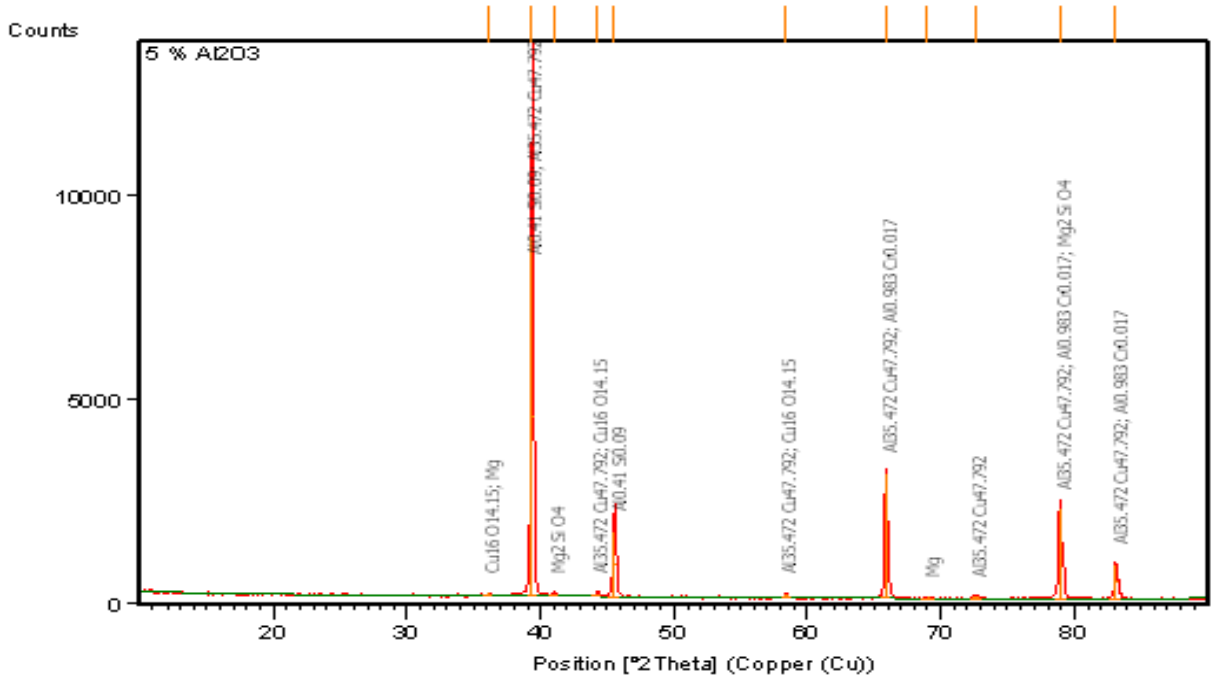

Figure 5.45- X-ray diffraction pattern of the alloy with 5 wt. % Al_2O_3 (Sample No.5)

Table 5.9- XRD results of alloy reinforced with 5% Al_2O_3

Ref.Code	Score	Compound Name	Chemical Formula	Weight fraction
01-074-5273	33	Aluminium Silicide	$Al_{0.41}Si_{0.09}$	49.0
01-072-3506	21	Aluminium Copper	$Al_{35.472}Cu_{47.792}$	7.0
01-071-0251	22	Copper Oxide	$Cu_{16}O_{14.15}$	1.0
01-074-5157	0	Aluminium Chromium	$Al_{0.983}Cr_{0.017}$	21.0
01-074-1684	9	Magnesium Silicate	Mg_2SiO_4	19.0
01-073-3812	15	Magnesium	Mg	19.0

Table 5.9 shows the X-ray diffraction pattern of the MMC (Sample No.5), which show the presence of Al and many other compounds. This confirms the presence of Al_2O_3 in the aluminium alloy 6061.

In X-ray difrracetion (Figure 5.45), Eleven peaks have been obtained in the 2θ span ranging from 10 to 100. From these peaks the maximum value of reletive intensity [%] is 100.00 at the position [^{0}2 Th.] of 39.3480 gives two assignments i.e. $Al_{0.41}Si_{0.09}$ and $Al_{35.472}Cu_{47.792}$. The peaks in the pattern can be indexed to a mixture of different compounds and other remaining minor peaks attributed to impurity.

Sample 6: X-ray diffraction pattern of the alloy with 5% Red Mud as a reinforcement

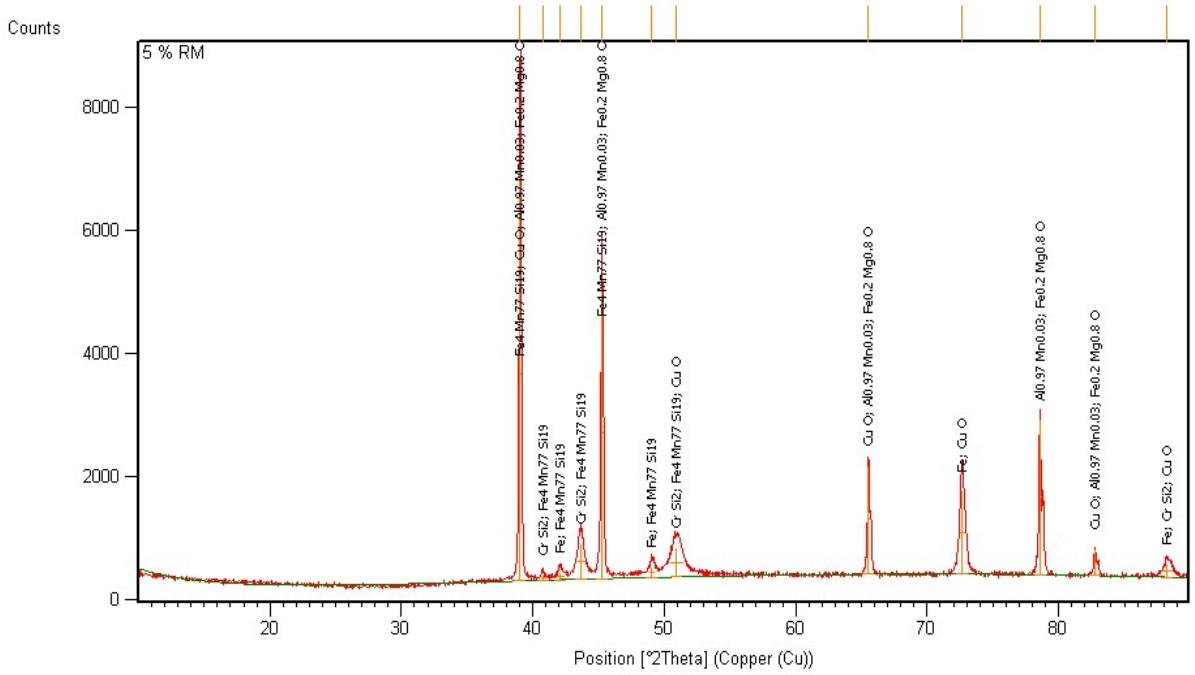

Figure 5.46- X-ray diffraction pattern of the alloy with 5 wt. % Red Mud (Sample No.6)

Table 5.10- XRD results of alloy reinforced with 5% Red Mud

Ref.Code	Score	Compound Name	Chemical Formula	Weight fraction (%)
01-071-4407	50	Iron	Fe	1.0

03-065-3546	26	Chromium Silicon	$CrSi_2$	7.0
03-065-9645	16	Iron Manganese Silicon	$Fe_4Mn_{77}Si_{19}$	16.0
01-089-5898	5	Copper Oxide	CuO	1.0
01-074-5245	82	Aluminium Manganese	$Al_{0.97}Mn_{0.03}$	65.0
01-075-7957	38	Iron Magnesium Oxide	$(Fe_{0.2}Mg_{0.8})O$	9.0

Table 5.10 shows the X-ray diffraction pattern of the MMC (Sample No.6), which show the presence of Al and many other compounds. This confirms the presence of Red Mud in the aluminium alloy 6061.

In X-ray difrracetion (Figure 5.46), Twelve peaks have been obtained in the 2θ span ranging from 10 to 100. From these peaks the maximum value of reletive intensity [%] is 100.00 at the position [^{0}2 Th.] of 39.0107 gives four assignments i.e. $Fe_4Mn_{77}Si_{19}$, CuO, $Al_{0.97}Mn_{0.03}$ and $(Fe_{0.2}Mg_{0.8})O$. The peaks in the pattern can be indexed to a mixture of different compounds and other remaining minor peaks attributed to impurity.

Sample 7: X-ray diffraction pattern of the alloy with 7.5% Silicon Carbide as a reinforcement

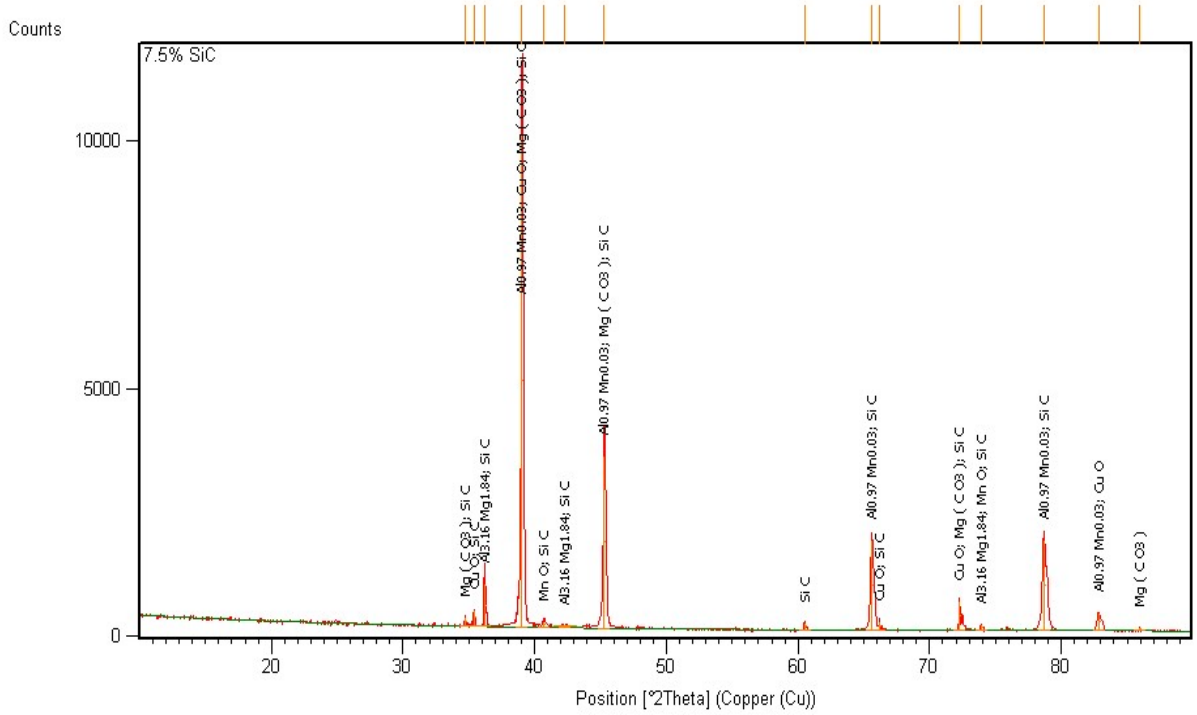

Figure 5.47- X-ray diffraction pattern of the alloy with 7.5 wt. % SiC (Sample No.7)

Table 5.11- XRD results of alloy reinforced with 7.5% SiC

Ref.Code	Score	Compound Name	Chemical Formula	Weight fraction
01-074-5245	72	Aluminium Manganese	$Al_{0.97}Mn_{0.03}$	68.0
03-065-6848	29	Aluminium Magnesium	$Al_{3.16}Mg_{1.84}$	3.0
01-089-2531	0	Copper Oxide	CuO	8.0
01-077-2363	20	Manganese Oxide	MnO	1.0
01-070-8513	19	Magnesium Carbonate	$Mg(CO_3)$	7.0
01-089-2352	9	Silicon Carbide	SiC	13.0

Table 5.11 shows the X-ray diffraction pattern of the MMC (Sample No.7), which show the presence of Al and many other compounds. This confirms the presence of SiC in the aluminium alloy 6061.

In X-ray difrracetion (Figure 5.47), fifteen peaks have been obtained in the 2θ span ranging from 10 to 100. From these peaks the maximum value of reletive intensity [%] is 100.00 at the position [^{0}2 Th.] of 39.0318 gives four assignments i.e. $Al_{0.97}Mn_{0.03}$, CuO, $Mg(CO_3)$ and SiC. The peaks in the pattern can be indexed to a mixture of different compounds and other remaining minor peaks attributed to impurity.

Sample 8: X-ray diffraction pattern of the alloy with 7.5% Alumina as a reinforcement

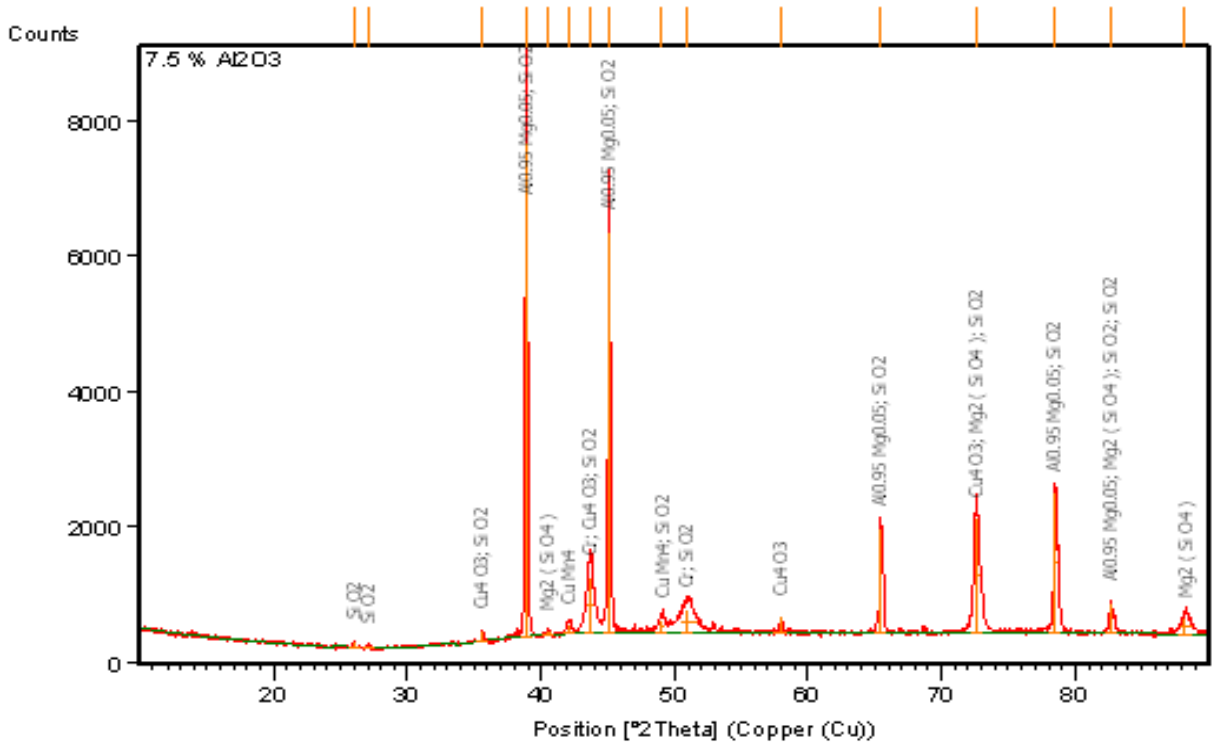

Figure 5.48- X-ray diffraction pattern of the alloy with 7.5 wt. % Al_2O_3 (Sample No.8)

Table 5.12- XRD results of alloy reinforced with 7.5% Al_2O_3

Ref.Code	Score	Compound Name	Chemical Formula	Weight fraction

01-074-5237	72	Aluminium Magnesium	$Al_{0.95}Mg_{0.05}$	75.0
01-088-2323	48	Chromium	Cr	5.0
03-065-5589	36	Copper Manganese	$CuMn_4$	1.0
01-083-1665	23	Copper Oxide	Cu_4O_3	2.0
01-087-2031	6	Magnesium Silicate	$Mg_2(SiO_4)$	12.0
01-089-8939	10	Silicon Oxide	SiO_2	4.0
01-083-2473	6	Silicon Oxide	SiO_2	4.0

Table 5.12 shows the X-ray diffraction pattern of the MMC(Sample No.8), which show the presence of Al and many other compounds. This confirms the presence of Al_2O_3 in the aluminium alloy 6061.

In X-ray difrracetion (Figure 5.48), Sixteen peaks have been obtained in the 2θ span ranging from 10 to 100. From these peaks the maximum value of reletive intensity [%] is 100.00 at the position [^{0}2 Th.] of 38.8608 gives two assignments i.e. $Al_{0.95}Mg_{0.05}$ and SiO_2. The peaks in the pattern can be indexed to a mixture of different compounds and other remaining minor peaks attributed to impurity.

Sample 9: X-ray diffraction pattern of the alloy with 7.5% Red Mud as a reinforcement

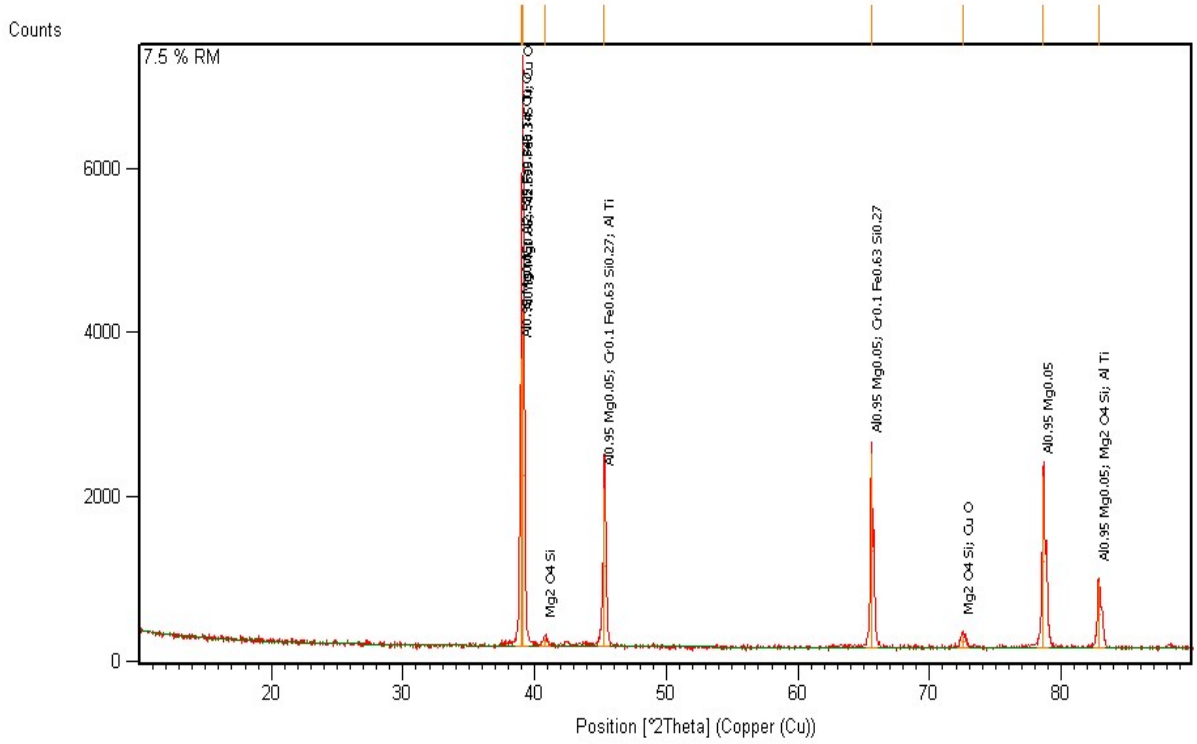

Figure 5.49- X-ray diffraction pattern of the alloy with 7.5 wt. % Red Mud (Sample No.9)

Table 5.13- XRD results of alloy reinforced with 7.5% Red Mud

Ref.Code	Score	Compound Name	Chemical Formula	Weight fraction
01-074-5237	74	Aluminium Magnesium	$Al_{0.95}Mg_{0.05}$	42.0
01-071-7545	32	Chromium Iron Silicon	$Cr_{0.1}Fe_{0.63}Si_{0.27}$	4.0
01-074-5204	25	Aluminium Iron Titanium	$Al_{2.535}Fe_{0.345}Ti$	33.0
01-087-2031	14	Magnesium Silicate	$Mg_2(SiO_4)$	3.0
01-074-5283	21	Aluminium Titanium	AlTi	3.0

01-073-6234	5	Copper Oxide	CuO	15.0

Table 5.13 shows the X-ray diffraction pattern of the MMC of (Sample No.9), which show the presence of Al and many other compounds. This confirms the presence of Red Mud in the aluminium alloy 6061.

In X-ray difrracetion (Figure 5.49), Eight peaks have been obtained in the 2θ span ranging from 10 to 100. From these peaks the maximum value of reletive intensity [%] is 100.00 at the position [^{0}2 Th.] of 39.1170 gives four assignments i.e. $Al_{0.95}Mg_{0.05}$, $Cr_{0.1}Fe_{0.63}Si_{0.27}$, $Al_{2.535}Fe_{0.345}Ti$ and CuO. The peaks in the pattern can be indexed to a mixture of different compounds and other remaining minor peaks attributed to impurity.

Sample 10: X-ray diffraction pattern of the alloy with 10% Silicon Carbide as a reinforcement

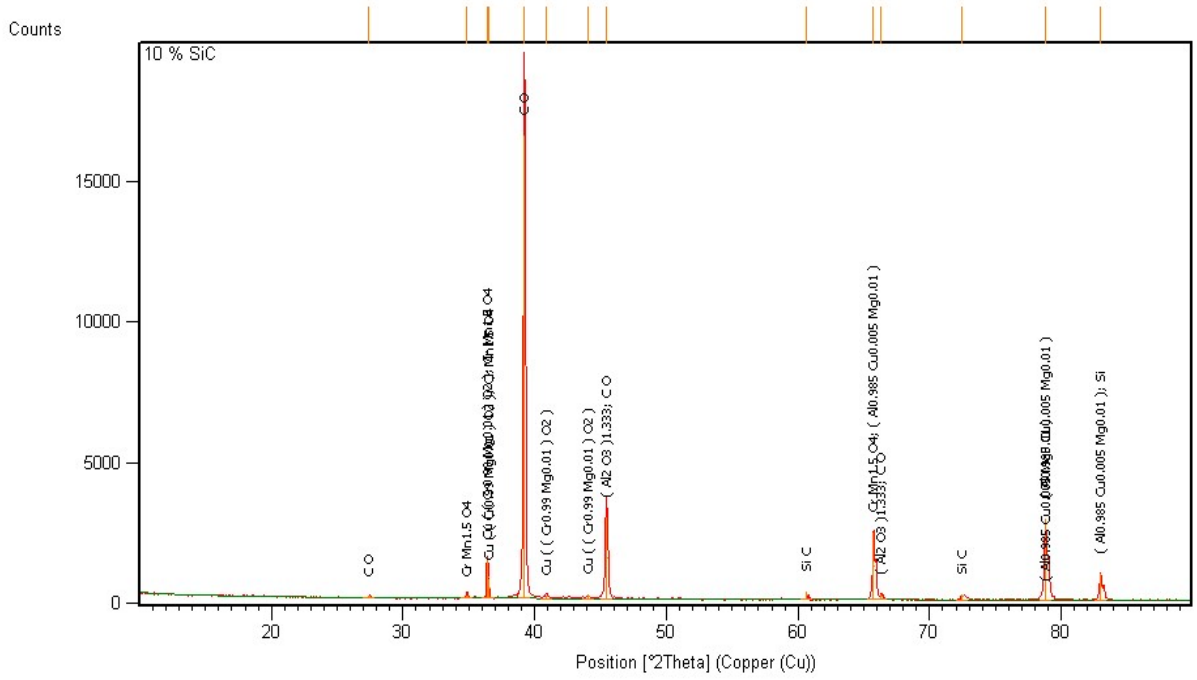

Figure 5.50- X-ray diffraction pattern of the alloy with 10 wt. % SiC (Sample No.10)

Table 5.14- XRD results of alloy reinforced with 10% SiC

Ref.Code	Score	Compound Name	Chemical Formula	Weight fraction
01-075-9817	24	Copper Chromium Magnesium Oxide	$Cu((Cr_{0.99}Mg_{0.01})O_2)$	4.0
01-071-0982	11	Chromium Manganese Oxide	$CrMn_{1.5}O_4$	1.0
01-074-5175	22	Aluminium Copper Magnesium	$Al_{0.985}Cu_{0.005}Mg_{0.01}$	10.0
01-075-0921	26	Aluminium Oxide	$(Al_2O_3)_{1.333}$	66.0
01-074-1229	0	Carbon Oxide	CO	10.0
01-073-1708	13	Silicon Carbide	SiC	6.0
01-071-3902	12	Silicon	Si	3.0

Table 5.14 shows the X-ray diffraction pattern of the MMC of (Sample No.10), which show the presence of Al and many other compounds. This confirms the presence of SiC in the aluminium alloy 6061.

In X-ray difrracetion (Figure 5.50), Fifteen peaks have been obtained in the 2θ span ranging from 10 to 100. From these peaks the maximum value of reletive intensity [%] is 100.00 at the position [^{0}2 Th.] of 39.1985 gives only one assignments i.e. CO. The peaks in the pattern can be indexed to a mixture of different compounds and other remaining minor peaks attributed to impurity.

Sample 11: X-ray diffraction pattern of the alloy with 10% Alumina as a reinforcement

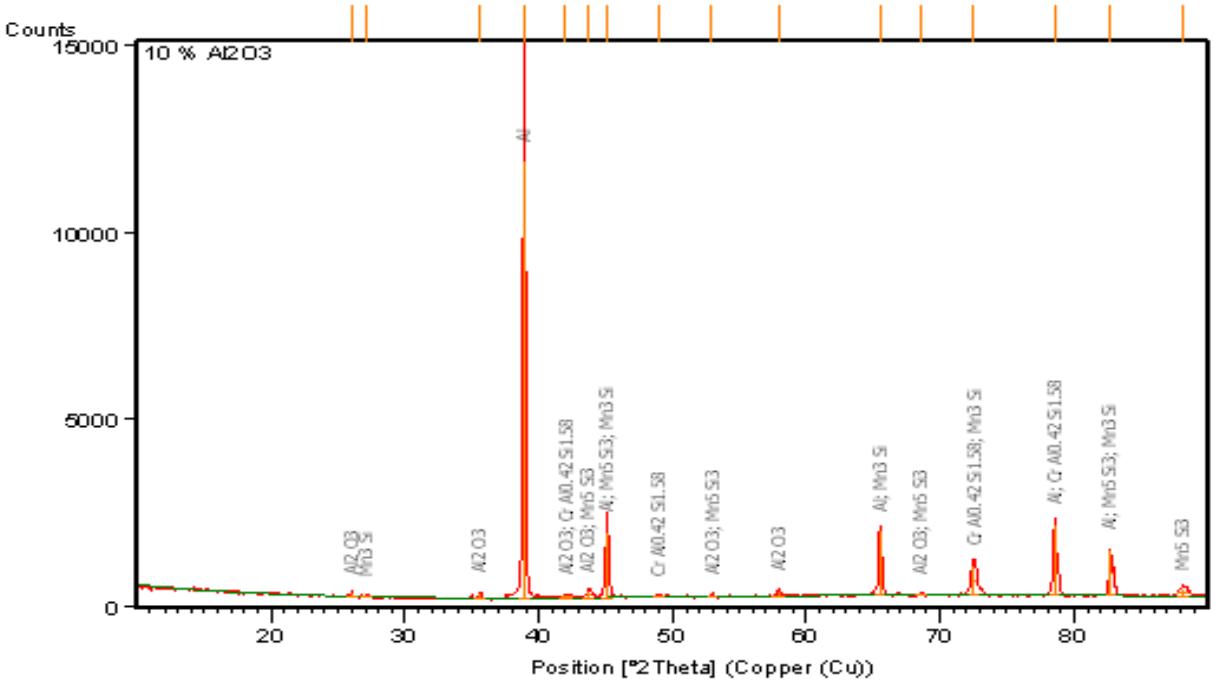

Figure 5.51- X-ray diffraction pattern of the alloy with 10 wt. % Al_2O_3 (Sample No.11)

Table 5.15- XRD results of alloy reinforced with 10% Al_2O_3

Ref.Code	Score	Compound Name	Chemical Formula	Weight fraction
01-089-2837	68	Aluminium	Al	81.0
01-088-0826	48	Aluminium Oxide	Al_2O_3	6.0
01-086-0329	19	Manganese Silicon	Mn_5Si_3	7.0
01-086-0329	13	Chromium Aluminium Silicon	$CrAl_{0.42}Si_{1.58}$	1.0
03-065-7191	39	Manganese Silicide	Mn_3Si	6.0

Table 5.15 shows the X-ray diffraction pattern of the MMC of (Sample No.11), which show the presence of Al and many other compounds. This confirms the presence of Al_2O_3 in the aluminium alloy 6061.

In X-ray difrracetion (Figure 5.51), Sixten peaks have been obtained in the 2θ span ranging from 10 to 100. From these peaks the maximum value of reletive intensity [%] is 100.00 at the position [^{0}2 Th.] of 38.8640 gives only one assignments i.e. Al. The peaks in the pattern can be indexed to a mixture of different compounds and other remaining minor peaks attributed to impurity.

Sample 12: X-ray diffraction pattern of the alloy with 10% Red Mud as a reinforcement

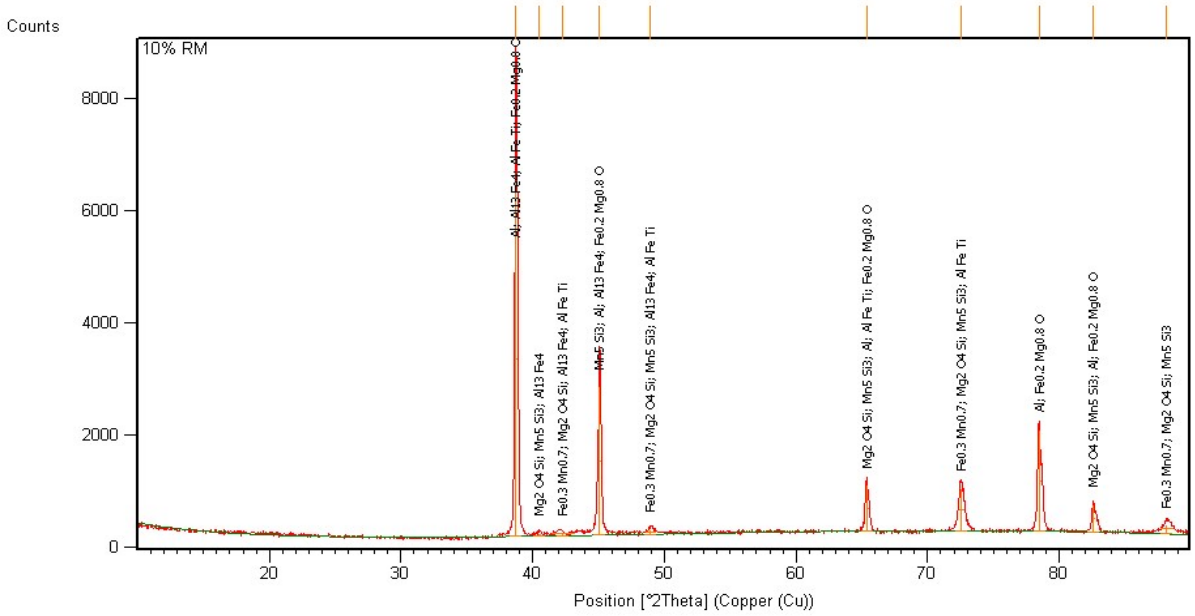

Figure 5.52- X-ray diffraction pattern of the alloy with 10 wt. % Red Mud (Sample No.12)

Table 5.16- XRD results of alloy reinforced with 10% Red Mud

Ref.Code	Score	Compound Name	Chemical Formula	Weight fraction
01-071-8284	38	Iron Manganese	$Fe_{0.3}Mn_{0.7}$	1.0
01-087-2031	17	Magnesium Silicate	$Mg_2(SiO_4)$	3.0
01-086-0329	5	Manganese Silicon	Mn_5Si_3	1.0

01-089-2837	85	Aluminium	Al	44.0
01-073-3008	10	Iron Aluminium	Fe_4Al_{13}	16.0
01-075-7821	12	Aluminium Iron Titanium	$Ti(Fe_{0.5}Al_{0.5})_2$	26.0
01-075-7957	50	Iron Magnesium Oxide	$(Fe_{0.2}Mg_{0.8})O$	8.0

Table 5.16 shows the X-ray diffraction pattern of the MMC of (Sample No.12), which show the presence of Al and many other compounds. This confirms the presence of Red Mud in the aluminium alloy 6061.

In X-ray difrracetion (Figure 5.52), Ten peaks have been obtained in the 2θ span ranging from 10 to 100. From these peaks the maximum value of reletive intensity [%] is 100.00 at the position [^{0}2 Th.] of 38.7283 gives four assignments i.e. Al, Fe_4Al_{13}, AlFeTi and $(Fe_{0.2}Mg_{0.8})O$. The peaks in the pattern can be indexed to a mixture of different compounds and other remaining minor peaks attributed to impurity.

Sample 13: X-ray diffraction pattern of alloy 6061without reinforcement

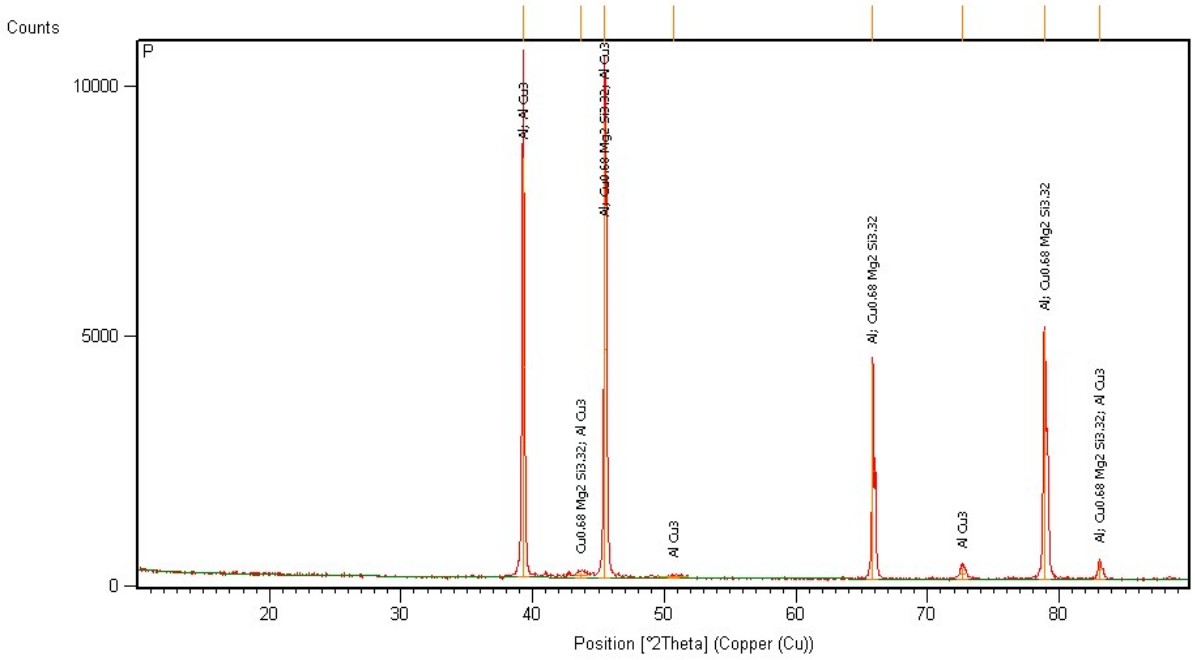

Figure 5.53- X-ray diffraction pattern of the Al alloy 6061 (Sample No.13)

Table 5.17- XRD results of alloy 6061without reinforcement

Ref.Code	Score	Compound Name	Chemical Formula	Weight fraction
01-089-2837	72	Aluminium	Al	48.0
01-071-4295	21	Copper Magnesium Silicon	$Cu_{0.68}Mg_2Si_{3.32}$	3.0
01-074-6895	32	Aluminium Copper	$AlCu_3$	49.0

Table 5.17 shows the X-ray diffraction pattern of the MMC of (Sample No.13), which show the presence of Al and many other compounds/ elements. This confirms the presence of different elements such Cu, Mg, and Si etc. in the aluminium to form aluminium alloy 6061.

In X-ray difrracetion (Figure 5.53), Eight peaks have been obtained in the 2θ span ranging from 10 to 100. From these peaks the maximum value of reletive intensity [%] is 100.00 at the

position [^{0}2 Th.] of 45.4807 gives three assignments i.e. Al, $Cu_{0.68}Mg_2Si_{3.32}$ and $AlCu_3$. The peaks in the pattern can be indexed to a mixture of different compounds and other remaining minor peaks attributed to impurity.

5.7 MICRO STRUCTURAL OBSERVATION OF WORN PIN SURFACES

The worn-out surfaces of some selected/ typical specimens (10 % wt. fraction of reinforcements) after the wear test were observed under optical microscope with magnification 200X.

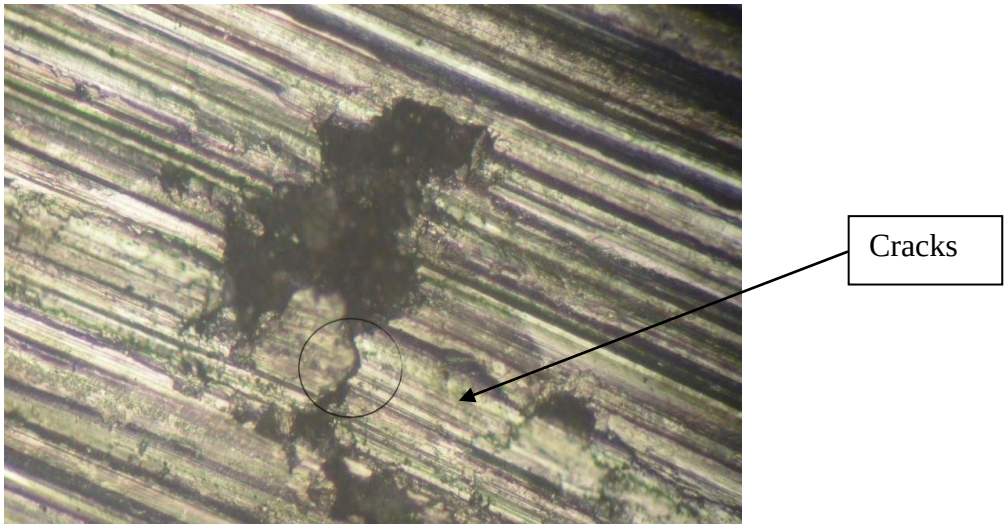

Figure 5.54- Micrograph showing wear surface of 10% Red Mud in Al alloy 6061

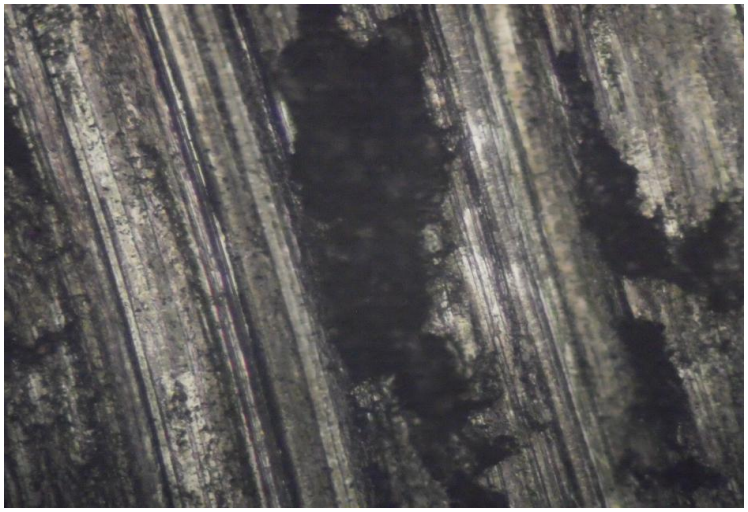

Figure 5.55- Micrograph showing wear surface of 10% SiC in Al alloy 6061

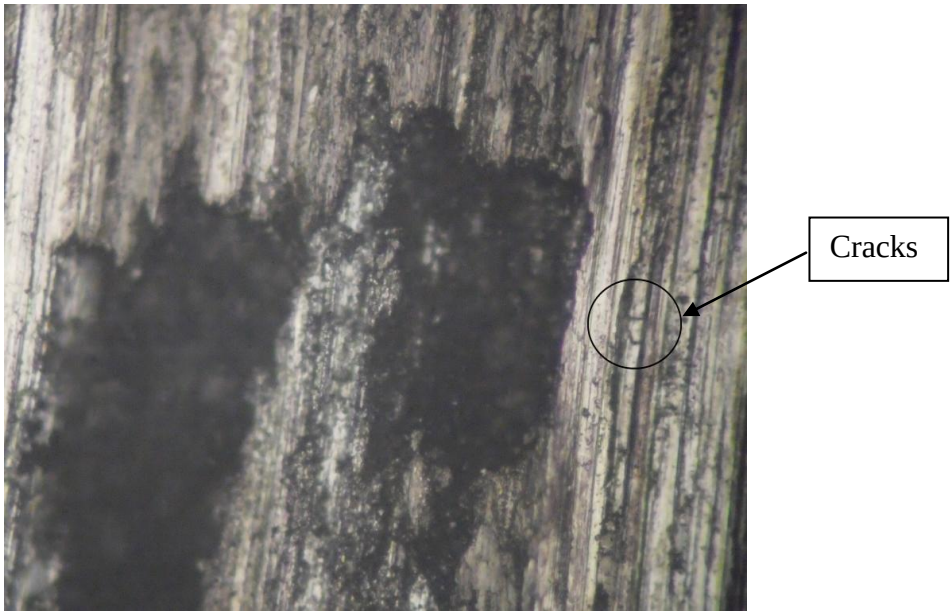

Figure 5.56- Micrograph showing wear surface of 10 % Al_2O_3 in Al alloy 6061

Figure 5.54-5.56 shows the surface morphology of aluminium alloy 6061 with 10% Red Mud, SiC and Al_2O_3 composite, tested under ambient temperature with constant load and speed.

The structures of the worn surfaces are greatly dependent on sliding speed, load and hardness of particles (reinforcement). Comparing these figures it can be visualized that one of the common features observed in all three MMCs, i.e. the formation of grooves and ridges running parallel to the sliding direction. These wear scars are the primarily characteristic of abrasive wear. On further analyzing, it has been found that grooves are fine on the worn pin surface of Al alloy 6061 with 10 % wt. fraction of SiC as compared to others. A similar observation was also reported in Al–Si alloy subjected to 24.5 N load in comparison to 53.9 N [15].

From the micrographs (Figure 5.54 and 5.56) some cracks have appeared and these cracks are propagated in different directions [1]. This might be due to strain hardening of aluminium based metal matrix composites with applied load and due to pulling up of hard phase particles i.e. red mud and alumina from the aluminium grain boundary.

CHAPTER 6 CONCLUSION AND SCOPE OF FUTURE WORK

6.1 CONCLUSION

The conclusions drawn from the present investigation are as follows:

- Aluminium based metal matrix composites have been successfully fabricated by stir casting technique with fairly uniform distribution of Red mud, Silicon carbide and Aluminium oxide particulates.
- For synthesizing of composite by stir casting process, stirrer design and stirrer position, stirring speed and time, particles preheating temperature, particles incorporation rate etc. are the important process parameters.
- The results confirmed that stir formed Al alloy 6061 with Red Mud, SiC and Al_2O_3 reinforced composites is clearly superior to base Al alloy 6061 in the comparison of microhardness i.e. the microhardness increases after addition of SiC, Al_2O_3 and Red Mud particles in the matrix.
- Dispersion of SiC, Red mud and Al_2O_3 particles in aluminium matrix improves the wear resistance of the composites.
- It is found that wear rate tends to decrease with increasing particles wt. percentage (2.5-10%), which confirms that silicon carbide, red mud and alumina addition is beneficial for reducing the wear rate of MMCs.
- The wear rate showed the two stages of wear for all the applied loads. At the initial stage run-in wear occurred up to 1 km sliding distance and in later stage wear approaches to steady state.
- It appears from this study, the wear rate trend starts decreasing with increase in weight percentage of SiC and Al_2O_3 in the matrix, but in case of Red Mud reinforcement, wear rate of the composite decreases due to addition of red mud particles up to 7.5% by weight. Beyond this wt. % the wear rate trend starts increases.

  This is because when red mud is added beyond 7.5% by weight in the matrix the viscosity of MMC increased and stirrer was not rotated properly, thereby poor interfacial

bonding takes place between the red mud and Al alloy matrix. MMC with 7.5% red mud reinforcement have approximately constant wear rate throughout the test and have maximum value of microhardness among all the experiments.

- XRD results showed the presence SiC, Al_2O_3 and Red Mud particles in alloy matrix. The oxide phases like Al_2O_3, Fe_2O_3 and TiO_2 etc. have dispersed uniformly through out in the Red Mud MMC thus strengthening the resulting composite.
- The Optical micrography and SEM images revealed that SiC, Red Mud and Alumina particulates are fairly distributed in Aluminium alloy Matrix. It also revealed from SEM images that at some places voids has been occurred before wearing. From the optical micrography grooves, ridges and some cracks have been appeared after wearing. The grooves and ridges running parallel to the sliding direction but cracks are propagated in arbitrary directions.
- Red mud, the waste generated from alumina production can be successfully used as a reinforcing material to produce Metal-Matrix Composites (MMCs). It can be replaced by other expensive reinforcement materials such as SiC and Al_2O_3. Thereby saving of expensive reinforcements could be achieved.

6.2 SCOPE OF FUTURE WORK

- Same metal matrix composites can be manufactured by using other manufacturing techniques like spray casting etc. and results can be compared with stir casting technique.
- In this study red mud, SiC and Al_2O_3 particles of sizes 103-150, 60- 90 and 30-50 microns have been used. This can further be extended by varying the particle size and then effect of particle size on the wear behaviour of the composite can be studied.
- Heat treatment of the MMCs at different temperature range and quenching media like water, oil and brine solution etc. can be used to achieve better results.

REFERENCES

[1] Prasad Naresh and Acharya S.K, "Development of Metal Matrix Composite Using Red mud an Industrial Waste for Wear Resistant Applications", Ph.D Thesis, National Institude of Technology, Rourkela, India, January 2006.

[2] Sanjeev kumar and Bikramjit Sharma, "Effects of Thermal Cyclic loading on Cast Aluminium Composite Reinforced with Silicon Carbide and Fly Ash Particles", M.E. Thesis, Thapar University, Patiala, India, July 2010.

[3] Narinder Singh, Shweta Goyal and Kishore Khanna, "Effect of Thermal Ageing on Al Alloy Metal Matrix Composite", Department of Mechanical Engineering, M.E. Thesis, Thapar University, Patiala, India, July 2010.

[4] Vishal Sharma and Sanjeev Das, "Synthesis and Interfacial Characterization of Al-4.5wt%Cu/ Zircon Sand/ Silicon Carbide Hybrid Composite", Department of Physics and Materials Sciences, M.E. Thesis, Thapar University, Patiala, India, June 2007.

[5] Shailove kumar, Kishore Khanna and V.P. Agrawal, "Effect of thermal ageing on Al -SiC MMC", Department of Mechanical Engineering, M.E. Thesis, Thapar University, Patiala, India, July 2010.

[6] Vladimir Cablik, "Characterization and applications of red mud from bauxite processing", pp. 27-38, 2007.

[7] M.Ramachandra and K. Radhakrishna, "Study of abrasive wear of Al-Si (12%)-SiC MMC synthesised using vortex method", Department of Metallurgical and Materials Engineering, pp.1- 12, December 2004.

[8] S. Sawla, S. Das, "Combined effect of reinforcement and heat treatment on the two body abrasive wear of aluminium alloy and aluminium particle composites", pp. 555–561, 2004.

[9] G. B. Veeresh Kumar, C. S. P. Rao, N. Selvaraj, M. S. Bhagyashekar, "Studies on Al6061-SiC and Al7075-Al_2O_3 Metal Matrix Composites", Journal of Minerals & Materials Characterization & Engineering, pp.43-55, Volume 9, 2010.

[10] N R Prabhu Swamy, C S Ramesh and T Chanderashekar, "Effect of heat treatment on strength and abrasive wear behaviour ofAl6061–SiCp composites", Indian Academy of Sciences, pp. 49–54, Volume 33, February 2010.

[11] Adem Kurt, Mustafa Boz, "The effect of Al2O3 on the friction performance of automotive brake friction materials", Journal of Science Direct, pp. 1161- 1169, February 2007.

[12] M.K. Surappa, R.K. Uyyuru, S. Brusethaug, " Tribological behavior of Al–Si–SiCp composites/automobile brake pad system under dry sliding conditions", Tribology International 40 (2007), pp. 365- 373, April 2006.

[13] Soner Buytoz, Serdar Osman Yılmaz, "Relationship between thermal and sliding wear behavior, of Al6061/Al_2O_3 metal matrix composites", Journal of Springer Science, pp. 4485–4493, volume 42, February 2007.

[14] Sanjeev Das, Siddhartha Das, Karabi Das, "Abrasive wear of zircon sand and alumina reinforced Al–4.5 wt% Cu alloy matrix composites – A comparative study", Journal of Science direct, pp. 746-751, June 2006.

[15] Kamalpreet Kaur, O. P. Pandey, "Dry Sliding Wear Behavior of Zircon Sand Reinforced Al–Si Alloy", pp. 377- 387, May 2010.

[16] Jaykant Gupta and S.K.Patel, "Mechanical and Wear properties of carburized mild steel samples", M.E. Thesis, National Institude of Technology, Rourkela, India, May 2009.

[17] Ashutosh Sharma and Sanjeev Das, "Study of the age hardening behavior of Al - 4.5Cu/ZrSiO4 composite in different quenching media", Department of Physics and Materials Sciences, M.E. Thesis, Thapar University, Patiala, India, June 2007.

[18] S.K. Varma et al., and Daniel Salas, "The Control of Grain Size and Distribution of particles in a 6061alloy and Al_2O_3 composite by solutionzing treatment", Department of Metallurgical and Materials Engineering, pp. 2023- 2034, volume 27 A, July 1996.

[19] Murphy et al., "freezing and melting treatment of red mud slurries to aid solid separation", United States Patent, feb.1973.

[20] S. Zahi, A.R. Daud, "Fly ash characterization and application in Al–based Mg alloys", Journal of Elsevier- Material and Design, pp.1-10, September 2010.

[21] Book: Technology Base Enhancement Program Metal Matrix Composites Prepared by BDM Federal, Inc August 1993.

[22] www.wikkipedia.com/ wear behavior

[23] www.wikipedia.com/aluminium alloy.html

[24] Mechanical Engineers Handbook: Seymour G. Epstein et al., "aluminium and its alloy", pp. 1-14, 1998.

[25] www.azom.com/ Al alloy 6061

[26] www.red mud Characteristics. Info

[27] www.ask.com/ encyclopaedia

[28] www.wikipedia.com/ silicon carbide/ Silicon carbide properties.html

[29] www.wikipedia.com/ aluminium oxide/ Al_2O_3 material properties.html

[30] Rohatgi, P. Cast Metal Matrix Composites. In Metals Handbook, 9th Ed.; ASM: Metals Park, OH, Vol. 15, Casting, pp.840–853, 1988.

[31] ASM Handbook: Materials Park, OH. pp. 823-873, 1995.

[32] Godfrey D, Peterson MB and Winer WO editors. Wear control handbook. New York: ASME, pp. 283–312, 1980.